The Sahlgrenska Academy

Molecular and cellular interactions on noble metal nanopatterned surfaces

– applications towards bone, soft tissue and infection control

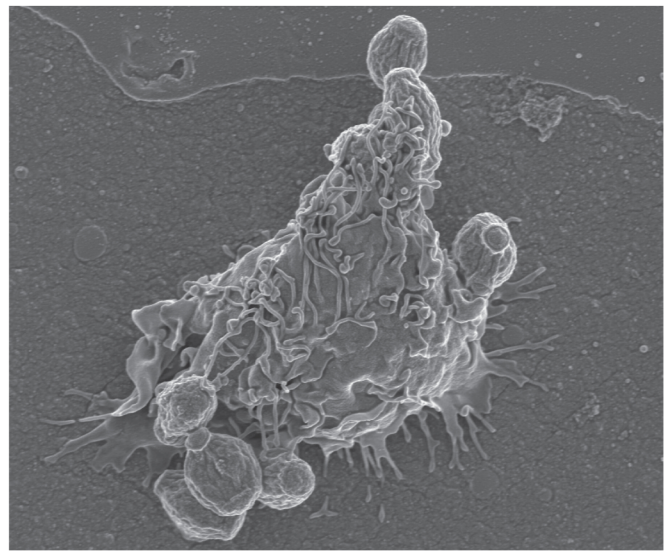

Sara Svensson

Institute of Clinical Sciences
at Sahlgrenska Academy
University of Gothenburg

UNIVERSITY OF GOTHENBURG

Molecular and cellular interactions on noble metal nanopatterned surfaces

- applications towards bone, soft tissue and infection control

Sara Svensson

Department of Biomaterials

Institute of Clinical Sciences

Sahlgrenska Academy at University of Gothenburg

UNIVERSITY OF GOTHENBURG

Gothenburg 2014

Cover illustration: Monocyte–zymosan interactions on nanopatterned noble metal coated silicone

Molecular and cellular interactions on noble metal nanopatterned surfaces

Department of Biomaterials
Institute of Clinical Sciences
Sahlgrenska Academy at University of Gothenburg
Box 412
405 30 Gothenburg
Sweden

ISBN 978-91-628-9004-9

Printed in Gothenburg, Sweden 2014
Ineko AB

Printed in 250 copies

Till Noel

ABSTRACT

Biomaterial-associated infection is recognised as one of the main risks for failure of medical devices. The presence of a foreign material in tissues has been suggested to compromise the ability of host cells to eradicate infection. In addition, a protective biofilm formed by bacteria limits the effectiveness of administered antibiotics, which underscores the importance of preventive measures. The use of implant surface modifications that resist bacteria is a promising approach to reduce the infection risk. A nanopatterned noble metal coating, applied on catheters, has shown up to 50% reduction of infections in the clinic. The aim of the present project was to investigate the material–tissue interactions of nanopatterned noble metal coatings, especially with respect to their role in inflammation and bioburden control. Several microscopy techniques, cellular and microbiological techniques, and molecular analyses have been used.

The results show that the processes of inflammation and fibrosis can be modulated depending on the combination of noble metals in the coating (silver, gold and palladium). Noble metal coated titanium implants displayed a comparable bone response to that of clinically used machined titanium and was shown to reduce *Staphylococcus aureus* adhesion *in vitro*. To separate the effects of noble metal chemistry from nanotexture, the specific effects of nanostructures on host defence cells (monocytes) and *Staphylococcus epidermidis* were evaluated using gold model surfaces with or without immobilised gold nanoparticles on the surface. The presence of nanostructures did not affect monocyte behaviour but reduced bacterial viability and biofilm formation on the surfaces, indicating a bactericidal effect induced by nanoscale surface features. An *in vivo* infection model to study early inflammatory events was developed. The presence of *S. epidermidis* induced significantly more inflammatory cell recruitment, cell activity and cell death. A trend towards a more intense inflammatory response and a reduced amount of viable bacteria was observed around the noble metal coated implants.

In conclusion, nanostructured noble metal coatings are biocompatible in soft tissue and bone, which render them a suitable option in many new application areas. The anti-infectious potential of the coatings may partly be related to physical interactions of bacteria with the surface nanostructures and partly related to an intensified inflammatory response due to the material surface chemistry.

Keywords: Nanotopography, noble metals, titanium, biocompatibility, osseointegration, inflammation, host defence, monocytes, infection control, antimicrobial, staphylococci

SAMMANFATTNING

Infektion i anslutning till implantat och proteser är en allvarlig komplikation. Förekomsten av ett främmande föremål i kroppens vävnader har visat sig leda till en sämre förmåga för kroppens försvarsceller att eliminera bakterier. Dessutom kan många mikroorganismer omge sig av en skyddande biofilm då de växer på en yta, vilket minskar effekten av antibiotika. Preventiva strategier utgörs dels av att modifiera implantatet så att en vävnadsintegrering underlättas och dels av att förändra implantatytans kemi och topografi i syfte att förhindra förekomst av bakterier. Ett kliniskt exempel är en ädelmetallbeläggning, endast några nanometer i tjocklek, som visat sig reducera kateter-relaterade infektioner med upp till 50%. I denna avhandling har betydelsen av ädelmetaller samt nanotextur på implantatytor för inflammation, vävnadsintegrering och bakterier undersökts i provrörsmiljö, mjukvävnad och ben. Flera olika mikroskoperingstekniker, cell- och molekylärbiologiska analysmetoder samt mikrobiologiska tekniker har använts.

Resultaten i denna avhandling visar att man genom att variera beläggningens olika komponenter (silver, guld och palladium) kan påverka både inflammatoriska förlopp och mängden fibrös vävnad som bildas runt implantatet. En ädelmetallbeläggning kunde, med gott resultat, påföras en titanyta och visade en liknande förmåga att integreras i ben som kliniskt använda maskinbearbetade titanytor. Dessutom bevarades den antimikrobiella effekten då en markant minskning av adherenta *Staphylococcus aureus* jämfört med kontrollytor kunde påvisas. För att ta reda på mer om hur de separata effekterna från beläggningens ädelmetallkemi och nanostruktur bidrar till dess antimikrobiella egenskaper användes modellytor av guld. Dessa guldytor belades med nanopartiklar av guld och användes för att undersöka adhesion och biofilmtillväxt av *Staphylococcus epidermidis* samt reaktion av humana försvarsceller (monocyter) vid mikrobiell stimulering. Nanostrukturerna påverkade inte monocyterna nämnvärt jämfört med den släta kontrollytan, men däremot påvisades lägre bakterieöverlevnad och en senarelagd biofilmsproduktion på de nanostrukturerade ytorna. En infektionsmodell utvecklades därefter för att studera tidiga inflammationsförlopp kring ytmodifierade titanimplantat i närvaro av *S. epidermidis*. Bakterierna inducerade en kraftig rekrytering av inflammatoriska celler, en ökad cellaktivitet och celldöd. Ädelmetallbelagt titan tenderade att öka det inflammatoriska svaret och hade också en lägre andel levande bakterier.

Sammanfattningsvis så har ädelmetallsbelagda ytor visat god vävnadvänlighet i både mjukvävnad och ben, vilket öppnar upp för möjligheten att utvidga dess kliniska användningsområde. Den antimikrobiella effekten kan delvis bero på fysiska interaktioner mellan bakterier och ytans nanostruktur och delvis på ett intensifierat inflammatoriskt svar orsakat av materialytans kemi.

LIST OF PAPERS

This thesis is based on the following studies, referred to in the text by their corresponding Roman numerals.

I. Suska F, Svensson S, Johansson A, Emanuelsson L, Karlholm H, Ohrlander M, Thomsen P. *In vivo* evaluation of noble metal coatings.
Journal of Biomedical Materials Research. Part B, Applied Biomaterials 2010; 92(1): 86-94

II. Svensson S, Suska F, Emanuelsson L, Palmquist A, Norlindh B, Trobos M, Bäckros H, Persson L, Rydja G, Ohrlander M, Lyvén B, Lausmaa J, Thomsen P. Osseointegration of titanium with an antimicrobial nanostructured noble metal coating.
Nanomedicine: Nanotechnology, Biology and Medicine 2013; 9(7): 1048-56

III. Svensson S, Forsberg M, Hulander M, Vazirisani F, Palmquist A, Lausmaa J, Thomsen P, Trobos M. Role of nanostructured gold surfaces on monocyte activation and *Staphylococcus epidermidis* biofilm formation.
International Journal of Nanomedicine 2014; 9: 775-94

IV. Svensson S, Trobos M, Hoffman M, Norlindh B, Petronis S, Lausmaa J, Suska F, Thomsen P. A novel soft tissue model for biomaterial-associated infection and inflammation – bacteriological, morphological and molecular observations.
In manuscript.

List of papers not included in the thesis

- Omar O, Suska F, Lennerås M, Zoric N, Svensson S, Hall J, Emanuelsson L, Nannmark U, Thomsen P. The influence of bone type on the gene expression in normal bone and at the bone–implant interface: experiments in animal model.
  Clinical Implant Dentistry and Related Research 2011; 13(2): 146-56
- Omar O, Svensson S, Zoric N, Lennerås M, Suska F, Wigren S, Hall J, Nannmark U, Thomsen P. In vivo gene expression in response to anodically oxidised versus machined titanium implants.
  Journal of Biomedical Materials Research. Part A 2010; 92(4): 1552-66
- Omar O, Lennerås M, Svensson S, Suska F, Emanuelsson L, Hall J, Nannmark U, Thomsen P. Integrin and chemokine receptor gene expression in implant-adherent cells during early osseointegration.
  Journal of Material Science. Materials in Medicine 2010; 21(3):969-80
- de Peppo G.M, Svensson S, Lennerås M, Synnergren J, Stenberg J, Strehl R, Hyllner J, Thomsen P, Karlsson C. Human embryonic mesodermal progenitors highly resemble human mesenchymal stem cells and display high potential for tissue engineering applications.
  Tissue Engineering. Part A 2010; 16(7): 2161-82

TABLE OF CONTENTS

ABBREVIATIONS

AFM	Atomic force microscopy
ALP	Alkaline phosphatase
AMP	Antimicrobial peptide
ANOVA	Analysis of variance
BAI	Biomaterial-associated infections
bFGF	Basic fibroblast growth factor
BMP	Bone morphogenetic protein
BSP	Bone sialoprotein
C3	Complement factor 3
CFU	Colony-forming units
CL	Chemiluminescence
CLSM	Confocal laser scanning microscopy
CoCr	Cobalt-chrome
CoCrMo	Cobalt-chrome-molybdenum
CoN	Coagulase-negative
CR3	Complement receptor type 3
ELISA	Enzyme-linked immunosorbent assay
FIB	Focused ion beam
FISH	Fluorescence *in situ* hybridisation
GFAAS	Graphite furnace atomic absorption spectroscopy
GM-CSF	Granulocyte-macrophage colony-stimulating factor
HA	Hydroxyapatite
HBSS	Hank's balanced salt solution
ICP-MS	Inductively coupled plasma mass spectrometry
IFN-γ	Interferon-gamma
IgG	Immunoglobulin
IL	Interleukin
IL-8R	Interleukin-8 receptor
LDH	Lactate dehydrogenase
LPS	Lipopolysaccharide
M-CSF	Macrophage colony-stimulating factor
MAC	Membrane attack complex
MCP-1	Monocyte chemoattractant protein-1
MIP-1α	Macrophage inflammatory protein-1 alpha
MIP-1β	Macrophage inflammatory protein-1 beta
NF-κB	Nuclear factor-kappa B
OC	Osteocalcin
OD	Optical density
OPG	Osteoprotegerin

OPN	Osteopontin
PAMP	Pathogen-associated molecular patterns
PBS	Phosphate buffered saline
PCL	Polycaprolactone
PDGF	Platelet derived growth factor
PDMS	Polydimethylsiloxane
PEG	Polyethylene glycol
PGA	Poly-γ-glutamic acid
PIA	Polysaccharide intercellular adhesin
PMA	Phorbol myristate acetate
PMN	Polymorphonuclear cells
PRR	Pattern-recognition receptor
PSM	Phenol-soluble modulin
PTFE	Polytetrafluoroethylene
PUUR	Polyurethane urea
RANK	Receptor activator of nuclear factor-kappa B
RANKL	Receptor activator of nuclear factor-kappa B ligand
ROS	Reactive oxygen species
RPMI	Rosewell Park Memorial Institute
RT-qPCR	Reverse transcriptase quantitative real-time polymerase chain reaction
Runx2	Runt-related transcription factor 2
SEM	Scanning electron microscopy
TGF-β	Transforming growth factor-beta
TLR	Toll-like receptor
TNF-α	Tumour necrosis factor-alpha
TOF-SIMS	Time-of-flight secondary ion mass spectrometry
TSB	Tryptic soy broth
UHMWPE	Ultra-high molecular weight polyethylene
VEGF	Vascular endothelial growth factor
XPS	X-ray photoelectron microscopy

1 INTRODUCTION

1.1 Biomaterials in the clinic

Biomaterials are defined as non-viable materials used in medical devices intended to interact with biological systems.[1] They can be used for the evaluation, treatment, augmentation and replacement of an injured or non-functional body structure for the restoration of its anatomy and function. Today, millions of biomedical implants are used, ranging from everyday use of contact lenses to life-sustaining pacemakers and mobility-supporting joint prostheses. This dependency on biomaterials is forecast to increase due to both a growing elderly population and expanding access to healthcare.

Biomaterials can be divided into several subgroups depending on the duration of tissue contact (temporary or permanent), their location in the body and which tissues they come into contact with. One distinction is made between external and internal medical devices. External devices come into contact with different types of epithelial cells and include wound dressings, urinary catheters or endotracheal tubes. Internal devices can be either partially internal, like dental implants, bone anchored hearing aids and amputation prostheses, breaking the epithelial lining, or completely internal, such as pacemakers or joint prostheses. The demands on implants differ depending on the anatomical site, the time of use and its intended function, but common for them all is the requirement for biocompatibility. For a material to be biocompatible it should perform with an appropriate host response in a specific application.[1]

Implanted medical devices can broadly be divided into soft tissue implants and bone anchoring implants. The tissue response towards these different implants differs due to their diverse surroundings (**Figure 1**). A common feature for all biomaterials that come into contact with biological components is the instantaneous adsorption of proteins on the surface. The first cells arrive from the blood stream within minutes, followed by an inflammatory response orchestrated mainly by macrophages, and subsequent healing.

In soft tissues, macrophages are often maintained in the area for a long time period, some which are fused into foreign body giant cells, forming a layer on the implant surface. The goal of the cells is to eliminate the foreign object, resulting in frustrated phagocytosis of the material. The macrophages secrete chemokines, cytokines and growth factors, and play an important role in the events following implantation. The

macrophages signal to fibroblasts to initiate repair, often resulting in a fibrous capsule around the implant. This is regarded as the normal foreign body reaction.

In bone, on the other hand, fibrous encapsulation is not always the case. The special features of bone enable integration of the implanted biomaterial, depending on the material. The ability of an implant to integrate in bone was first discovered with titanium in the late sixties, and was termed "osseointegration" some years later.[2] Osseointegration requires primary stability, enabling bone progenitor cells from the existing bone or bone marrow to deposit new bone matrix around the implant material. The integration of the implant in the bone tissue provides biomechanical stability and enables load-bearing.

The success rate of implants is generally very high, but complications do occur, which compromise the function of the device and lead to pain, disease or even life-threatening conditions for the patient. One of the major complications is infection. The infection rate varies depending on implant site, time of use and level of contamination,[3] but is also dependent on the health status of the patient and the surgical conditions. Infection rates for various medical devices used in different applications are shown in **Table 1**. Biomaterial-associated infections (BAI) are difficult to treat due to the persistence of bacteria on the material surfaces. Surface-adherent bacteria have the ability to deposit a biofilm that protects them from host defence mechanisms as well as antibiotic treatment.[4-6] Hence, preventive measures are of great importance and include the use of laminar air-flow operation halls, use of adequate prophylaxis protocols, as well as modifications of the biomaterial.

Figure 1. Schematic illustration of the tissues surrounding a pacemaker and a bone-anchored amputation prosthesis. An implant in soft tissue (left) is commonly surrounded by a fibrous capsule, which is mainly comprised of collagen fibres arranged in parallel with the material surface, fibroblasts and blood vessels. At the material surface, one- to two cell layers of macrophages and multinuclear foreign body giant cells are normally present. In bone (right), implants have the possibility to become integrated in the bone tissue. New bone forms around the implant and provide stabilisation to the implant, thus enabling load-bearing. For both examples, the presence of nanoscale features on the implant surface may have the possibility to direct cell responses, e.g. via the activation of cell surface receptors.

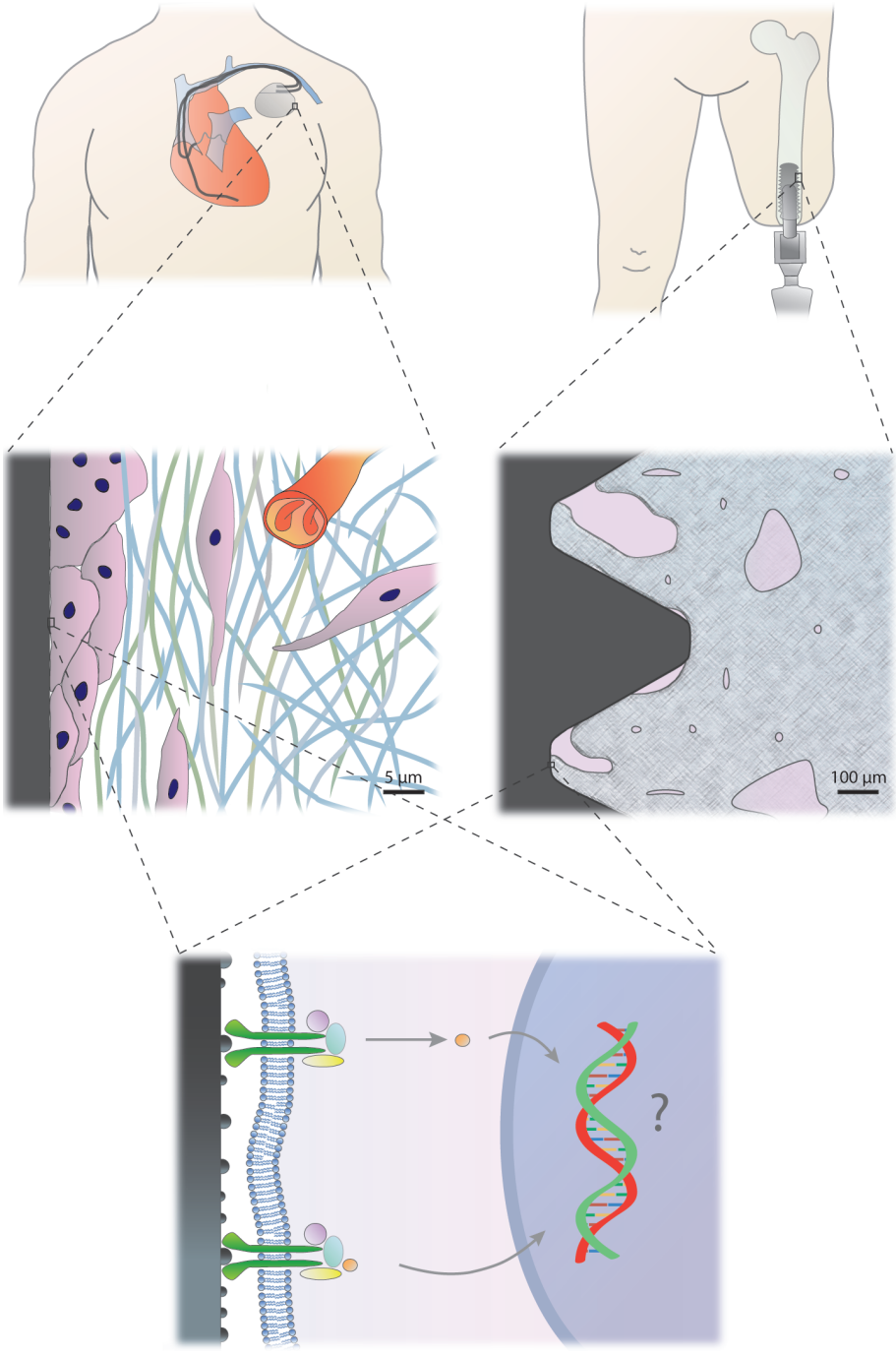
5 µm
100 µm
?

Table 1. Infection rates of biomaterial-associated infections for various medical implants and devices

Implant or device	Infection rate (%)	Reference
Urinary tract		
Urinary catheter	10-100	[7]
Percutaneous		
Central venous catheter	3-8	[8]
Heart assist device	25-50	[8]
Ventricular assist device	18-59	[9]
Fracture fixation device	5-10	[8]
Suture	2-5	[10]
Airways		
Mechanical ventilation (endotracheal tube)	9-23	[11]
Transmucosal		
Dental implant	5-10	[8]
Soft tissue		
Pacemaker	0.1-20	[12]
Mammary prosthesis	1-2	[8]
Penile prosthesis	1-3	[8]
Ventricular shunt	5-15	[13]
Eye		
Contact lens	0.5-4	[14]
Intraocular lens	0.1	[15]
Circulatory system		
Mechanical heart valve	1-3	[8]
Vascular graft	1-5	[8]
Bone		
Hip arthroplasty	1.4	[16]
Knee arthroplasty	0.5-1.5	[17]
Tibial nail	1-7	[18]

1.2 Wound healing

When a wound is created, there is a disruption in the normal anatomical structure and function. The response is immediate and initiates an ordered sequence of events with the aim to restore haemostasis and heal the wound. Wound healing is characterised by four distinct but overlapping phases: haemostasis, inflammation, proliferation and remodelling.[19]

1.2.1 Haemostasis

Tissue injury causes the disruption of blood vessels with accompanying loss of blood. When blood components come into contact with the surrounding damaged tissue, e.g. exposed collagen, platelets become activated and release clotting factors, cytokines and growth factors from their granules.[19] The coagulation cascade is initiated with a resulting platelet aggregation and fibrin clot at the site of injury that restores haemostasis. The fibrin clot is composed of several cross-linked fibrin fibres forming a provisional matrix that plays an important role in tissue repair, leukocyte cell adhesion and endothelial migration during angiogenesis.[20]

1.2.2 Inflammation

Inflammatory cells, such as neutrophils and macrophages, are recruited to the wound site in response to chemotactic signals released from microorganisms, platelets, damaged tissue or signals generated during the activation of coagulation- and complement protein cascades.[21] Mast cells play an important role in the extravasation of leukocytes through the endothelium due to degranulation of histamine, enzymes and other active amines.[22] The granular content causes surrounding blood vessels to dilate and increase their permeability, thereby facilitating the extravascular accumulation of plasma proteins and extravasation of inflammatory cells. These events also give rise to the typical signs of inflammation, which are redness, heat, swelling and pain.

Neutrophils are among the first cells to arrive at the wound site and are the predominant cells during the first days of inflammation. Their main functions are to prevent infection by phagocytosis, to kill microorganisms and to break down foreign particles and damaged tissue. Phagocytosis is facilitated by recognition and attachment, engulfment, and subsequent degradation of the ingested material and is aided by complement (C3b) or immunoglobulin (IgG) opsonisation.[23] The internalised phagosome is fused with granules containing various proteases and antimicrobial substances that, together with production of reactive oxygen species (ROS), degrade the object. If compromised, these enzymes and oxygen metabolites can be released from the cells, with tissue injury as a result.[23,24] Neutrophils have a short life span (hours to days) and when their mission is fulfilled, the neutrophils

undergo apoptosis and are phagocytised by incoming macrophages or extruded as pus.[25]

Macrophages, recruited from the blood as monocytes, gradually replace the neutrophils in the wound site. The monocytes differentiate into macrophages of different types depending on the signals present in the surroundings. Macrophages have multiple roles in wound healing. They are highly phagocytic and clear cellular debris, necrotic tissue and remaining bacteria from the wound site, which is associated with highly active proteases and pro-inflammatory mediators.[19,26] They also produce a large repertoire of cytokines and growth factors of importance for transition from the inflammatory phase to the proliferative phase of healing, recruiting fibroblasts and endothelial cells to the site.[27-29] Due to their diverse functions, a crude distinction is made based on the macrophage phenotype. Classically activated macrophages (M1) exert pro-inflammatory actions, eradicate invading microorganisms and promote a Th1 immune response, whereas alternatively activated macrophages (M2) are involved in debris scavenging, angiogenesis, tissue remodelling and resolution of inflammation.[26]

Lymphocytes enter the wound site at a later stage. The precise role of lymphocytes in wound healing is not clear, but has been suggested to be of regulatory nature.[28]

1.2.3 Proliferation and remodelling

The presence of macrophages in the wound is an indication that the proliferative phase is initiated. During the proliferative phase, the provisional fibrin matrix is replaced with granulation tissue consisting of extracellular matrix, macrophages, fibroblasts and numerous blood vessels. In response to growth factors such as platelet derived growth factor (PDGF), transforming growth factor-β (TGF-β) and basic fibroblast growth factor (bFGF), fibroblasts are stimulated to proliferate and migrate into the wound area where they synthesise, deposit and remodel the extracellular matrix.[27] The formation of new blood vessels, angiogenesis, is stimulated in response to vascular endothelial growth factor (VEGF), TGF-β, bFGF as well as local factors in the wound microenvironment.[19] Re-epithelisation of the wound includes proliferation and migration of epithelial cells at the margin of the wound, extending in between the newly formed granulation tissue and the fibrin clot.[27]

Once the granulation tissue is formed, some fibroblasts will transform into myofibroblasts and contract the wound. The maturation of granulation tissue to scar tissue is associated with ceased angiogenesis and reduced amount and activity of fibroblasts and macrophages.[27] Fibroblasts will start to remodel the matrix and type III collagen, synthesised at high levels during the initial phase of wound healing, is gradually replaced by type I collagen, the dominant collagen type in native skin. The

tensile strength of a wounded area will never reach the same breaking strength as uninjured tissue, but will increase during the remodelling phase as a result of increased cross-linking between collagen molecules and formation of larger collagen bundles.[27]

1.3 Biomaterials in soft tissue

When a biomaterial is introduced into soft tissues it is generally associated with a certain degree of tissue damage and a wound healing response is initiated in order to restore homeostasis. However, the presence of an abiotic, non-self material affects this process. Normal host responses to an implanted material include protein adsorption, acute inflammation, chronic inflammation, granulation tissue formation and fibrosis, i.e. formation of a fibrous capsule around the material. An outline of the sequential and overlapping events including cell types is shown in **Figure 2**, whereas a schematic drawing of the events at the implant surface is shown in **Figure 3**.

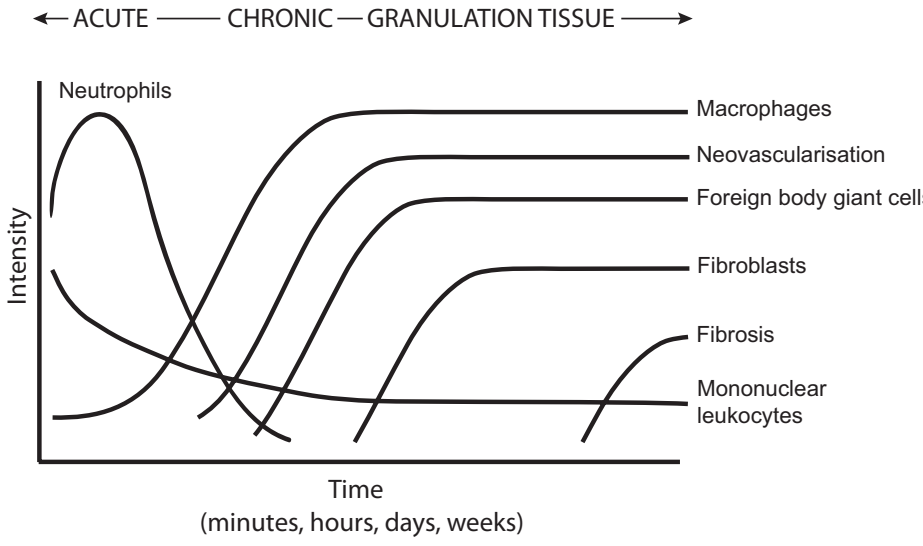

Figure 2. The temporal variation in the acute inflammatory response, chronic inflammatory response, granulation tissue development and foreign body reaction to implanted biomaterials. Adapted from Anderson.[30]

1.3.1 Protein adsorption

Protein adsorption to surfaces is a complex phenomenon which is influenced by surface chemistry, surface topography, surface charge, hydrophilicity, hydrophobicity, solvent effects and protein composition.[31-33] For example, the specific curvature of surface nanofeatures changed the conformation of fibrinogen and albumin upon adsorption.[34] This nanotopographical effect was however weaker than that produced by hydrophobicity. Protein orientation and conformational changes upon surface adsorption alter the peptides exposed to cells and, as a consequence, influence the cell response.

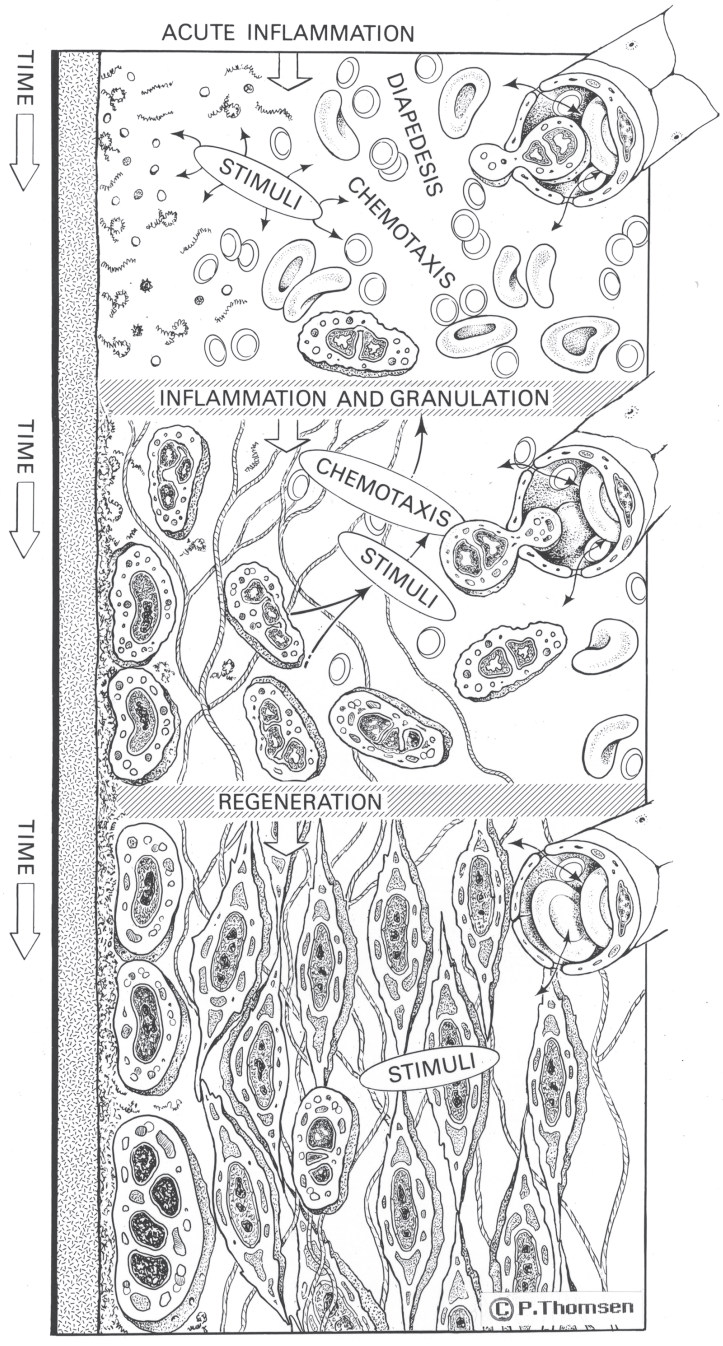

Figure 3. Schematic drawing of the healing events around an implant in soft tissue. Printed with permission from P. Thomsen.[35]

Although the interaction between surface-adsorbed proteins and cells is likely to be of paramount importance for early tissue responses to biomaterials, very little information is available on protein adsorption to biomaterial surfaces *in vivo*. A comparison between *in vitro* and *in vivo* experiments indicated different deposition patterns on titanium and calcium phosphate surfaces.[36] After introduction of an implant into the body an instantaneous protein adsorption will occur on the material surface. The injury of vascularised tissues will result in activation of the extrinsic and intrinsic coagulation systems, the complement system, the fibrinolytic system, the kinin-generating system and platelets.[37] Proteins derived from these systems, together with other plasma proteins (e.g. albumin), will form a conditioning film on the implant surface and constitute the basis of a provisional matrix on and around the biomaterial. It is with these proteins that the cells and possible microorganisms will interact. Rosengren *et al.* detected a protein and cell rich fluid space containing albumin, fibrinogen, immunoglobulin and complement factor 3 (C3) by using titanium implants inserted into the abdominal wall of rats.[38,39] The proteinaceous and fibrin-rich interfacial zone acts like a provisional scaffold for cell migration and adhesion and is subsequently replaced by matrix secreted by fibroblasts.[40]

1.3.2 Inflammatory response to implanted materials

The acute inflammatory response to an implant is characterised by the exudation of fluid and plasma proteins from the blood vessels and the infiltration and accumulation of leukocytes in the tissue.[30] Leukocytes migrate from the blood vessels, via extravasation through the endothelium, to the site of injury in response to chemotactic factors. Both the surgical trauma and the presence of a biomaterial give rise to production of chemotactic mediators.[37] At the early stages of acute inflammation there is a predominance of polymorphonuclear cells (PMN), particularly neutrophils. The assembly of macrophages at the implant site further propagates the chemotactic signalling, which recruits even more macrophages, and results in a shift towards a higher proportion of mononuclear cells in the exudate.[30] One of the major functions of both neutrophils and, at a later stage macrophages, is the removal of microorganisms, damaged tissue and foreign objects. However, the presence of a non-phagocytosable material, i.e. an object too large to be engulfed by the phagocytes, may result in extracellular release of granular content as well as generation of ROS at the material interface in an attempt to degrade the foreign object.[41,42] This kind of frustrated phagocytosis may have detrimental effects for materials that readily undergo degradation and/or corrosion. It also causes damage to the tissue surrounding the material and recruitment of more inflammatory cells to the site. It has been suggested that another consequence is an inferred inability to combat incoming pathogens since the cells are exhausted, resulting in a compromised immune defence around the implant.[4]

After the predominance of neutrophils, the shift towards mononuclear cell dominance with monocytes, macrophages, lymphocytes and plasma cells, is characteristic for the chronic inflammatory response. As for normal wound healing, macrophages are key players in inflammatory events as well as repair and remodelling around the implant due to the large repertoire of molecules that they produce. Macrophages also have a decisive role in the development of the adaptive immune response, although the role of lymphocytes at the implant site remains to be elucidated. Since the presence of a non-degradable biomaterial will continue to constitute an inflammatory stimulus for the cells, all implants are associated with some degree of chronicity. The chemical and physical properties of a material, but also the mobility of the material in the implant site, may produce chronic inflammation.[30]

1.3.3 Tissue repair and fibrous capsule formation

The healing response to an implant is initiated already during the initial inflammatory response, where platelets and recruited macrophages release a wide variety of chemokines, cytokines and growth factors. Some of these soluble mediators stimulate the migration, proliferation and activation of repair cells such as fibroblasts and endothelial cells. Endothelial cells are responsible for the process of angiogenesis, whereas fibroblasts synthesise, deposit and organise new tissue matrix and exchange the provisional protein matrix with granulation tissue.[27] A granulation tissue consisting of extracellular matrix, macrophages, fibroblasts and varying amounts of capillaries is typically formed. In addition, the presence of one- to two cell layers of macrophages and foreign body giant cells (fused macrophages) at the surface is a common feature of implanted materials.[30,43] This is sometimes referred to as the foreign body reaction. The end result of the soft tissue repair is often fibrous encapsulation of the implant, which may adventure the function of the implant. This response may be interpreted as a way of shielding the body from the implanted material. The mechanism for the fibrous encapsulation is not fully understood, but different material properties such as porosity,[44,45] topography,[46-49], chemistry[46,50] as well as implant mobility[48,51] have been suggested to affect cell behaviour and the end-stage healing response to an implant.

1.3.4 Cell–material surface interactions

Various research groups have evaluated the inflammatory and cytotoxic potentials of different implant surfaces *in vitro*. Implant surfaces prepared from different materials and with different processing techniques possess a wide range of surface characteristics such as chemistry, charge, hydrophilicity/hydrophobicity and topography. Below follows a brief review of selected cell types and their responses to surface chemistry and surface topography.

Inflammatory cells

Different inflammatory cell types interact with the implant surface and its adsorbed proteins. In fact, depending on the scientific question, a large number of *in vitro* studies have addressed the interactions between individual types of inflammatory cells and different materials (both as solid substrates and as particulates). By virtue of their versatility and longevity at the implant surface *in vivo*, macrophages are often recognised as the most important cell in determining the fate of an implant. With its large repertoire of secreted chemokines, cytokines and growth factors it has the potential to influence several other cell types and are thought to orchestrate the healing events around implants (reviewed in Anderson 2008[37] and Thomsen & Gretzer 2001[52]).

Effects of chemistry

Several *in vitro* studies have demonstrated that different surface chemistries elicit distinct effects in the behaviour of monocytes/macrophages, most commonly analysed by measurement of secreted cytokines. For example, monocytes on smooth titanium up-regulated the production of several cytokines, including macrophage inflammatory protein (MIP)-1α, MIP-1β, interleukin 6 (IL-6), IL-10 and IL-12, compared with smooth glass and polycaprolactone (PCL) after 48 hours.[53] After 24 and 48 hours, higher levels of tumour necrosis factor-α (TNF-α), IL-1β and IL-6 were detected in human monocyte cultures on titanium alloy (Ti6Al4V) and cobalt-chrome (CoCr) compared with polyethylene (UHMWPE) and polystyrene, but no difference due to polyethylene crosslinking was observed.[54] Bhardway *et al.* demonstrated a time dependent secretion pattern of TNF-α, IL-8, IL-10 and granulocyte-macrophage colony-stimulating factor (GM-CSF) of monocytes on different polymers, with polystyrene causing a relatively weaker inflammatory response than silicone, polyurethane and Teflon.[55] The effect of increased hydrophilicity of microrough titanium resulted in a general down-regulation of pro-inflammatory cytokine genes (significant for TNF-α, IL-1α, IL-1β and monocyte chemoattractant protein (MCP)-1) after 24 hours using a murine monocyte cell line.[56] The same study, in contrast to Ainslie and co-workers,[53] showed a reduction in pro-inflammatory gene expression of cells on polished titanium versus cells on glass. During the first 48 hours human monocytes on titanium produced more TNF-α as well as IL-10 compared with copper, and were associated with fewer apoptotic and necrotic cells.[57] In a study by Gretzer *et al.* both titanium and polystyrene gave rise to higher TNF-α levels than polyurethane urea (PUUR), which coincided with a higher proportion of apoptotic or necrotic cells on titanium and polystyrene using non-stimulated human monocytes.[58] Stimulation with lipopolysaccharide (LPS) increased cell viability on all materials and resulted in higher TNF-α levels on polystyrene and PUUR in comparison with titanium. In addition, immersion of titanium and zirconium implants in blood for up to 24 hours resulted in a higher up-regulation of

genes for IL-8 and IL-8R on titanium compared to zirconium.[59] This behaviour was not affected by LPS-stimulation.

Effects of topography

Human monocytes have been shown to produce more inflammatory cytokines and higher levels of ROS when grown on microscale silicon compared with nanoscale or smooth silicon.[60] Likewise, human monocytes secreted more IL-1β and expressed higher levels of several pro-inflammatory cytokines and chemokines (e.g. IL-1β, IL-6, TNF-α, MCP-1, MIP-1α) when adherent to rougher expanded polytetrafluoro-ethylene (PTFE).[61] Microroughening of titanium resulted in an up-regulation of several inflammation-associated genes.[56] Using a murine macrophage cell line, Khang *et al.* demonstrated higher cell density on micron and submicron alumina (Al_2O_3) compared with nanotextured alumina and smooth glass.[62] The cells were rounded on all alumina surfaces, whereas more spread on glass. However, no functional assessment of the cells was performed. Wojciak-Stothard *et al.* cultured murine cell line macrophages on microfabricated grooves and steps, 30-282 nm deep and 2 or 10 μm wide.[63] The macrophages were shown to align along the grooves, with an increasing degree of orientation, with an increasing depth and with a decreasing width of the grooves. Groove depths of 70 nm or more stimulated the cells to increase their initial adhesion and to phagocytise more beads compared to smooth control surfaces.

The effect of nanotopography on inflammatory cells *in vitro* is presented from selected references in **Table 2**. Nanotopographic features (nanotubes or nanowires) on titanium, glass and PCL showed less inflammatory response in human monocytes compared with their smooth counterpart, as revealed by less inflammatory cytokines, less ROS production and more rounded morphology.[53] Similar results were obtained on a variety of titanium nanotopographies using a murine macrophage cell line.[64,65] Reduced TNF-α levels as well as an increased ability to quench free radicals were seen on titanium nanotubes with a diameter of 70 nm compared to non-modified titanium, whereas other nanotube diameters (30, 50 and 100 nm) had an intermediate effect.[66] Furthermore, studies on alumina with pores of either 20 or 200 nm revealed more spread and active monocytes, with higher TNF-α and IL-1β levels, on 200 nm compared with 20 nm structures.[67] On the contrary, human neutrophils on the same surfaces appeared morphologically much more active on the 20 nm pores,[68] suggesting that nanotopographic features affect different cell types to varying degree. However, other studies have failed to show an effect on inflammatory cells based on nanotopography.[60,69]

Table 2. Selected in vitro studies of monocytes/macrophages on nanotopography

Chemistry, feature size	Cell type	Time	Adhesion, morphology	Activity	Ref
Titanium Nanosized protrusion (rms=4.8) Smooth (rms=0.4)	Mouse macrophage cell line (J774A)	5, 12, 24, 28 h	More rounded cells on nano (5 h) Cells migrated longer distances with higher speed on smooth	Less iNOS (24 h) and NO production (48h) on nano Lower TNF-α and IL-1β mRNA levels (12 h) on nano	[64]
Tantalum oxide Nanobumps with diameters of 15, 58, 95 and 212 nm Smooth control	Primary mouse peritoneal macrophages	72 h	Cells spread more on 10 and 50 nm and less on 100 and 200 nm compared with smooth surfaces More viable cells on 50 nm Lost cytoskeleton organisation on 100 and 200 nm	TNF-α mRNA higher on 50 nm IL-6 mRNA higher on 200 nm Slow increase in IL-10 with increasing nanostructure diameter No difference in MCP-1 and MIP-1α	[70]
Titanium, glass, PCL Nanotubes (70 nm) or nanowires (40 or 196 nm)	Human blood monocytes	48 h	More rounded cells on nano for all surface chemistries Rounded cells also on smooth Ti but spread on smooth glass and PCL	Less cytokines on nano, depending on material (IL-1β, IL-6, IL-10, IL-12, TNF-α, MIP-1α, MIP-1β, IFN-γ) Lower ROS on nano vs. smooth Ti	[53]
Titanium Nanotubes (d=40–70 nm), nanotextured, conventional	Mouse macrophage cell line (IC21)	24 h	Reduced adherence and more rounded cells on nano compared with conventional Ti		[65]
Titanium Nanotubes (30, 50, 70, 100 nm), conventional	Mouse bone-marrow derived macrophages	24 h	Generally more cell adhesion on nano More spread cells on 50-100 nm, whereas more filopodia extensions on 30 nm and conventional Ti	Less TNF-α production on nano (significant for 70 nm nanotubes)	[66]
Titanium 110 nm high hemispherical protrusions of varying coverage Smooth control	Human blood monocytes	24 h, 7 d	Similar cell adhesion on all surfaces Rounded cells on all surfaces	Similar IL-1β and TNF-α production on all surfaces	[69]
Alumina 20 and 200 nm pores	Human blood monocytes	24 h	More adherent and rounded cells on 20 nm	More IL-1β and TNF-α production on 200 nm	[67]

Fibroblasts

Fibroblasts are abundant cells in soft tissues. They play a critical role in wound healing and are responsible for the fibrous capsule formation around many implanted materials. *In vitro* fibroblast cultures can be used for initial screening of various surface modifications to assess cytotoxicity. Some research groups are using fibroblasts for morphology studies, e.g. contact guidance, whereas others are analysing fibroblast behaviour on surfaces to assess possible properties of the material on fibrous tissue growth on and around the implant *in vivo*.

Effects of chemistry

Fibroblast cultures are often used as a first measure to assess biological toxicity or cytocompatibility of materials and material modifications. A human fibroblast cell line showed similar morphology and proliferation between 1 and 10 days when cultured on titanium, stainless steel and the titanium alloy Ti6Al7Nb.[71] However, when comparing the standard titanium with standard Ti6Al7Nb, which both have rough surfaces, it was found that fibroblast proliferation was inhibited on the Ti6Al7Nb surface, demonstrating non-cytocompatibility. Another study found equal fibroblast viability on polyethylene glycol (PEG), silicone (PDMS) and paylene C, all materials used for coating of bladder sensors.[72] Wrzeszcz *et al.* aimed to inhibit fibrosis over a cochlear implant and designed a dexamethasone-releasing hydrogel coating that was subsequently tested in fibroblast cultures.[73] Test results showed a highly significant reduction of fibroblast proliferation after 7 days. On the contrary, a study investigating different degree of polydimethylsiloxane (PDMS) crosslinking found an optimal molecular mobility for cured PDMS that allowed the best cell attachment and proliferation.[74]

Effects of topography

Fibroblasts have been extensively used for investigations of surface topography, in particular with respect to cell adhesion and morphology. In general, fibroblasts show alignment along grooves and ridges.[75-77] Nanoscale topography produced by silica nanoparticles (diameter 7, 14 and 21 nm) had a pronounced effect on cell spreading and was associated with round, easily detached and non-proliferating murine fibroblasts compared with smooth control surfaces.[78] Also nanosized pits with a diameter of 35, 75 and 120 nm reduced fibroblast adhesion.[79,80] Using polymer demixing of polystyrene and polybromostyrene to produce nanometric islands with height differences of 13, 35 and 95 nm, Dalby *et al.* demonstrated an increased fibroblast spreading and proliferation on 13 nm islands compared with smooth control surfaces, whereas reduced spreading was seen on 95 nm islands.[81] The 13 nm islands promoted increased initial and long-term adhesion[82] and were shown to up-regulate several genes related to cell signalling, proliferation, cytoskeleton and production of extracellular matrix proteins.[83]

1.3.5 Tissue–material surface interactions

In vitro models are often superior to *in vivo* models to study the details of cell–implant interactions, but studies in the more complex *in vivo* environment are important for increasing our understanding of inflammation and repair/regeneration at implant surfaces. Several surface properties of a material may influence the biological response, such as chemistry, microstructure, topography, surface energy, implant shape and contaminations.[35] It is important to keep in mind that the animal species and the implantation site play an important role in the determination of biocompatibility. Furthermore, it is also important to state that the fibrogenic response may be the most important factor for long-term function, e.g. overgrowth of connective tissue at sensor surfaces or openings of catheters, since it markedly reduces the functional performance.

Effects of chemistry

The soft tissue reactions to biocompatible materials, exemplified by titanium, have been correlated to an early (12–24 hours) and transient leukotactic response, predominance of mononuclear cells in exudates and an early but transient production of pro-inflammatory cytokines (IL-1α, TNF-α, IL-6).[84-86] On the contrary, cytotoxic materials, exemplified by copper, induced a high and extended leukotactic response with predominance of neutrophils in exudates, high degree of cellular damage and high and persistent secretion of pro-inflammatory cytokines.[84-86] Copper also induced the formation of a thick and dense fibrous capsule, containing a large amount of inflammatory cells, whereas titanium gave rise to a thinner, more well-organised capsule.[50] Titanium and Ti6Al4V did not reveal any differences neither with respect to cell types and numbers at the interface, nor fibrous capsule thickness, after 1–12 weeks.[87] Comparing titanium to polymer materials, inflammatory cells were more frequently associated with PTFE than titanium.[40,88] In addition, a thicker fibrous capsule was found around PTFE compared with titanium after 12 weeks in the abdominal wall of rats.[89] The effect of hydrophilicity/hydrophobicity was investigated on hydroxyl- or methyl-functionalised gold surfaces. The results showed that the chemical surface properties influence early (1–7 days) inflammatory cell recruitment and distribution, with fewer cells on the hydrophobic implants, but not at a later stage (28 days), when similar fibrous capsules were found.[90,91] Furthermore, the cells adherent to hydroxyl-functionalised gold mounted a higher oxidative response (H_2O_2) in response to phorbol myristate acetate (PMA) than methyl-functionalised gold and unmodified gold implants after 3 and 24 hours of implantation.[90]

Effects of topography

In vivo experiments have shown that the topography of an implant influences the soft tissue reactions. Rosengren and co-workers showed an increased capsule thickness

around smooth compared with coarse (10−−50 μm surface irregularities) polyethylene after 1, 6 and 12 weeks of implantation.[47,48] In one of the studies this correlated with a higher amount of newly recruited macrophages around smooth implants,[47] whereas in the other with a higher number of dead cells around the implant after 1 week.[48] It was suggested that mechanical shear at the interface (which was assumed to be higher around smooth implants) could be an initiator of cell necrosis at the implant site, which in turn stimulates the recruitment of additional leukocytes and results in a thicker fibrous capsule.[48] However, the relationship between increased surface roughness and reduced capsule thickness is not straightforward, as demonstrated by Ungersböck *et al.*[92] In addition, microgrooved implants gave rise to thicker capsules, whereas implants with random microscale roughness yielded thinner capsules compared with smooth implants.[46]

The porosity of an implant also influences the tissue response and the fibrous encapsulation. Porous materials often heal in a less fibrotic manner compared with smooth materials.[44,45] Porous polymer scaffolds with a uniform pore size diameter of 30–40 μm have been shown to have a high macrophage infiltration, high vascularisation and good healing properties.[93] Bryers *et al.* hypothesized that the large number of macrophages in the pores are ultimately directed towards a regenerative phenotype (M2), which can explain the improved healing around these implants.[93] For example, an increased proportion of macrophages expressing markers of alternative activation (M2) have been observed for these implants after 4 weeks of implantation.[45] In contrast, a recent study by Sussman *et al.* demonstrated a shift towards the pro-inflammatory phenotype (M1) inside the pores as well as on the outer implant surfaces, whereas M2-macrophages to a higher degree were present in the fibrous capsule.[94]

The effect of nanotopography has been evaluated with respect to soft tissue response. Titanium implants modified with TiO_2 nanotubes showed significantly reduced capsule thickness after 1 and 6 weeks, which was coupled to a higher nitric oxide scavenging effect of the modified surface.[49] Although the scavenging effect of titanium is most likely related to the increased surface area when using nanoscale modification, this result underscores the fact that nanoscale topographical surface modifications also result in a change of other properties such as charge, conductivity, porosity, wettability, friction as well as physical and chemical reactivity,[95] making it difficult to exclusively study the effect of an individual surface parameter.

1.4 Bone healing

Bone is one of few tissues in the body with the capacity to regenerate without forming a fibrous scar. Bone healing is comprised of a complex, overlapping sequence of biological events involving a variety of cell types, molecular mediators and extracellular matrix. Depending on the extent, location and stability of an injury, bone can heal either with direct apposition of new bone matrix in the defect (intramembranous bone formation), or indirectly, via the formation of cartilage (endochondral bone formation). These two processes often take place in parallel and will eventually result in the regeneration of the bone structure to its original shape.[96] The different phases of bone healing are outlined below.

1.4.1 Haemostasis and inflammation

When an injury occurs, the vasculature is damaged with subsequent blood loss and formation of a blood clot (haematoma). The blood clot is mostly comprised of aggregated platelets and polymerised fibrin molecules, but also of bone marrow cells. It serves as a source of signalling molecules, such as PDGF and TGF-β, and as a provisional matrix forming a template for callus formation.[97] Inflammatory cells are recruited to the site of injury and further propagate the inflammatory response, which peaks within 24 hours and usually is resolved within 7 days.[98,99] Important cytokines and growth factors during this phase include TNF-α, IL-1, IL-6, PDGF, TGF-β, VEGF and bone morphogenetic proteins (BMPs).[100] These mediators facilitate the recruitment of additional inflammatory cells, recruitment, proliferation and differentiation of mesenchymal stem cells towards the chondroblastic and osteoblastic lineages, and also promote angiogenesis.[101-104] Over time, capillaries grow into the clot which is reorganised into a fibrin-rich granulation tissue.[105]

1.4.2 Soft callus formation

Most bone injuries are associated with mechanical instability, promoting healing via formation of an intermediate cartilaginous callus, also known as a soft callus. The soft callus forms within the haematoma-derived granulation tissue and connects the fracture ends of the bone, thereby providing stability to the fracture.[98] This pathway of bone healing is called endochondral bone formation.

Mesenchymal stem cells attracted to the injury site form early mesenchymal condensations, within which cells differentiate into chondroblasts.[106] The chondroblasts are subsequently stimulated to proliferate and synthesise a type II collagen-rich cartilaginous matrix. These cells become progressively embedded within their own matrix, thus changing phenotype into chondrocytes. Once the granulation tissue is replaced, the chondrocytes undergo an additional phenotype shift and become large, hypertrophic chondrocytes, responsible for the

mineralisation of the surrounding matrix.[107] Hypertrophic chondrocytes also secrete factors that attract blood vessels, haematopoietic cells and osteoprogenitor cells, thus directing bone cells to invade and replace the newly formed cartilage.[106]

1.4.3 Hard callus formation

Hard callus formation refers to the formation of woven bone, either through replacement of the cartilaginous soft callus or by direct, intramembranous, bone formation in the absence of a cartilaginous template. The majority of bone injuries involve some level of intramembranous bone formation, originating from the interior lining of bone structures.[107]

The formation of a hard callus represents a very active period of osteogenesis, characterised by high levels of osteoblast activity and formation of mineralised bone matrix. While cartilage is essentially avascular, the formation of bone requires adequate blood supply and is dependent on revascularisation. The transition from the soft callus to new bone formation is a crucial step in the repair process and involves coordinated events of chondrocyte apoptosis, cartilaginous matrix degradation and removal, vascularisation and osteogenic cell recruitment, differentiation and bone matrix production.[108] TNF-α initiates chondrocyte apoptosis as well as cartilage resorption, and promotes the recruitment of mesenchymal stem cells.[100] However, the regulation of matrix resorption is linked to receptor activator of nuclear factor kappa B ligand (RANKL) and macrophage colony-stimulating factor (M-CSF).[108] The matrix resorption takes place in parallel with recruitment of more mesenchymal stem cells which differentiate into osteoblasts and form woven bone. Both osteoblasts and hypertrophic chondrocytes express high levels of VEGF, thereby promoting the invasion of blood vessels into the newly formed bone.[109] As the hard callus formation progresses and the calcified cartilage is replaced with woven bone, the callus becomes more solid and mechanically rigid.

1.4.4 Bone remodelling

The woven bone in the hard callus is a primitive bone type laid down rapidly by the osteoblasts. Although providing biomechanical stability to the injured site, woven bone is weaker and more flexible than normal, lamellar bone. In the final stage of bone healing the woven bone is exchanged to that of mature, lamellar bone.

The remodelling process is a coupled process between osteoclasts and osteoblasts. Osteoclasts, expressing RANK on the cell surface, become activated to resorb bone by binding to RANKL expressed by osteoblasts.[110] Osteoblasts also express osteoprotegerin (OPG), which competitively binds to RANKL and thereby prevents osteoclast activation.[111] Hence, the OPG/RANK/RANKL triad is important in the process of bone regeneration and bone remodelling. The remodelling phase is

believed to be orchestrated by IL-1 and TNF-α.[96,108] The osteoclasts, which are large multinucleated cells of haematopoietic origin, adhere to a mineralised surface and form a tightly sealed zone in which bone resorption proceeds by acidification and protease degradation. The resorption creates erosive pits on the bone surface, where osteoblasts are able to lay down new bone. Osteoblasts synthesise and secrete type I collagen, osteopontin (OPN), bone sialoprotein (BSP) and osteocalcin (OC), which form an osteoid. As the bone matrix takes form, mineralisation occurs and osteoblasts trapped within the bone matrix are phenotypically transformed into osteocytes. When the bone remodelling is finalised, the resulting regenerated bone is indistinguishable from that of normal, non-injured bone, with cortex or trabecular structures as well as a marrow.

1.5 Biomaterials in bone

Biomaterials introduced into bone have the unique opportunity to be totally integrated within the host bone tissue, given the right material characteristics. This ability was first discovered by Per-Ingvar Brånemark in the late sixties when elaborating with titanium chambers as means for intra-vital observations of the microcirculation. The discovery has strongly influenced the profession of dentistry and has given rise to an important medical device industry with applications such as oral implants, bone anchored hearing aids, amputation prostheses and tools to monitor implant–bone stability. The ability to integrate a material in bone, i.e. the ability of an implant to be surrounded and in close contact with living bone in order to withstand functional loading, is referred to as osseointegration. The biological events leading to osseointegration resembles those for normal bone healing via the intramembranous route, i.e. direct bone formation without intermediate cartilage formation. However, the modulatory role of material surface properties for the stimulation or inhibition of specific biological events is not fully understood.

1.5.1 Bone healing around implants

Bone healing around implants has been studied immensely during the last couple of decades. The reader interested in different aspects of osseointegration is referred to different reviews.[112-116] The introduction of implants in bone is inevitably associated with blood contact, both from damaged vessels in the soft tissue and from bone marrow, and results in an instantaneous deposition of proteins at the implant surface. Platelets within the blood become activated, aggregate and form a clot which is stabilised by the polymerisation of fibrin. The fibrin clot forms a three-dimensional provisional matrix filled with adhesive plasma proteins as well as cytokines and growth factors.[117] The inflammatory process at the bone–implant interface has not been well characterised, but is generally believed to be necessary for bone healing to be initiated. For example, both TNF-α and TGF-β1 have been implicated to be involved in the recruitment and/or the differentiation of mesenchymal stem cells and osteoprogenitor cells.[118,119] Experimental studies have indicated a peak in gene expression of IL-1β and TNF-α in cells adherent to the titanium implant surface at 1 and 3 days, respectively.[120] Moreover, ultrastructural studies of the titanium–bone interface in rabbits have demonstrated the presence of multinuclear giant cells at the implant surface for as long as 4 weeks after implantation.[121] The role of these cells is not known, but they gradually disappear when the bone–titanium contact increase.

Metabolically active osteogenic cells require a blood supply, thus angiogenesis is essential. The bone is formed by osteoblasts. Osteoblasts originate either from the differentiation of mesenchymal stem cells or from precursor cells lining the endosteal or periosteal surfaces, i.e. the surfaces around cortical or trabecular bone.[122] The new

bone is to a large extent formed from the existing bone in a direction towards the machined titanium implant, but also in the form of solitary islands inside the screw threads.[123] These islands are the result of mesenchymal stem cell condensation and subsequent differentiation to committed bone cells. Notably, these islands were separated from the titanium implant surface and then fused with bone trabeculae from the endosteum. The bone–implant interface zone was the last part to become mineralised, and this occurred via gradual deposition of bone mineral aggregates in the organic matrix in contrast to that seen in osteoid seams.[121] However, on implant surfaces with more complex topography or with an apatite-covered surface, a direct apposition of bone on the implant surface may occur.[124-127]

Upon installation, the primary stability of the implant is a requirement for successful healing.[128] The formation of woven bone around the implant provides the implant with secondary stabilisation, which is important as the primary stability declines upon resorption of dead bone tissue next to the implant due to surgical trauma and thermal necrosis.[129] In fact, an increased amount of bone in the bone–implant interface correlates with the stability of the implant as evaluated by torque tests.[130] The final phase of osseointegration is the remodelling of the rapidly deposited woven bone around the implant into more structurally organised and mechanically stronger lamellar bone. This remodelling includes the coupled action between osteoclasts and osteoblasts and the mechanical stress in the bone surrounding the implant. This process continues throughout the lifetime of the implant.

1.5.2 Cell–material surface interactions

In vitro cultures of osteoblasts or osteogenic progenitor cells, e.g. mesenchymal stem cells, on material surfaces are normally used to assess different aspects of bone formation such as adhesion, differentiation and matrix mineralisation. Today, *in vitro* studies are far less complex than the *in vivo* environment in which the implants are inserted, but they are useful for screening purposes as well as for providing insights into the mechanisms that lead to osseointegration.

Effects of chemistry

The effect of surface chemistry on attachment and differentiation between titanium and its alloys has been assessed with murine calvarial cells.[131] The results showed higher initial spreading and higher alkaline phosphate (ALP) activity on pure titanium and Ti6Al4V after 5 days of culture compared with TiNb30 and TiNb13Zr13. Another study by Lincks *et al.* showed higher differentiation of MG63 cells, a human osteoblast cell line, on titanium than Ti6Al4V with similar roughness.[132] Ti6Al4V stimulated the production of more extracellular matrix proteins and mineralised matrix by osteoblast-like cells than did cobalt-chrome-molybdenum (CoCrMo) and glass.[133] Murine mesenchymal stem cells showed higher

mineralisation on smooth poly-L-lactic acid than on smooth polystyrene.[134] The role of substrate hydrophilicity has been demonstrated in a study by Liao *et al.*, that showed increased osteoblast differentiation on hydrophilic silicone in relation to hydrophobic silicone.[135] Calcium phosphate coatings such as hydroxyapatite (HA) are commonly used due to their similarity with bone apatite. Higher levels of ALP activity and mineralised nodules were found on HA compared with titanium, with glass having intermediate levels.[136]

Effects of topography

Microgrooves (heights 0.5-1.5 μm) on poly-L-lactic acid or polystyrene have been shown to induce alignment and differentiation of rat bone marrow cells.[134] Microcolumns made on titanium did not influence osteoblast differentiation but revealed cell alignment.[131] MG63 cells cultured on titanium alloy (Ti6Al4V) with increasing micro-roughness supported less cell adhesion and less ALP activity, but increased production of OC, OPG, prostaglandin E2 and TGF-β1.[137] Similar results were obtained on pure titanium,[132] suggesting that roughness on the microscale is important for osteogenic differentiation. Synergistic effects of surface hydrophilicity and microscale topography were demonstrated in studies with murine cells on silicone with 30 μm pyramids, on which cells differentiated to a higher degree compared with its smooth counterpart.[135]

The introduction of surface nanotopographies has in general been shown to promote osteoblast cell adhesion and differentiation.[138,139] Some studies have reported an increased proliferation as well as an increased differentiation.[140-142] However, proliferation has also been linked to a decreased differentiation.[143] Interestingly, murine osteoblasts seeded on surfaces exhibiting a gradient of nanoparticles (diameter 70 nm) showed reduced cell adhesion and proliferation when the particle density was high.[144] Increased adhesion has been demonstrated for both progenitor cells and osteoblasts on a variety of materials such as nanophase materials,[145] nanotubes[142] and nanopores.[141,146] Osteogenic differentiation has also been shown to increase in response to a number of nanoscale features.[140-142,146] Furthermore, randomly distributed nanoscale features have been found to increase osteogenic differentiation of human mesenchymal stem cells.[147] In addition, 100–500 nm nodules on top of micro-pitted titanium surfaces showed enhanced osteoblast proliferation and differentiation up to 21 days compared to surfaces with only micropits.[148] These positive, topographically induced effects on bone cell differentiation have been regarded as more selective than the overall up-regulative action of dexamethasone (up-regulates all gene pathways), which is routinely used to induce osteogenic differentiation *in vitro*.[139]

1.5.3 Tissue–material surface interactions

There is a great interest for surface modifications of bone implants in order to optimise integration in both healthy and compromised patients. A number of studies have evaluated different surface chemistries and topographies, but the relative importance of chemical versus roughness properties for the cellular events in the bone–implant interface has not yet been elucidated.

Effects of chemistry

The *in vivo* bone response of titanium has demonstrated better integration (higher removal torque) than Ti6Al4V after 6 and 12 months in rabbit tibia,[149] but no significant differences between the materials were found based on morphological evaluation after 3 months in the same model.[150] Zirkonium has been found to have similar bone response as titanium after 1 and 6 months in rabbit tibia.[151] Gold, on the other hand, was associated with a markedly lower amount of bone and bone–implant contact, which may be related to the lack of an oxide layer on the gold surface.[151] A comparison between Ti6Al4V and CoCr implants revealed lower interfacial shear strength for CoCr, but no difference in bone–implant contact was present after 12 weeks of implantation.[152] The authors acknowledged the presence of more unmineralised bone in the interface of CoCr as one possible explanation for this result. Different types of calcium phosphate coatings, e.g. HA, have been applied to titanium to improve biocompatibility and to reduce the time for bone integration. HA-coated implants have shown increased bone–implant contact and higher interface strength as compared with titanium.[153,154] In addition, the thickness, microstructure, composition and roughness of the titanium oxide on the implant surfaces have been related to an altered bone response.[112] However, when modifying the surface chemistry, it is difficult to avoid topographical differences between materials caused by the modification techniques and vice versa.

Effects of topography

For bone implantation purposes there is general consensus that roughening of the implant surface leads to a stronger bone response.[113,155,156] For example, TiO_2-blasted screws and cylinders showed higher removal torque than machined titanium after 12 weeks in dog mandible.[157] TiO_2-blasting with specific size of the particles revealed increased bone–implant contact and removal torque for 25 and 75 μm particles compared with machined titanium.[158] On the other hand, blasting with 250 μm particles resulted in a reduced bone–implant contact compared with 25 μm particles after 4 weeks, demonstrating the advantage of a moderately rough over a highly rough surface texture.[159] Nevertheless, it has been suggested that microrough implants are biocompatible but have limited ability to directly affect the initial fate of the surrounding tissue.[138] This is proposed to be overcome with the use of nanoscale

modifications of the implants, which can alter the cellular and tissue responses and may improve osseointegration.

Many *in vitro* studies have suggested a beneficial effect of nanoscale topography for bone cell adhesion and mineralisation. Less evidence has yet been obtained from *in vivo* studies since it is difficult to keep the chemistry constant and vary the nanotopography. Moreover, most studies have a combination of microscale and nanoscale surface features. Recent studies applying intentional nanoscale surface modifications without altering the implant chemistry have demonstrated positive effects of titanium nanotopography on osseointegration (histology, ultrastructure and removal torque).[127,160,161] A hydrofluoric acid treatment of TiO_2-blasted titanium implants, resulting in 100 nm features on the implant surface, demonstrated higher differentiation of adherent cells as judged by gene expression of Runx2, ALP and BSP up to 7 days *in vivo*.[162] A similar treatment resulted in an increased bone–implant contact after two weeks in dog when compared to its microrough counterpart.[163] An increased bone–implant contact was also demonstrated for titanium and Ti6Al4V implants modified with discrete nanocrystalline deposition of calcium phosphate on top of the microstructure of the implants.[164] Similar results were obtained by Meirelles *et al.* by modifying very smooth titanium implants with nanoscale HA-particles.[165] When adding either HA nanocrystals or titania nanostructures to the same, smooth, titanium implants, a higher bone–implant contact was obtained with nano-titania after 4 weeks in rabbit tibia.[166] The authors suggested that bone healing was more dependent on the size and distribution of nanofeatures than on the chemistry. In contrast, there have also been studies that have failed to show a beneficial effect of nanostructures,[167,168] demonstrating the complexity of these studies.

In general, the difficulty to separate the biological effects of micro- and nano-topographical surfaces features from chemical surface properties is a major dilemma also during the critical interpretation of *in vivo* results. Another difficulty is to apply intentional nanoscale topographic patterns on the complex three-dimensional configurations of clinically used implants. A recent example of such a strategy, using a colloidal lithographic technique, was the successful application of nano-bumps with varying size on screw-shaped titanium implants.[169] The results of this study demonstrated a higher bone–implant contact for 60 nm sized bumps compared with larger bumps (120 nm) or machined control after 4 weeks of implantation in rabbit tibia. It is anticipated that the diameter, height, density and curvature of the nanostructures are related to one another. It is probably also important to control these parameters on the complex implant geometries and shapes used *in vivo*.

Another relevant aspect which has not been sufficiently investigated is the ability of the surrounding microenvironment to ”sense” the nanotopographical cues after the

initial repair phase. Moreover, from an application point of view the long-term safety and functional effects in both soft and hard tissues are important to evaluate.

1.6 Biomaterial-associated infections

1.6.1 Clinical perspective

Biomaterial-associated infections have been recognised as one of the main risks for failure of medical devices and represent the major cause of nosocomial infections.[170] The consequences of BAI can be devastating for the patient and often lead to the need for surgery and long-term treatment with antimicrobial agents, thus causing a major individual and societal burden and cost.[170,171] The prevalence of infections associated with a variety of medical devices is outlined in **Table 1** (section 1.1). The consequences of these infections vary depending on implant type and location. For example, urinary catheters have an infection risk of 10-100% depending on the length of catheterisation, but are attributable to low morbidity.[7] In contrast, aortic grafts are associated with infection rates of 2%, but infectious complications are lethal in almost 90% of the patients.[170] Furthermore, although mortality rates attributed to infections associated with certain devices are low, such infections can result in major morbidity and long-term hospitalisation.

From a treatment perspective, the most reliable way to eradicate BAI is by removal of the device followed by extensive antimicrobial regimens.[170,172,173] The removal of a device may result in tissue damage and lead to long-term morbidity and discomfort for the patient. In addition, re-implantation procedures have generally much higher infection rates compared with first time procedures,[8,174,175] since the tissue surrounding the implant can be infected, compromised, inflamed and possibly necrotic.[176] A two-stage procedure is therefore advisable where the infected device is removed, allowing healing of the surrounding tissue and eradication of the infection, before re-implantation of a new device. However, some applications do not allow a two-stage procedure, e.g. vascular grafts or left ventricular assist devices, necessitating single-surgery exchanges in contaminated tissue conditions.

Lately, the level of antimicrobial resistance in bacteria causing BAI has increased worldwide,[177] leaving infected patients with fewer treatment options. Hence, one of the main challenges with the use of medical devices is to prevent infection from occurring, and as far as possible, not contribute to the emergence and dissemination of resistant bacteria by the extensive usage of antimicrobial agents.

1.6.2 The causative agents

The microorganisms responsible for BAI are a variety of gram-positive and gram-negative bacteria and fungi (**Table 3**). Staphylococci, especially *Staphylococcus aureus* and *Staphylococcus epidermidis*, are the predominant species found at sites of BAI, accounting for about 66% of the infections.[170]

Table 3. Common microorganisms reported for various medical implants and devices

Implant or device	Bacterial/Fungal Species	Reference
Urinary tract		
Urinary catheter	*Escherichia coli*, enterococci, *Pseudomonas aeruginosa*, *Candida* species, *Klebsiella pneumoniae*	[7]
Percutaneous		
Ventricular assist device	*Staphylococcus epidermidis*, *Staphylococcus aureus*, enterococci, *Pseudomonas aeruginosa*, *Enterobacter*, *Klebsiella*, *Candida* species	[9]
Central venous catheter	*Staphylococcus epidermidis*, *Candida albicans*	[178]
Intravascular catheter	Coagulase-negative staphylococci, *Staphylococcus aureus*, gram-negative bacilli, *Candida albicans*	[173]
Suture	*Staphylococcus epidermidis*, *Staphylococcus aureus*	[178]
Airways		
Endotracheal tube	*Staphylococcus aureus*, *Streptococcus pneumoniae*, *Haemophilus influenzae*, *Proteus* species, *Serratia marcescens*, *Klebsiella pneumoniae*, *Esherichia coli*, *Pseudomonas aeruginosa*, *Acinetobacter* species, *Enterobacter* species	[179]
Soft tissue		
Pacemaker	*Staphylococcus aureus*, coagulase-negative staphylococci, streptococci	[180]
Mammary prosthesis	*Staphylococcus aureus*, *Serratia marcescens*	[181]
Penile prosthesis	*Staphylococcus aureus*, *Staphylococcus epidermidis*	[178]
Eye		
Contact lens	*Pseudomonas aeruginosa*, *Serratia marcescens*, coagulase-negative staphylococci, *Staphylococcus aureus*	[182]
Intraocular lens	*Staphylococcus epidermidis*, *Staphylococcus aureus*, *Enterococcus faecalis*, *Streptococcus pneumonia*, gram-negative bacteria, fungal species	[15]
Circulatory system		
Mechanical heart valve	*Staphylococcus epidermidis*, *Staphylococcus aureus*	[178]
Vascular graft	Gram-positive cocci	[178]
Bone		
Joint prosthesis	*Staphylococcus epidermidis*, *Staphylococcus aureus*, *Escherichia, Klebsiella*, *Proteus*, *Enterobacter*	[172]

It has been demonstrated that the presence of a medical device within the body significantly reduces the number of bacteria required to produce infection.[183,184] For example, in a subcutaneous model in guinea pigs a dose of 10^8 CFU *S. aureus* did not result in abscesses, whereas 10^2 CFU was sufficient to infect the animals in the presence of a biomaterial.[184] Neutrophils around the materials have been found to have decreased phagocytic and bactericidal activities as well as an increased bacterial adherence, suggesting a favourable environment for infections at implant sites.[184,185]

A common virulence trait is the ability to produce biofilm. The biofilm protects bacteria from opsonising antibodies, phagocytic uptake and significantly reduces their sensitivity to antimicrobial treatment,[4,6,186] making them difficult to eradicate. Poor antimicrobial penetration, slow bacterial growth and induction of biofilm phenotype, are factors that allow biofilm bacteria to tolerate much higher concentrations of antimicrobial agents compared with their planktonic counterparts, contributing to antimicrobial resistance development.[187-189] Among clinical isolates, biofilm-forming strains are also more frequently multiresistant to several antimicrobial agents compared with non-biofilm-producing strains.[189]

1.6.3 Gram-positive bacteria

Gram-positive bacteria differ from gram-negative by their thicker cell wall that surrounds the cytoplasm membrane. The cell wall of gram-positive bacteria is composed of multiple layers of peptidoglycan, a structure of repetitive sugar molecules linked via short peptide chains. Teichoic acid and lipoteichoic acid, two long anionic molecules unique for gram-positives, are often incorporated in the cell wall.

Host cell recognition

Gram-positive bacteria are detected by eukaryotic cells via different pathways: via direct recognition of conserved structures on the bacterial cell wall, or via opsonisation by host complement proteins or immunoglobulins.

The pattern-recognition receptors (PRRs) recognise evolutionary conserved structures on pathogens, the so-called pathogen-associated molecular patterns (PAMPs).[190] Toll-like receptor 2 (TLR2) on the host cell surface recognises peptidoglycan and lipoteichoic acid on the bacterial cell wall and plays a major role in the detection of gram-positive bacteria.[191] Studies in TLR2-deficient mice have shown decreased survival after infection with *Staphylococcus aureus* and *Streptococcus pneumonia* in comparison with wild-type mice,[192,193] demonstrating the importance of TLR2 in host defence against gram-positive bacteria. Furthermore, the endosome-bound TLR9, which recognises unmethylated CpG DNA,[194] and the cytoplasmic NOD2 and NALP1 receptors,[195,196] which both recognise the

peptidoglycan-derivative muramyl dipeptide, are involved in the recognition of gram-positive and gram-negative bacteria. For further details, the reader is referred to recent reviews on Toll-like receptors.[190,197]

Alternative ways of bacterial detection are via the complement system or via Fcγ-receptor recognition of IgG-opsonised bacteria, the latter as part of the humoral response against bacteria. The complement system has three major roles in the host defence against bacteria.[198,199] Firstly, the complement fragments C3b and C3bi function as relatively unspecific opsonins, thus aiding internalisation of bacteria by phagocytic cells. Secondly, C5a acts like a chemoattractant for phagocytic cells. Thirdly, C5b-9 forms a membrane attack complex (MAC) causing bacterial lysis. However, complement-mediated bacterial lysis is limited to gram-negative bacteria due to the thicker cell wall of gram-positive bacteria, but the MAC may have alternative roles for gram-positive bacteria since inhibitors that block MAC-formation have been found in *Staphylococcus aureus* and *Streptococcus pyogenes*.[198,200]

Staphylococcal virulence

The genus *Staphylococcus* comprises several species that are characterised by their round shape (diameter 0.5–1.0 μm) and their formation of grape-like clusters when they divide.[201] They are non-motile, non-spore forming, facultative anaerobes that are categorised based on their ability to produce coagulase.[202] *Staphylococcus aureus* is a coagulase-positive bacterium, whereas *Staphylococcus epidermidis* belongs to the coagulase-negative (CoN) group. *Staphylococcus aureus* colonises mainly mucosal surfaces, is more aggressive and often associated with early and acute infections, whereas the less virulent *S. epidermidis* is a commensal bacterium of the skin mainly involved in delayed or chronic infections.[203,204]

Staphylococcus aureus

Staphylococcus aureus is a virulent pathogen that can avoid host defence mechanisms and kill host cells by the secretion of toxins (reviewed by Foster[205]). It can express a variety of adhesins that interact with host extracellular ligands such as elastin, laminin, collagen, fibronectin, fibrinogen and bone sialoprotein.[206] *Staphylococcus aureus* has the ability to inhibit chemotaxis, block recruitment of neutrophils and compromise neutrophil access to bound complement and antibodies by formation of a polysaccharide capsule.[205,207] In addition, the ability to form biofilm is also likely to be important. This bacterium can avoid phagocytosis by several mechanisms, e.g. by binding of complement factors, cleavage of surface-bound C3b and IgG, by neutralisation of IgG and by becoming coated with fibrinogen. However, *S. aureus* can also trigger internalisation into many types of host cells via formation of a fibronectin bridge, where it can survive in a semi-dormant state.[208] Once inside of neutrophils, *S. aureus* can interfere with endosome fusion, resist the action of antimicrobial peptides (AMPs) and avoid lethal effects of oxygen free radicals, e.g. by

removal of O_2^{-}.[205,209] The aggressiveness of *S. aureus* is much attributed to the production of various toxins with cytolytic effects, such as enterotoxins, leukocidins and phenol-soluble modulins (PSMs).[210] Some toxins act as superantigens, which can alter the function of T-cells and induce immunosuppression.[205] This bacterium also produces an array of proteases and other tissue and cell component degrading enzymes, thus facilitating tissue destruction and spreading.

Staphylococcus epidermidis

Staphylococcus epidermidis possesses a wide range of virulence factors, many of them related to persistence by circumvention of host defence system mechanisms rather than aggressively attacking the host (reviewed by Otto[211,212]). For example, *S. epidermidis* has multiple genes for attachment, both to abiotic surfaces and to matrix proteins such as collagen, fibrinogen, elastin and others. Upon attachment, intercellular aggregation occurs as well as production of protective exopolymers, the so-called biofilm. The exopolymer poly-γ-glutamic acid (PGA) is crucial for *S. epidermidis* resistance to neutrophil phagocytosis and AMPs,[213] whereas the polysaccharide intercellular adhesin (PIA) protects from neutrophil killing, complement deposition, immunoglobulins and both cationic and anionic AMPs.[214,215] This bacterium has also the capability to degrade or avoid the action of antimicrobial peptides by a recently discovered antimicrobial peptide sensing system, causing up-regulation of AMP-defensive systems upon activation.[216] Moreover, a variety of proteases involved in degradation of fibrinogen and complement factor C5 and possibly tissue damage can also be produced by *S. epidermidis*.[211] The toxin production of *S. epidermidis* is mostly limited to PSMs. However, despite carrying genes for the very potent cytolytic PSMδ, *S. epidermidis* keeps its production at a very low level, reflecting a passive defence strategy compared to the use of aggressive toxins produced by *S. aureus*.[204]

Biofilm formation

The formation of biofilm is a surface-related phenomenon. Bacterial biofilms are defined as structured communities of bacterial cells enclosed in a self-produced polymeric matrix and adherent to inert or living surfaces.[178] The biofilm matrix consists of extracellular polymers such as polysaccharides, proteins and oligonucleotides, but does also contain large amounts of water.[217] The biofilm mode of growth causes genome-wide adaptations and includes down-regulation of basic cell processes such as nucleic acid, protein and cell wall synthesis.[218] Hence, the biofilm offers bacteria a protective environment that can withstand host immune responses and renders bacteria less susceptible to antibiotics compared with bacteria in the planktonic state.[4,6,219,220]

Both *S. aureus* and *S. epidermidis* are prominent biofilm producers and the molecular basis of biofilm formation in these species has been reviewed.[211,221] The general biofilm process is outlined in **Figure 4**. In summary:

1. In the human body, the first step of biofilm formation on a surface is the ***adherence*** to human matrix proteins by either specific or non-specific interactions.
2. Once attached, the ***accumulation*** phase starts and bacterial cells divide and express genes required for the synthesis of extracellular polysaccharide. The proteins encoded by the *ica*-operon (responsible for the production of PIA) play important but not absolute roles in staphylococci biofilm development.[222]
3. ***Maturation*** of the biofilm is characterised by intercellular aggregation and biofilm structuring, leading to a three-dimensional appearance with mushroom-like cell towers.
4. Lastly, detachment and ***dispersal*** of planktonic bacteria from the biofilm occurs, enabling spread of the infection to other areas.

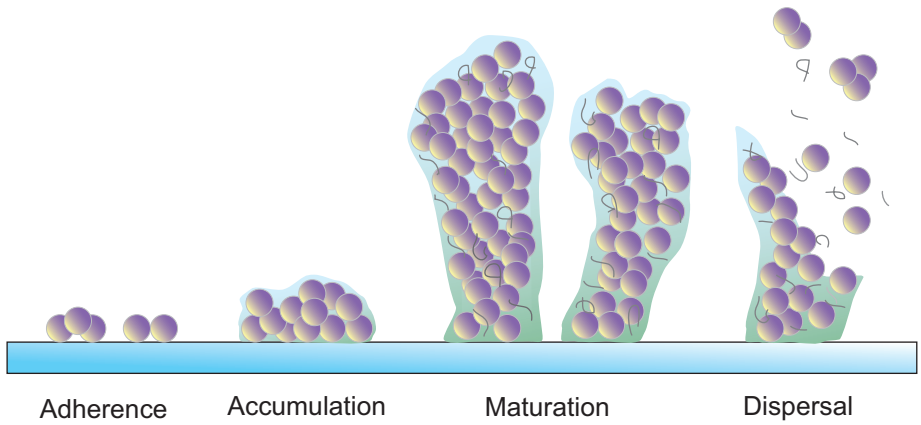

Figure 4. Schematic drawing of the biofilm process. Adapted from Otto.[221]

1.6.4 Bacteria–material surface interactions

Bacterial adhesion to a material surface is a complex process influenced by many factors, including the bacterial properties, the material surface characteristics and environmental factors such as the presence of serum proteins and flow conditions.[223] The process of bacterial adhesion includes two phases; one initial, instantaneous and reversible physical phase, followed by a time-dependent and irreversible molecular and cellular phase which involves biofilm formation.[224]

Primary attachment of bacteria to a material surface depends primarily on physicochemical interactions, i.e. hydrophobic and electrostatic interactions.[225] Thus, the hydrophobic and negatively charged cell wall of most bacteria results in increased attachment to hydrophobic or positively charged surfaces but in decreased attachment to hydrophilic or negatively charged surfaces.[226-229] The second phase of adhesion comprises molecular reactions between bacterial surface structures and the substratum and depends on the presence of specific bacterial adhesins to host proteins.[224]

Surface roughness, especially in the microscale, increases bacterial adhesion and biofilm deposition[230,231] as well as bacterial adhesion strength[232] compared with smooth surfaces. Moreover, bacteria seem to preferentially adhere to irregularities in the size-range of the bacteria itself, whereas grooves that are much larger and wider in size have more similarities with smooth surfaces.[223,231] Explanations for the increased bacterial attachment onto rough and porous surfaces can be the larger surface area available for bacteria interactions as well as crevices providing shelters for the bacteria in a flow environment. Long-term (7 days) bacterial attachment to titanium was shown to be directly related to surface roughness, with most bacterial cells on the rougher surface.[233]

The role of nanotopography on bacterial adhesion is less well studied. Due to the rigid cell wall of bacteria, the capability to deform upon attachment is limited, implying that they do not react to structures smaller than themselves.[234] Nevertheless, very small nanofeatures on glass have been shown to reduce attachment in eight different bacterial species in comparison to nanosmooth surfaces, of which *S. aureus*, *P. aeruginosa* and *E. coli* are relevant for BAI.[235,236] Nanorough titanium was shown to reduce attachment of *S. aureus*, *S. epidermidis* and *P. aeruginosa* compared to conventional titanium.[237] In contrast, nanotubular and nanotextured titanium showed increased attachment, both of live and dead bacterial cells.[237] However, it is difficult to conclusively determine that these results are solely due to nanotopography, mainly because of external factors in the fabrication process that may have an effect on the surface chemistry. Moreover, some studies have failed to show a relationship between nanotopography and bacterial adhesion, but demonstrated a major impact of the presence of serum proteins.[238]

In summary, both surface chemistry and surface topography influence bacterial adhesion and biofilm formation, but the relative importance of these factors is poorly understood. Furthermore, the environment into which the material will be placed and the subsequent protein adsorption will influence bacterial attachment sites. It has been suggested that a microtopography of specific size increases bacterial attachment, although the role of nanotopography for bacterial attachment remains to be elucidated.

1.6.5 Strategies for reducing biomaterial-associated infections

Most infections associated with medical devices arise as a consequence of the introduction of bacteria into the implant site during surgery or during the early postoperative procedure prior to wound healing. There is also a risk for haematogenous spread, i.e. spread of infection from another part of the body via the blood stream. The best strategy to prevent infection is to avoid colonisation of the device. Over the past decades, major improvements have been made concerning the hygiene in operation theatres, aseptic surgical procedures, preoperative antimicrobial prophylaxis and postoperative care, which altogether have reduced the infection rates.[172] Another important factor is the implant material, which can be engineered to counteract bacterial attachment and persistence on the device. Different surface modifications with different antimicrobial modes of action that can help prevent BAI are outlined in **Figure 5**.

Anti-adhesive surfaces

Anti-adhesive surfaces are likely to be of greatest relevance in temporary implant applications such as catheters, endotracheal tubes and contact lenses, due to their lack of tissue integration. Anti-adhesiveness can be obtained by changing the surface chemistry and/or topography, or by conditioning of the surface by pre-adsorbed molecules that either increase hydrophilicity, hydrophobicity or compete with the adsorption of host adhesins.[239] A clinically used example is the heparin coating, introduced to increase hydrophilicity of catheters and intraocular lenses, which has been shown to reduce bacterial adhesion.[240,241] Current approaches to achieve anti-adhesive properties often utilise self-assembled mono or multilayers, polymer brushes, surface grafting, zwitterionic polymers or hydrogels.[242-245]

Another clinically used example, that partly can be regarded as anti-adhesive, is noble metal coated devices. The coating is currently applied on urinary catheters, central venous catheters and endotracheal tubes (under clinical investigation) and has been shown to reduce infection rates with up to 50%.[7,246,247,248]

Bactericidal surfaces

Surfaces with bactericidal properties can differ in their mechanism of action. *Contact-killing* surfaces kill bacteria following direct interaction with the bacterial cell, whereas other *drug eluting* surfaces rely on leakage of antimicrobial substances. The benefits with the "killing-upon-contact" surfaces are the self-sterilising effect and long-lasting activity, but this effect may potentially be masked and inactivated by proteins adsorbing to the material surface.

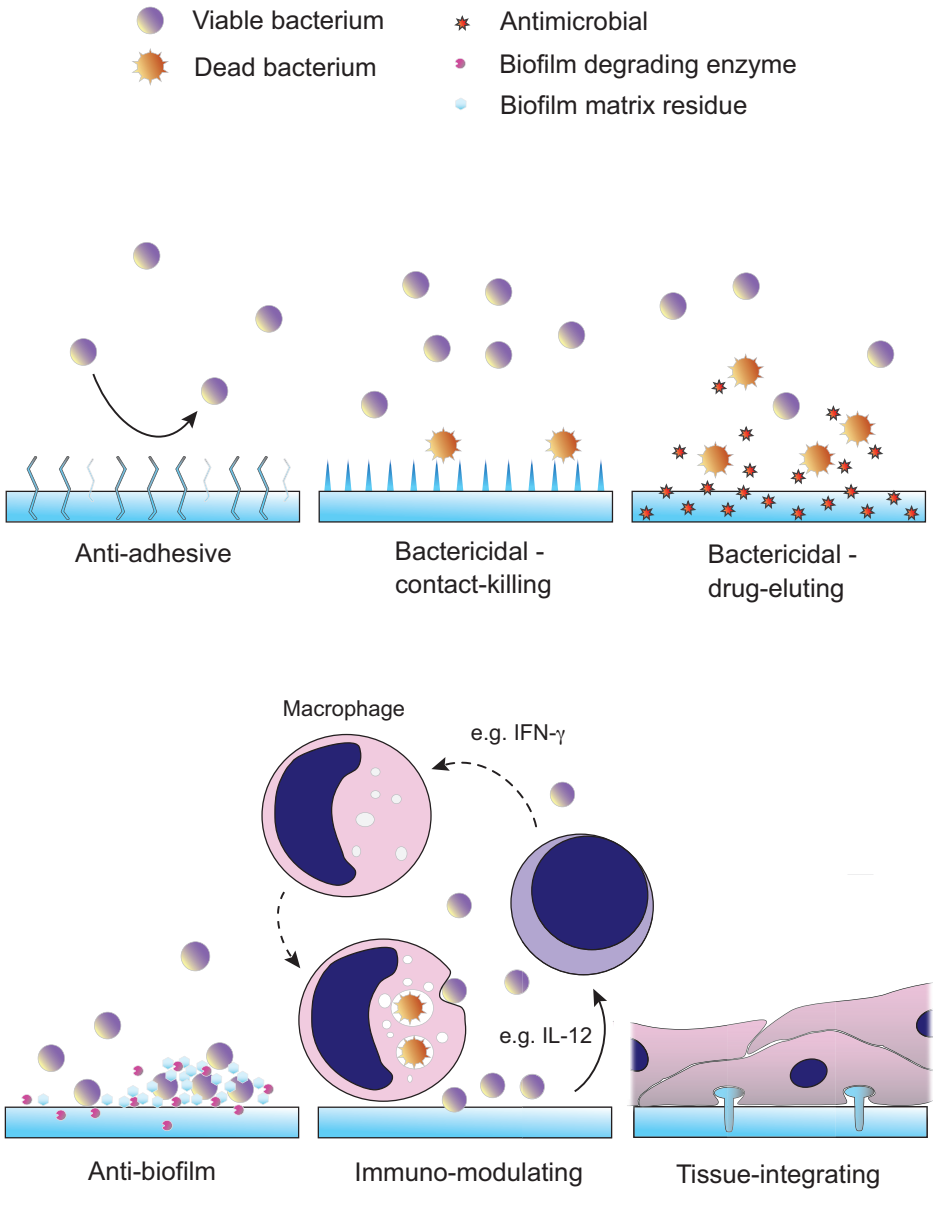

Figure 5. Schematic drawing of different strategies to reduce biomaterial-associated infections. Inspired from Busscher et al.[176] and Campoccia et al.[239]

The most clinically accepted methodology so far includes antibiotic-releasing surfaces.[176] Commonly, antimicrobial agents are applied to surfaces by grafting of antimicrobial molecules or by coating with single or multilayer films delivering antimicrobial molecules, e.g. triclosan, chlorhexidine, silver, antibiotics and AMPs.[249-253] Polymer coatings with functional groups that have bactericidal activity, e.g. tertiary amines and N-alamines, have also been used.[254,255] Other approaches utilise coatings with photo-induced bactericidal effect, e.g. titania (TiO_2) with or without silver,[256,257] or polymer coatings releasing nitric oxide or reactive oxygen species.[258,259] Lastly, nanostructured surfaces or coatings with nanostructured materials have been suggested as an alternative to reduce infection rates.[260-262] Nanostructures can be added both on the material surface and in the bulk material (such as chemical nanophase). Nanostructured materials as well as certain formulations of nanoparticles have shown strong antibacterial activity *in vitro*.[239,263] Due to the high surface-to-volume ratio in nanostructured materials, nanotechnology can also be used to enhance the antimicrobial action of photocatalytic surfaces or of surfaces releasing nitric oxide.[239] The role of nanostructures on a surface and as soluble particles for the fate of bacteria remains to be clarified. Furthermore, it is of importance to determine if nanostructures elicit toxic responses, e.g. in cells of the host defence and immune system.

Anti-biofilm surfaces

The growing knowledge of the molecular mechanisms involved in biofilm formation has enabled new opportunities to avoid bacterial colonisation on biomaterials. Substances that interfere with biofilm mechanisms and thereby attenuate the bacterial virulence may promote clearance of bacteria by host defence cells. These substances can either be grafted on implant surfaces or released by appropriate surface coatings.[239] Potential molecules with *anti-biofilm* capabilities include enzymes that degrade the extracellular substances of biofilm, e.g. dispersin B and rhDNase I,[264,265] that inhibit expression of biofilm genes, e.g. *N*-acetylcysteine,[266] that destruct cell wall or permeabilise cytoplasmic membranes, e.g. lysostaphin and AMPs,[267,268] or that target quorum sensing, e.g. furanones.[269] The use of these substances may be limited due to a rather narrow spectrum of activity, targeting only few bacterial species, but studies show promising synergistic effects combined with antimicrobial agents.[270,271]

Modulation of host immune system

Another approach to combat pathogens at the implant site is to *modulate the local immune system* of the host rather than directly counteracting bacterial colonisation. Macrophages are often found at sites of implantation and have a key role in host defence as well as wound healing.[19,37,52] Coatings with macrophage attracting molecules, e.g. MCP-1, or coatings that may induce bactericidal activity of macrophages, e.g. IL-12 or IFN-γ, can reduce infection rates *in vivo*.[272,273] Material

surfaces modified with antibody fragments against monocyte integrin receptors showed more adhesion, reduced cytokine production per cell and higher bacterial killing efficiencies when compared to surfaces modified with cell adhesion peptides (RGD) *in vitro*.[274] Thus, by the use of different signalling molecules on, or released from, a biomaterial surface, the inflammatory response can be directed by stimulating differentiation of monocytes into different phenotypes.[275] Thereby, by releasing molecules in multiple waves, the macrophages can be directed towards the classical microbe-killing phenotype (M1) directly after implantation, followed by a shift towards a wound healing and tissue regenerating phenotype (M2). A study using a murine model has shown the possibility to modulate the immune response also after an infection has occurred, thus enabling the clearance of surviving intracellular bacteria after administration of IFN-γ.[276]

Host tissue integration

Perhaps the best infection prevention strategy of all is to create a desirable integration of the implant in the tissue, leaving an uncompromised immune system to deal with incoming pathogens. However, since most BAI arise from contamination during surgery or wound closure, the implant is left unprotected. Then "a race for the surface" will start between bacteria and host tissue cells,[277] which may favour bacteria in the lack of additional protection strategies.[176] However, host tissue integration with establishment of a normal host immune response at the implant site would offer the best protection against infections via the haematogenous spread route, when antimicrobial coatings typically have lost their efficacy.

Implant surfaces may be tuned to promote cell and tissue adhesion by incorporation of cell adhesive motifs[278,279] or by means of micro- and nanotopography.[148,169,280] A challenge with these approaches is that the surfaces often facilitate bacterial adhesion too, since microorganisms use many of the same adhesive mechanisms as host tissue cells. This fact pushes the need for dual or multifunctional coatings that selectively encourage tissue cell attachment but at the same time impede bacterial adhesion or even kill microorganisms.[260,281-283]

Few of the modifications listed above have reached the clinic, partly because of the time-consuming and very costly clinical trials that need to be pursued. The most accepted strategies in the clinic involve heparin coated (anti-adhesive) catheters and lenses, silver-releasing catheters and wound dressings, as well as antibiotic-releasing implants of various kind (catheters and orthopaedic implants among others). However, a drawback of antibiotic-releasing implants is the difficulty in maintaining an acceptable concentration over a longer time (weeks), contributing to the burden of antimicrobial resistance. In addition, the type of antibiotics is important, especially after removal of infected internal devices, since intracellular bacteria may reside in the tissues at the site of infections.[284]

2 AIMS

The overall aim of the present thesis was to investigate cell and tissue responses to nanostructured noble metal coatings and to develop models and techniques to enable analysis of microbial–host defence interactions at the biomaterial–tissue interface.

The specific aims of the included studies were:

- To explore the role of different amounts and compositions of noble metals in the coatings for the inflammatory and fibrotic responses *in vivo*.

- To study and compare the bone response, both qualitatively and quantitatively, between noble metal coated titanium implants and clinically used, machined titanium implants.

- To investigate the role of surface nanotexture, without changing the surface chemistry, for bacterial adhesion and biofilm formation as well as for the behaviour of monocytes in response to microbial stimuli.

- To develop an *in vivo* infection model and to evaluate the initial effects of surface chemistry and nanotexture on biomaterial-associated inflammation and infection.

3 MATERIALS AND METHODS

3.1 Materials

Three types of materials with or without chemical and/or topographical modifications on the material surface have been used in the thesis. In three studies (paper I, II, IV), the implants were modified with a nanotextured noble metal coating consisting of silver (Ag), gold (Au) and palladium (Pd) and in one study (paper III), surfaces with immobilised gold nanoparticles were used. A summary of the different experimental surfaces can be found in **Table 4**.

3.1.1 Noble metal coating (paper I, II, IV)

The noble metal coating was applied to the implant surfaces of silicone (paper I) and titanium (paper II, IV) through the Bactiguard® proprietary surface technology (Bactiguard AB, Sweden). The coating procedure is a multi-step wet deposition process which involves dipping of the materials in several aqueous solutions in order to pre-treat and activate the surface for subsequent deposition of noble metals on the surface. The noble metal elements are deposited from solutions of metal containing salts, a reduction agent that reduces the salt to form the metallic noble metals and a deposition control agent that prevents metals from nucleating in the solution. The end result is a mixture of noble metal deposits consisting of Ag, Au and Pd that have formed a heterogenous nanopattern on the implant surfaces.

3.1.2 Silicone (paper I)

Silicone in the form of PDMS is a polymer that has been frequently used as a biomaterial in a broad spectrum of biomedical applications, including contact lenses, catheters and pacemakers.[285] In paper I, sheets of PDMS of 1 mm thickness were coated with five different combinations of the noble metals Ag, Au and Pd. Uncoated PDMS served as control. The sheets were then punched into disks with a diameter of 10 mm and sterilised by ethylene oxide.

3.1.3 Titanium (paper II, IV)

Titanium is a widely used implant material and is a common component of orthopaedic, dental and reconstructive implants due to its high strength-to-weight ratio, corrosion resistance and biocompatibility. In paper II, titanium (grade 1) was machined into screws, 4 mm in length and 3.75 mm in external diameter, for use in the bone study, in which noble metal coated and non-coated implants were compared.

Disk-shaped titanium (grade 2) implants with a diameter of 9 mm and a thickness of 2.2 mm were used in soft tissues (paper IV). Electropolishing was performed in order to obtain very smooth surfaces. Two thirds of the implants were modified with a noble metal coating, of which half were subsequently sputter-coated with a 5 nm thick layer of titanium in order to hide the noble metal chemistry but retain the nanotopography. This experimental setup enabled the analysis of the role of chemistry (noble metals versus titanium) and nanotopography (nanostructured versus smooth).

3.1.4 Immobilised gold nanoparticles (paper III)

Gold is considered as an inert material due to its non-reactive noble metal character (with filled electron d shell). Solid gold is rarely used in medical devices, but has had some applications in dentistry. In its ionic form gold is used to treat arthritis due to its anti-inflammatory effect.[286] In paper III, gold-sputtered silicon disks were used due to their smooth surface. These disks were modified with gold nanoparticles synthesised from gold salts via an attached cysteine layer. The attached nanoparticles became partly sintered into the underlying gold substrate upon washing with a basic piranha solution consisting of 3:1:1 Milli-Q water, ammonia and hydrogen peroxide.[287] The result was a surface with 35–40 nm sized nanospheres homogenously distributed over the surface.

Table 4. Summary and abbreviation of surfaces in paper I–IV

Experimental surfaces	Abbreviations
Paper I	
Uncoated PDMS	uncoated/control
Nanostructured noble metal coated PDMS with different Ag, Au and Pd contents (five coatings)	coated
Paper II	
Uncoated machined titanium	uncoated/control
Nanostructured noble metal coated machined titanium	coated
Paper III	
Smooth gold	Au
Nanostructured gold (35–40 nm hemispherical protrusions)	AuNP
Tissue culture polystyrene	TCP
Tissue culture treated polystyrene cover slips	Thx
Paper IV	
Smooth titanium	sTi
Nanostructured titanium	nTi
Nanostructured noble metal coated titanium	nNoble

3.1.5 Control cell culture substrates (paper III)

Tissue culture plastic (TCP), made from a surface treatment of polystyrene, is a commonly used substrate *in vitro* for anchorage-dependent cells. TCP and tissue culture treated plastic coverslips (Thermanox®, Thermo Fisher Scientific) were used as control surfaces in paper III.

3.2 Material characterisation

The material surfaces used were characterised, both qualitatively and quantitatively, using a variety of chemical and topographical techniques as outlined below. In addition, surface wettability (hydrophilicity/hydrophobicity) was also measured.

3.2.1 Topographical analysis techniques

Scanning electron microscopy (paper II-IV)

Scanning electron microscopy (SEM) utilises a focused beam of electrons that is scanned over a sample, that interacts with the atoms at the sample surface, and then collects backscattered or secondary electrons to retrieve information about surface topography and/or composition. In the present thesis, SEM was performed for qualitative (paper II–IV) and quantitative (paper III, IV) assessment of the implant surface topography. The surfaces were viewed at different magnifications in the secondary electron mode to mainly generate topographic contrast using an in-lens detector for optimal resolution. Nanoparticle (paper III) or nanodeposit (paper IV) size and surface coverage were analysed using ImageJ software (National Institutes of Health, USA).

Interferometry (paper II, IV)

Optical interferometry was used to measure the microscale surface roughness. The technique utilises light and gains information of surface topography based on interference of the reflected light. In paper II, screws were analysed in three distinct areas (peaks, valleys and flanks) on three consecutive threads, each area being 200×260 μm (MicroXAMTM, Phaseshift. USA). A high-pass Gaussian filter (size 50×50 μm) was used to remove the influence of implant shape and waviness. In paper IV, two areas of 230×300 μm on the disks were evaluated using the vertical scanning interferometry mode (Veeco Instruments Inc., USA). Different roughness parameters are described in **Table 5**.

Atomic force microscopy (paper I, III, IV)

For quantitative analysis of nanoscale surface roughness atomic force microscopy (AFM) was employed. This technique uses a cantilever with a sharp tip, a few nanometers in radius, to scan a sample surface area of some micrometers to obtain a

two- or three-dimensional surface profile. The surfaces were scanned over at least two measuring areas per sample in tapping mode, using the Bruker Dimension 3100 system (Bruker Corporation, USA). Different roughness parameters are described in **Table 5**.

Table 5. Surface roughness parameters

	2D	3D	Paper
Amplitude parameters			
Arithmetic average height deviation (nm)	Ra	Sa	I–IV
Root mean square roughness (nm)	Rq, Rms	Sq	I, III, IV
Surface scewness	Rsk	Ssk	IV
Surface kurtosis	Rku	Sku	IV
Ten point height roughness (nm)	Rz	Sz	IV
Mean peak height (nm)	Mean Ht		I
Spatial parameter			
Density of summits (μm^{-2})		Sds	II, IV
Peak-to-valley distance (nm)	Rpv		I
Hybrid parameter			
Developed surface area ratio (%)		Sdr	II, IV
Functional index			
Core fluid retention index		Sci	IV

3.2.2 Chemical analysis techniques

Graphite furnace atomic absorption spectroscopy (paper I)

To obtain quantitative information of the noble metal content on the implant surfaces graphite furnace atomic absorption spectroscopy (GFAAS) was used. The silicone implants (paper I) were digested in a mixture of nitric acid (HNO_3), hydrofluoric acid (HF) and hydrogen peroxide (H_2O_2) inside a Teflon vessel in a microwave at elevated temperature and high pressure until completely dissolved. The metal concentrations in the liquid were analysed using AAS (SIMAA 6100 AS 800 Autosampler, PerkinElmer instruments) and were normalised by the surface area of the implants.

Inductively coupled plasma mass spectrometry (paper II)

Inductively coupled plasma mass spectrometry (ICP-MS) is a quantitative chemical analysis method using high temperature plasma to convert sample atoms into ions, which are then separated and detected by a mass spectrometer. Noble metal coating adherence to titanium screws was evaluated by insertion and removal in a rigid polyurethane foam (paper II). The samples were then boiled in a mixture of

hydrochloric acid (HCl) and nitric acid (HNO_3) to dissolve the metals and were then diluted in water. The noble metal content on the implants and the plastic was then analysed by ICP-MS (Element 2, Thermo Fisher Scientific, USA) and quantified using standard curves.

X-ray photoelectron microscopy (paper II, IV)

X-ray photoelectron microscopy (XPS) is a surface sensitive technique that enables the detection of the surface chemical composition (in atomic %) for the outermost 2–10 nm of surfaces. Not only the elemental composition, but also information about different states of an element can be obtained, such as different functional groups, chemical bonding and oxidation state, based on the peak intensities of the emitted photoelectron and shifts in their kinetic energies. The samples were analysed using a monochromatic Al X-ray source over a surface area of approximately 1 mm^2. In paper II, a PHI 5500 XPS system (Physical Electronics, USA) was used and in paper IV, a Kratos AXIS $Ultra^{DLD}$ system (Kratos analytical, UK) was used.

Time-of-flight secondary ion mass spectroscopy (paper IV)

Another highly surface sensitive chemical analysis technique, measuring only the outermost 1–2 nm of a surface, is time-of-flight secondary ion mass spectroscopy (TOF-SIMS). By short pulses of primary ions bombarding the surface, scanning over the surface, secondary ions will be emitted and accelerated into a high-resolution mass spectrometer, in which they are sorted according to their masses. In paper IV, the shielding effect of the on top-sputtered titanium layer was evaluated by comparing signal intensities from Ag-, Au- and Pd-containing ions with those from noble metal coated samples. The analysis was performed using 25 keV Bi_3^+ primary ions at a current of 0.1 pA in a TOF-SIMS IV instrument (ION-TOF Technologies GmbH, Germany).

3.2.3 Physico-chemical technique

Wettability (paper III)

Static water contact angle measurements were used to determine the degree of hydrophilicity or hydrophobicity, i.e. the wettability of the surfaces used in paper III. A 5 µL water droplet (MilliQ, 18.2 MΩ) was applied to the surface, and a side view image of the droplet was captured with high-magnification macrophotography. Contact angles were then measured using the angle tool in ImageJ software.

3.3 *In vitro* systems

3.3.1 Monocyte isolation and culture (Paper III)

Primary human monocytes were isolated from buffy coats obtained from healthy blood donors using Ficoll separation followed by negative selection on a magnetic column (MACS, Miltenyi Biotec). The buffy coat content was diluted in 2 mM EDTA in phosphate buffered saline (PBS) without calcium and magnesium and layered on top of Ficoll-Paque PLUS (GE Healthcare) in leukocyte separation tubes (Leukosep®, Greiner Bio-One). A 15 minute centrifugation step at 800 g (no brake) produced an enriched cell fraction of lymphocytes, monocytes and platelets. After repeated washings, the purified cells were re-suspended in 0.5% bovine serum albumin in EDTA/PBS and then magnetically labelled by an antibody cocktail non-specific for monocytes. The cell suspension was loaded onto LS Columns in a magnetic MACS separator, upon which unlabeled cells (i.e. monocytes) were passed through the columns and collected. The viability of the cells was determined by trypan blue dye exclusion. The monocyte purity was assessed by labelling the cells with CD14-PE and CD45-FITC antibodies followed by flow cytometry (BD FACSCalibur™, BD Biosciences) analysis.

The isolated monocytes were suspended in Rosewell Park Memorial Institute (RPMI) 1640 medium with GlutaMAX™ supplemented with 5% fetal bovine serum at a concentration of 1×10^6 cells/mL. One mL of the cell suspension was directly seeded onto newly cleaned gold surfaces or polystyrene control surfaces and cultured at 37°C with 5% CO_2 and 95% humidity. After 18 hours the medium was exchanged in order to keep only the adherent cells and remove possible stress factors from the isolation process. After an additional 24 hours, the cells were challenged with either serum-opsonised zymosan A particles (final concentration 2×10^7 particles/mL; Sigma-Aldrich) or serum-opsonised *S. epidermidis* (final concentration 10^8 CFU/mL) for 1 hour.

3.3.2 Bacteria culture (paper III, IV)

A biofilm-producing strain of *Staphylococcus epidermidis* (ATCC 35984; Culture Collection, University of Gothenburg) was used in paper III and IV. This strain was originally obtained from a patient with catheter sepsis. The identification of the strain was confirmed by API Staph (bioMérieux, France). Susceptibility to several antibiotics was tested by a commercially prepared, dehydrated panel GPALL1F test (Sensititre, Trek Diagnostic, UK). The strain was found resistant to ampicillin (minimum inhibitory concentration >8 μg/mL) among others (data not shown).

The strain was stored at −80°C in freezing media containing tryptic soy broth (TSB) and 20% glycerol. Upon use, the strain was streaked on blood agar plates and

incubated over night in humidified air at 37°C. Single colonies were then added to RPMI 1640 medium (paper III) or 0.9% saline (paper IV) until an optical density ($OD_{546\ nm}$) of 0.25 was reached, corresponding to approximately 10^8 CFU/mL. Inoculum suspensions between 10^4 and 10^9 CFU/mL were then prepared by diluting or concentrating the OD suspension. The bacterial concentrations in the OD- and inoculum suspensions were confirmed by plating 20 µL spots of 7 tenfold dilutions in saline and 0.1% triton-X on duplicate blood agar plates and incubated at 37°C for 18–20 hours.

Opsonisation of *S. epidermidis* (paper III) was performed as follows: two colonies from a blood agar plate were separately sub-cultured in 4 ml TSB for 4 hours to reach the exponential growth phase. The cultures were then pooled, washed in Hank's balanced salt solution (HBSS), incubated with 10% active human serum (pooled from three individuals) in HBSS (total volume of 2 mL) for 5 minutes, washed again and diluted to a concentration of 10^9 CFU/mL before added (100 µL) to the monocytes.

In paper II, *Staphylococcus aureus* (ATCC 12600; Culture Collection, University of Gothenburg), isolated from pleural fluid, was used for evaluation of primary adhesion adapted from the method described by Gabriel *et al.*[288] The strain was cultured in TSB for 18 hours at 37°C under shaking, harvested and washed twice in 0.9% saline. An inoculum of 10^6 to 10^7 CFU/mL was prepared in PBS and added to the implants for 24 hours under shaking conditions at 37°C.

3.4 *In vivo* models

3.4.1 Soft tissue inflammation model (paper I)

Female Spraque-Dawley rats (200–300 g), fed on a standard pellet diet and water, were used to study the inflammatory response and fibrous encapsulation around different material surfaces. Isoflurane inhalation was used to initiate and maintain anaesthesia throughout the surgery. The back of the rats was shaved and cleaned with 5 mg/mL chlorhexidine. After skin incision and the creation of subcutaneous pockets by blunt dissection, the implants were placed in the pockets before wound closure. All rats received one implant of each type (six in total). After 1, 3 and 21 days of implantation, the animals were sacrificed by an overdose of pentobarbital (60 g/L) after short anaesthetic induction with isoflurane. The implants were retrieved and the surrounding exudates were obtained from the pockets by repeated aspiration with a total volume of 300 µL of HBSS and kept on ice. For evaluation of the fibrous capsule after 21 days, the implants together with the surrounding tissue were excised *en bloc* for fixation and further processing. The study was approved by the Local Ethical Committee for Laboratory Animals (Dnr 112/04).

3.4.2 Soft tissue inflammation and infection model (paper IV)

A rat infection model was developed to study inflammation and infection around biomaterials in the presence or absence of bacteria. This model was developed from the soft tissue inflammation model using the same rat species and surgical procedures. The surgery was performed under sterile conditions inside a class II safety cabinet. An infectious dose of 10^6 CFU of *S. epidermidis* in 50 µL saline was pipetted inside the subcutaneous pockets with or without inserted implants. To avoid leakage from the pockets and ensure proper healing, the wounds were carefully sealed by intracutaneous sutures followed by 2–3 single stitches. Control animals were kept separate and received 50 µL sterile saline. Three different material surfaces were evaluated in the study. At most, the rats received eight pockets of which two were sham sites, i.e. surgical sites without an implant, representing the surgical trauma, and saline injection with or without *S. epidermidis*. The early inflammatory events as well as viable counts and distribution of *S. epidermidis* were analysed after 4 hours, 1 day and 3 days. The implants were retrieved and the exudates were aspirated with PBS and kept on ice. In separate sites subjected to histological examination, the implants were retrieved and the pockets received 200 µL Zn-formalin in a pre-fixation step. The pockets with surrounding soft tissues were then excised and immersed in Zn-formalin. The ethical approval for the study was provided by the Local Ethical Committee for Laboratory Animals (Dnr 254/11).

3.4.3 Bone model (paper II)

Adult female New Zealand White rabbits weighing 3.5 to 5 kg and fed *ad libitum* were used to evaluate the bone response around different material surfaces. The animals were sedated and anaesthetised with diazepam and fentanyl/fluanisone. The legs were shaved and disinfected before surgery. Implantation holes were prepared using a series of dental implantation drills with increasing diameters (up to a diameter of 3.5 mm) under profuse cooling with sterile saline. Four implantation screws (outer diameter 3.75 mm) were installed, one in each tibia and femur, before rinsing and suturing of fascial layers and skin separately. The same surgeon inserted all implants. Analgesics and antibiotics were given for 3 and 5 days after surgery, respectively. After 6 and 12 weeks the animals were sedated, sacrificed by an overdose of barbiturate and fixated by perfusion via the left heart ventricle with 2.5% glutaraldehyde in 0.05 M sodium cacodylate buffer (pH 7.4). The study was approved by the Local Ethical Committee for Laboratory Animals (Dnr 306/06).

3.5 Evaluation methods

3.5.1 Cell quantification (paper I, III, IV)

The number of cells in medium, exudate, or adherent to material surfaces was determined using a Nucleocounter® system (ChemoMetec A/S). The cells were lysed directly after retrieval and then stabilised with disaggregation buffer. The cell mix was loaded in Nucleocassettes™ pre-coated with fluorescent propidium iodide that stains the cell nuclei and quantified in the Nucleocounter®.

3.5.2 Cell type (paper I, III, IV)

Determination of cell type in the exudate, i.e. mononuclear cells versus polymorphonuclear cells, was achieved by Türk staining (paper I) or May-Grünewald Giemsa staining (paper IV) followed by light microscopy. Türk-stained cells (10 µL cell suspension) were counted in a Bürker chamber within hours after retrieval, whereas May-Grünewald Giemsa-stained cells (100 µL cell suspension or 5×10^4 cells) were applied in a thin layer on a microscope slide, dried, stained and counted on a later occasion.

The proportion of monocytes isolated from blood was determined by flow cytometry (paper III). Samples of 10^5 cells were labelled with CD14-PE (characteristic for monocytes) and CD45-FITC (characteristic for all blood cells), fixated in 2% paraformaldehyde and analysed in a FACSCalibur™ (BD Biosciences, USA). Unlabelled cells and isotypic controls served as controls.

3.5.3 Cell viability (paper I, III, IV)

Cell viability from *in vivo* exudates and *in vitro* cultures was determined by trypan blue dye exclusion using light microscopy or by measuring the lactate dehydrogenase (LDH) content in the cell-free suspension/medium. LDH is an enzyme that leaks out from the cytoplasm upon cell membrane injury. LDH catalyses the conversion between lactate and pyruvate, and this conversion can be evaluated spectrophotometrically by measuring the reduction of NAD^+ to NADH at 340 nm (C-laboratory, Sahlgrenska University Hospital, Sweden).

3.5.4 Gene expression (paper III, IV)

Monocytes adherent onto gold surfaces *in vitro* (paper III) and pelleted exudate cells *in vivo* (paper IV) were analysed with respect to gene expression of cytokines, cell adhesion receptors and enzymes involved in tissue destruction and bacterial killing by reverse transcriptase quantitative real-time polymerase chain reaction (RT-qPCR). Cells were lysed in RLT buffer (Qiagen, Germany) supplemented with β-merkaptoethanol (Sigma-Aldrich) and frozen at −80°C. Total RNA was extracted

using the Nucleospin® RNA XS kit (Machery-Nagel, Germany) (paper III) or RNeasy® micro kit (Qiagen) (paper IV) as described by the manufacturers. The RNA concentration was measured using a nanospectrophotometer (IMPLEN NanoPhotometer™ Pearl, Implen GmbH, Germany; NanoDrop, Thermo Fisher Scientific, USA) and the RNA quality was evaluated by chip electrophoresis in an Agilent 2100 Bioanalyzer (Agilent Technologies, USA).

Total RNA was converted to cDNA using TATAA GrandScript cDNA Synthesis Kit (TATAA Biocenter AB, Sweden) in 10 µL reactions. Diluted samples were mixed with TATAA SYBR® GrandMaster Mix (TATAA Biocenter AB) and primers (final concentration 400 nM) and subjected to RT-qPCR analysis on the QuantStudio 12K Flex platform (Life Technologies) or on the LightCycler®480 system (Roche Applied Science). Inclusion of a ValidPrime assay (TATAA Biocenter AB) was used for detection of contaminating genomic DNA. Gene expression levels were normalised to two reference genes and analysed in GeneEx (MultiD Analyses AB, Sweden) using the relative comparative Cq method.

3.5.5 Cell secreted factors (paper I, III)

The amount of secreted proteins (cytokines and growth factors) in the exudate retrieved from the pocket in soft tissue (paper I) or cell culture medium (paper III) was evaluated by enzyme-linked immunosorbent assays (ELISA). The exudates/media were centrifuged at 400 g for 5 minutes and supernatants stored at −80°C until analysis. Commercial (human or rat) ELISA kits were utilised according to manufacturers' instructions. The optical density was measured at 540 nm with a microplate reader (SPECTRAmax, Molecular devices, UK or FLUOstar Omega, BMG Labtech, Germany) and translated to protein levels using accompanying software.

3.5.6 Production of reactive oxygen species (paper III)

Surface adherent monocytes were evaluated for their ability to mount an oxidative response upon stimulation with serum-opsonised zymosan or *S. epidermidis* by using luminol-mediated chemiluminescence (CL). The luminol (5-amino-2,3-dihydro-1,4-phtalazinedione; Sigma-Aldrich) molecule can pass through the cell membrane and can therefore detect both intra- and extracellular ROS.[289] The reaction was carried out in HBSS in opaque 24-well plates to diminish cross-talk between wells. Monocyte/macrophage cells were exposed to microbial stimuli, inserted into a microplate reader with luminescence optics (BMG Labtech), automatically injected with luminol (final concentration 5×10^{-5} M), and CL was read every minute for up to 90 minutes. Measured data points were transferred to MATLAB® (MathWorks Inc., USA), approximated to a curve using the smoothing spline method, and analysed in

respect to total CL (area under the curve), maximum CL and time to maximum CL for x values between 3 and 80 minutes.

3.5.7 Quantification of bacteria (paper II-IV)

A standard method to quantify bacteria is plate counting that estimates the number of bacterial cells present based on their ability to form colonies under specific conditions (nutrient medium, temperature and time). In theory, one viable cell can develop into a colony by multiplication. Since solitary cells are rare in nature, the progenitor of the colony is probably a mass of cells deposited together (*Staphylococcus* grows in clumps). Therefore, colony-forming unit (CFU) is an estimate of viable bacterial numbers. Columbia agar supplemented with 5% horse serum (blood agar plate) is a general purpose medium for the growth of most bacteria and indicates haemolytic activity. Selective plates are used for the growth of specific bacterial species with certain metabolism, tolerance or antimicrobial resistance. The use of selective media is important when analysing *in vivo* samples to ensure only the quantification of the administered strain. For example, staphylococci agar supplemented with 8 μg/mL ampicillin was used to estimate the number of viable *S. epidermidis* from *in vivo* samples (paper IV). For cultivation and enumeration of strains *in vitro* (paper II, III) blood agar plates were used.

Enumeration of bacteria was performed by the viable counting method. A bacterial suspension of unknown concentration was serially diluted (ten fold) and plated on duplicate plates. For spread counting, 100 μL of the dilutions was spread over the agar plate. For spot counting, 20 μL from each dilution was pipetted onto the agar and allowed to dry before incubation. After 1 to 2 days of incubation at 37°C the colonies were manually counted and the highest dilution not exceeding 300 colonies per spread plate or 50 colonies per spot was used to estimate the concentration (CFU/mL, CFU/implant).

Before quantification of implant-adherent *S. epidermidis*, the samples were sonicated at 40 kHz for 30 seconds followed by vortexing at maximum speed for 1 minute to detach the bacterial cells and break aggregates. Thereafter the viable counting method was performed as described above.

In paper II, the screws were first carefully rinsed to remove loosely adherent bacteria. Implant-adherent *S. aureus* was dislodged by 2 minutes vortexing in 0.05% Tween-20 in PBS prior to quantification using the viable counting method.

3.5.8 Fluorescence staining (paper III)

The biofilm-forming capacity and viability of surface-adherent *S. epidermidis* were assessed *in situ* by using a two-colour fluorescence assay, in which live cells are

stained green (SYTO 9) and dead cells are stained red (propidium iodide). Prior to analysis, the surfaces were carefully rinsed to remove non-adherent bacteria and incubated with 200–250 µL premixed staining solution (FilmTracer™ LIVE/DEAD® Biofilm Viability kit, Invitrogen) for 30 minutes in the dark. The surfaces were then carefully rinsed, kept in saline and visualised either by confocal laser scanning microscopy (CLSM; LSM 710, Carl Zeiss) for the quantification of three-dimensional biofilm images, or by measuring the total fluorescence in a microplate reader (FLUOstar Omega, BMG Labtech).

For CLSM visualisation, the surfaces were placed in 6 cm petri plates covered in saline and analysed at five different random spots (425×425 µm) over the surface (corners and centre) using a x20 water-dipping objective. The images were quantitatively analysed using the COMSTAT2 software in respect to total biomass, maximum thickness and area occupied at the surface of live and dead bacterial cells. The fluorochromes were excited at 488 nm and 561 nm, and emitted light was measured using band-pass filters of 505–530 nm and 585–690 nm for green and red light, respectively.

For fluorescence plate readings, the surfaces were transferred to black 24-well plates to reduce background fluorescence and analysed by top optic readings. Both fluorochromes were excited at a wavelength of 485 nm, whereas the emission was analysed at 520 nm and 615 nm for green and red, respectively.

3.5.9 Fluorescence *in situ* hybridisation (paper IV)

In fluorescence *in situ* hybridisation (FISH), fluorescent labelled nucleic acid probes are used to detect and localise specific DNA sequences. In paper IV, a CoN-specific Peptide Nucleic Acid (PNA) probe kit (AdvanDx, USA), specific for 16S, was used for localisation of *S. epidermidis* in the tissue. De-paraffinised tissue sections on glass were hybridised with 15 µL PNA probe at 55°C for 30 minutes and subsequently washed at 55°C for 30 minutes, air dried and mounted. Stained slides were kept in dark at 4°C until visualised in an epifluorescence microscope (Nikon Eclipse E600) with a Texas Red filter (excitation 540–580 nm, emission 600–660 nm).

3.5.10 Cell, bacteria and tissue morphology – electron microscopy techniques (paper II-IV)

Scanning electron microscopy was used to visualise the relationships between eukaryotic cells, bacterial cells and the material surface after *in vitro* cultures (paper III), and to visualise interactions between eukaryotic and bacterial cells and extracellular matrix at the implant surface after *in vivo* experiments (paper IV). Furthermore, to visualise the interior of eukaryotic cells and details of bacteria–surface interactions (paper III), a focused ion beam (FIB) was used for

accurate milling of selected eukaryotic and bacterial cells, before viewing in SEM. In paper II, SEM was used on plastic embedded titanium implants with surrounding tissue to evaluate the bone–implant interface. Information about the degree of mineralisation was obtained since mineralised bone backscatter electrons more strongly than newly synthesised bone.

Implant-adherent cells were fixated in Karnovsky's (2% paraformaldehyde, 2.5% glutaraldehyde in 0.15 M sodium cacodylate buffer), washed in sodium cacodylate buffer and postfixated with 1% osmium tetroxide in 0.1 M sodium cacodylate buffer for 2 hours at 4°C. Contrast enhancement was performed with 1% thiocarbohydrazide for 10 minutes at room temperature, followed by incubation in 1% osmium tetroxide in 0.1 M sodium cacodylate buffer for 1 hour at 4°C according to a modified version of the OTOTO post-fixation method.[290] Dehydration was performed in a graded series of ethanol (70–99.5%) and critical point drying was achieved by hexamethyldisilazane evaporation. The samples were mounted on stubs and coated with palladium before visualisation with a mixture of secondary and backscattered electrons in a Zeiss 982 Gemini SEM operated at 3 kV.

Milling of the cell and bacteria samples was performed in a dual-beam FIB system (Strata DB 235, FEI or Versa 3D, FEI) operated at 16.0–30.0 kV (Ga^+ ions) and 5–10 kV (electrons). The larger sized cells were sputtered with a platinum layer prior to ion milling in order to protect the cells, whereas this was not needed for the smaller bacterial cells due to shorter time of ion exposure. Cross sections of the eukaryotic and bacterial cells were then imaged by SEM.

Representative samples of the plastic embedded screw–tissue specimens were carefully ground, mounted on stubs, coated with palladium and then viewed in the backscattered electron mode in SEM (LEO Ultra 55 FEG SEM, Zeiss) operating at 20–30 kV.

3.5.11 Preparation of histological specimens (paper I, II, IV)

Histological evaluation can be performed on plastic resin embedded or paraffin embedded specimens. The main advantage with plastic embedded specimens is that the implant can stay in place and be cut through together with the tissue, giving a more intact interface between the cells in the tissue and the material, optimal to perform histomorphometry. However, few sections can be produced. Paraffin embedded specimens can yield several sections, allowing multiple staining and labelling procedures to be used for analysis of the tissue sections. In the present thesis, soft tissues were excised *en bloc* with (paper I) or without (paper IV) the implant, for plastic resin and paraffin embedding, respectively. In paper II, the

implant and the surrounding bone were excised together for further processing towards plastic resin embedding.

3.5.12 Histology and histomorphometry

Analysis of fibrous capsule formation around the implants was performed on 1–2 µm thick sections stained by Richardson solution (paper I). The thickness of the fibrous capsule was analysed at five equally located points on both sides of the implant disk.

Bone–implant specimens (15–20 µm thick) were stained with toluidine blue prior to light microscopy evaluation (paper II). Histomorphometry was used to quantify the amount of bone within the threads of the screws (bone area, BA) as well as the amount of bone in contact with the screws (bone–implant contact, BIC).

In paper IV, histological analysis was performed on 3–5 µm thick paraffin sections of tissue surrounding the implant, but the implant had been removed. Tissue sections were either stained with Mayers hematoxylin and eosin, May-Grünewald Giemsa or labelled with a 16S-specific FISH probe (described above) for evaluation of tissue structure, cell types and detection of bacteria.

All specimens were evaluated in a Nikon Eclipse E600 light microscope connected to image analysis software (Image Analysis 2000, Tekno Optik AB).

3.6 Statistics

Different statistical tests were used to assess significant differences between groups. Specific tests were selected in relation to the type of data and the number of groups investigated. Non-parametric tests were used when data could not be assumed to have a normal distribution.

In general, non-parametric tests were used for all results obtained from *in vivo* experiments. Wilcoxon signed rank test for related samples was used when comparing different types of material modifications, whereas comparison between different treatments or time points was accomplished by using the Kruskal-Wallis test followed by Mann-Whitney U tests for independent samples. Parametric tests were used for analysis of *in vitro* results as well as material roughness measurements, where one-way ANOVA followed by Tukey's post hoc test or t-tests were performed. All gene expression analyses were performed on logarithmic values and analysed using parametric tests. Throughout the work a significance level of 5% was used.

4 SUMMARY OF RESULTS

4.1 Paper I

The first study was performed to evaluate the interfacial soft tissue response to systematic variations in the composition of the noble metal coating. Five coatings on silicone (PDMS) were manufactured to systematically alter the gold and palladium contents, whereas the silver content was kept constant (**Figure 6**). Coated and uncoated silicone disks were then analysed in a subcutaneous *in vivo* model with respect to inflammatory events and subsequent repair processes after 1, 3 and 21 days of implantation.

All coatings had total metal levels below 1.6 μg/cm^2. The coating process resulted in a small increase in surface nanoroughness compared with an uncoated silicone control surface. No major release of noble metals was detected after *in vivo* implantation.

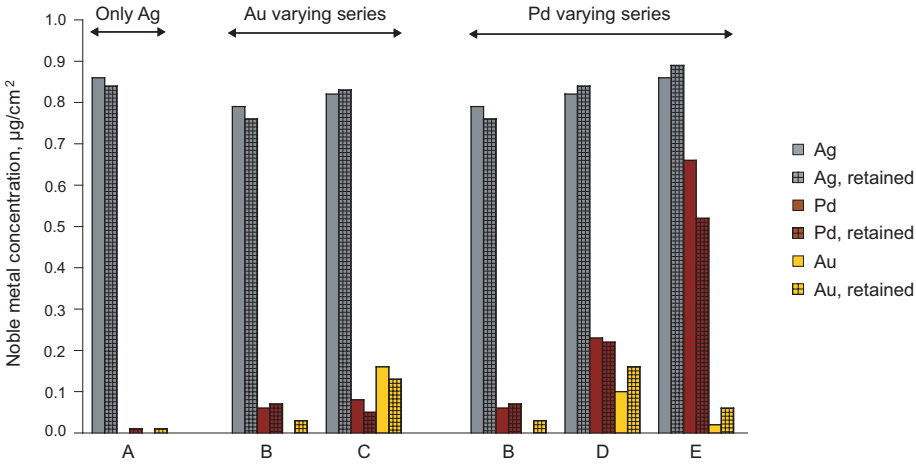

Figure 6. Noble metal content in the different coatings before (solid bars) and after 21 days of implantation (crossed bars).

Alterations in the noble metal composition influenced the pattern of inflammatory events during implantation. Coatings with Ag and medium amounts of Pd and Au (D) had the lowest amount of implant-adherent cells at 1 and 3 days, with significant differences compared to coatings with low amounts of Pd and low to medium amounts of Au (B, C).

During the first days after implantation, coatings of Ag only (A), or Ag with medium amounts of Au and low to medium Pd content (C, D) were associated with a decreased recruitment of inflammatory cells to the exudates, a lower percentage of neutrophils, higher cell viability and lower production of MCP-1, compared with the other coatings and the control.

The coating with only Ag (A) was distinguished by lower cell recruitment to the exudate at 1 day, whereas it was associated with more implant-adherent cells at 21 days. The introduction of Pd and Au to the coatings increased the amount of exudate cells at 1 day to levels similar to that of uncoated silicone. No trends in changes of the number of implant-adherent cells were seen as a result of Pd and Au additions to the coatings. The concentrations of MCP-1 in the exudates correlated with the exudate cell numbers and may explain the lower recruitment of inflammatory cells to the coating with only Ag (A).

The total amount of recruited inflammatory cells decreased over time, indicating a transient inflammatory response for all materials. The majority of the recruited cells was found in the exudate at day 1. On the contrary, the majority was found adhered to the surfaces on day 3 and 21.

Mononuclear cells were the predominant cell type in the exudate at all time points with increasing levels over time. The proportion of PMN at day 1 was higher around the control surface compared with most coatings, but decreased to very low values at 3 days.

The fibrous capsule around the implants was evaluated after 21 days. A thinner capsule was observed for the uncoated control (88 μm), whereas the addition of metals increased the capsule thickness (>100 μm). Coatings with a higher Pd content (C, D) gave rise to the thickest capsules, whereas the coating with only Ag had a thinner capsule.

The study demonstrated that by varying the noble metal ratio at implant surfaces it is possible to modulate inflammation and fibrosis in soft tissue.

4.2 Paper II

The second study evaluated the bone response of noble metal coated titanium implants and the osseointegration was compared with that of clinically used machined titanium implants. Noble metal coated and uncoated titanium control screws were inserted in the tibia and femur of rabbits. After 6 and 12 weeks, the bone–implant contact and bone area was evaluated.

Chemical analysis of the implants revealed a main contribution of TiO_2 on both implant types, whereas only coated implants had additionally small amounts of Ag, Au and Pd (<1 μg/cm^2) on the surfaces. The coating gave rise to a distinct nanotopography in the form of 10–150 nm noble metal deposits, with fewer and more separated deposits in the thread valleys but densely packed on the thread peaks. However, no significant quantitative topographical differences were detected on the micron level.

In vitro adhesion test with *S. aureus* showed a two log reduction in adherent bacteria on coated versus control screws.

A qualitatively and quantitatively similar bone response was observed for the coated and uncoated screws, as determined by histology, histomorphometry and electron microscopy. After 6 weeks of implantation, bone formation and remodelling was demonstrated in femur and tibia, whereas most of the bone, especially around femoral implants, was already remodelled and closely resembled highly organised lamellar bone after 12 weeks. The bone area within the threads increased over time in both tibia and femur, but did not differ between coated and control implants. The bone–implant contact did not change over time and was similar for the two implant types, with an exception for femur after 12 weeks which revealed a lower bone–implant contact for coated screws compared with controls.

In summary, the results demonstrated a similar bone response to machined and noble metal coated titanium implants.

4.3 Paper III

In study III, the impact of nanostructured surfaces on monocyte activation and *S. epidermidis* adhesion and biofilm formation was investigated. Gold surfaces with 35–40 nm gold nanoparticles immobilised on the surface were produced and compared with smooth gold surfaces. Two smooth polystyrene surfaces were used as controls in the monocyte experiment.

Quantification of live surface-associated bacteria showed no differences between the materials when evaluated with the viable counting method at any time point analysed (2, 24 and 48 hours). In contrast, fluorescent viability staining demonstrated a significantly lower amount of live *S. epidermidis* on nanostructured surfaces, which was more pronounced on surfaces with higher nanoparticle coverage. Furthermore, confocal analysis revealed that nanostructured surfaces were associated with a larger innermost surface area occupied by dead bacteria (2 and 24 hours) as well as more dead total biomass (2 hours). Smooth surfaces showed earlier (24 hours) intercellular adhesions between *S. epidermidis* cells and were generally associated with thicker and

more mature biofilms (higher tower formations) at 48 hours, as observed in SEM and confocal microscopy. In addition, single bacterial cells on the smooth surface were shown to be in continuous contact with the substrate, whereas adherent bacterial cells on the nanostructured surface relied on a few, discrete attachment points.

Human monocytes were allowed to attach to the substrates for 18 hours before media change. After an additional 24 hours of incubation, monocytes were stimulated with either opsonised zymosan (non-living microbial stimuli) or opsonised, live *S. epidermidis* for 1 hour. High cell viability of monocytes was found on all surfaces, independent of stimuli. Unstimulated monocytes demonstrated low activation, reduced gene expression of pro- and anti-inflammatory cytokines, and low cytokine secretion. In contrast, stimulation with either of the preys resulted in elevated production of ROS, higher gene expression of TNF-α, IL-1β, IL-6 and IL-10 as well as increased secretion of TNF-α, demonstrating the ability of the cells to elicit a response and actively phagocytise the preys. Zymosan was the most potent prey to elicit ROS production, whereas *S. epidermidis* caused a more pronounced up-regulation in gene expression and cytokine secretion. No differences between the nanostructured and smooth gold surfaces could be discerned, but rather between the gold surfaces and the control polystyrene surfaces. Upon stimulation, monocytes cultured on the gold surfaces displayed a different adhesion pattern and more rapid oxidative burst than those cultured on polystyrene.

4.4 Paper IV

In the fourth study, a soft tissue biomaterial-associated infection model was developed, focusing on the initial events between host defence cells and bacteria on the material surface, in the exudate and in the surrounding tissue. Titanium disks, with or without nano-coatings of either titanium or noble metals, were implanted subcutaneously for 4, 24 and 72 hours in the presence or absence of *S. epidermidis* (10^6 CFU dose). Sham sites without implants were used as controls.

The control sites without bacteria were associated with a low and transient inflammatory response, as demonstrated by a peak of infiltrating inflammatory cells at 24 hours, early predominance of PMN with a shift to mononuclear dominance, a low degree of cell death and early but transient gene expression levels of TNF-α, IL-6, IL-8, TLR2, TLR4 and elastase. The presence of a biomaterial resulted in a relatively higher cell recruitment, similar low degree of cell death, initially a higher proportion of mononuclear cells, but similar or lower gene expression of all analysed genes compared with sham sites.

The addition of *S. epidermidis* to the sham and implant sites resulted in significantly higher recruitment of inflammatory cells, predominance of PMN throughout the

study, higher and continuous cell death and an overall increase in gene expression of TNF-α, IL-6, IL-8, TLR2 and elastase. Very few viable *S. epidermidis* were detected at 4 hours, whereas considerably higher amounts (100 fold) were found at 24 and 72 hours. More bacteria were quantified from the exudates compared with the implants at all time points. The total amount of bacteria decreased, although non-significantly, from 24 to 72 hours with the least reduction seen at sham sites. Fluorescently labelled *S. epidermidis* in the tissue demonstrated high presence in the interface zone, between the implant and the tissue proper. Furthermore, bacteria were observed both extra- and intracellularly. After 72 hours it was evident that repair processes had started and the presence of *S. epidermidis* had induced a more condensed interface with a higher presence of inflammatory cells in comparison with controls.

Small differences were seen between the different materials, but a trend was found towards an increased inflammatory response (higher cell infiltration, higher gene expression and higher proportion of PMN) as well as a reduced amount of viable bacteria, associated with the noble metal coated titanium in comparison with smooth and nanostructured titanium.

5 DISCUSSION

5.1 Methodological considerations

In the present thesis a combination of *in vivo* and *in vitro* models has been employed to assess biocompatibility in bone and soft tissue, and to investigate material surface-, host defence cell- and bacterial cell-interactions. The focus has been towards nanopatterned noble metal coatings. Different strategies have been applied to analyse separate contributions from noble metal chemistries and topographies.

Biocompatibility and specific events related to inflammation were evaluated using bone and soft tissue models in rabbits and rats, respectively. These models have previously been used to evaluate different aspects of material modifications and they offer the ability to discriminate between materials in comparison with clinically relevant controls.[50,85,291,292] The models can be used to indicate safety and to provide quantitative data on inflammatory and repair processes. It should be noted that the bone study (paper II) did not include a functional assessment of implant stability, which is necessary to perform prior to introduction of such coated implants under load-bearing conditions in humans.

The last two studies addressed the role of nanotexture and nanochemistry on host defence cells and *S. epidermidis in vitro* and *in vivo*. The choice of *S. epidermidis* is justified by the large representation of CoN staphylococci at sites of BAI. It should not be excluded that different bacterial species, and strains within one species, can possess different virulence, growth and adhesion properties on different biomaterial surfaces.[223]

The two main advantages of *in vitro* studies as compared with *in vivo* studies are: (i) the reduced number of variables that affect the outcome, and (ii) the ability to focus on specific cellular events during interactions with either a material surface, a particular cell type or a certain molecule. In paper III, single and co-culture models of primary human monocytes and *S. epidermidis* were used. Co-culture models can imitate perioperative or late hematogenous bacterial spreading, depending on whether bacteria adhere to a surface before or after host cell seeding.[293] In paper III, a bacterial challenge was introduced for a short period of time (1 hour) after the pre-establishment of monocytes on the surfaces. Other co-culture models have shown that when eukaryotic cells are allowed to reach a critical cell surface coverage before a bacterial challenge, the possibilities for bacteria to colonise a surface are strongly reduced, supporting the belief that tissue integration is the most important protection for a permanent implanted device.[176,293] *In vitro* co-culture models require a suitable culture medium that supports a balanced growth of both eukaryotic cells

and bacterial cells. Heat inactivated serum was used in the monocyte cultures, whereas no proteins were added to bacterial cultures when investigating bacterial cell–surface interactions. The use of protein-free medium offers the possibility to study the effects of isolated material surface properties on bacterial adhesion and behaviour. The models can be made more complex, e.g. by introducing active serum, by including more cell types, or by adding a matrix on the surfaces. However, interpretations should be restricted to the *in vitro* situation and extrapolations to *in vivo* conditions need to be made with caution.

In paper IV, an *in vivo* model was developed to investigate the inflammatory events pertaining to BAI. Such a model will aid the understanding of the functional and possible dysfunctional aspects of host defence cells in the presence of a biomaterial and the possible modulation of cell behaviour by material properties. Rats, although generally considered immunocompetent, have been proven useful as a model system for implant-related infections in bone as well as non-biomaterial associated infections.[294-297] In the present approach we based the new model on a previously described, aseptic soft tissue model.[40,298] In addition, although no strict boundaries exist, the sample collection from three different compartments (implant, exudate and tissue) enables pin-pointing the location of cells and bacteria and assessing their function at a cellular and molecular level. To fully understand the in depth mechanisms and further exploit the model, the following potential improvements have been identified: homogenisation and bacterial counts also from tissue, bacterial viability evaluation, functional assessment of both surface associated host cells and bacteria by gene expression analysis, cytokine measurements and ROS production, and the inclusion of bactericidal control materials. Moreover, longer time points as well as the use of different bacterial species and strains exerting different virulence are needed to validate the model. Due to the complex *in vivo* environment, a major dilemma is the inability to separate direct versus indirect effects on bacterial colonisation, i.e. the role of the surface versus the role of host defence. Additional drawbacks include the more limited sources of rat specific commercial products and the difficulties for genetic modifications in comparison with mice.

5.2 Inflammatory response and fibrous capsule formation around nanostructured noble metal coatings

In paper I, the surface of silicone was modified with five differently composed noble metal coatings which were evaluated in soft tissue with respect to inflammation and fibrosis. All coatings showed a similar or lower inflammatory response compared with uncoated PDMS after 1, 3 and 21 days. Specifically, the coating containing only Ag caused a lower recruitment of cells to the exudate at day 1, which could be

coupled to a lower secretion of the chemoattractant MCP-1. The pure Ag coating also gave rise to an initially lower proportion of PMN. Previous studies have indicated an anti-inflammatory role of silver both *in vitro* and *in vivo*, which may serve as an explanation for this result. Nanoparticles of silver or silver ions have shown a down-regulatory effect on the pro-inflammatory nuclear factor-kappa B (NF-κB), IFN-γ and TNF-α in monocytes *in vitro*,[299,300] whereas a reduced infiltration of inflammatory cells, an increased apoptosis of inflammatory cells and lower levels of pro-inflammatory IL-1β, IL-12, TNF-α and metalloproteinases have been found *in vivo*.[301-304] Interestingly, the introduction of small amounts of Au and Pd into the coating reversed the anti-inflammatory potential of the Ag coating, indicating an interaction between the different metals in the coating. Further addition of Au and Pd to the coatings again modified the inflammation depending on the amount of the individual metals. Those coatings containing low and intermediate amounts of Pd and intermediate amounts of Au were more similar to the pure Ag coating. Adhesion studies on fibroblasts *in vitro* showed a sudden decrease in attachment to coatings containing Ag and small amounts of Au and Pd in contrast to coatings containing only one of the metals.[305] This supports the observation that the combination of several metals in the coating influences cell behaviour. Furthermore, by adding higher amounts of Au and Pd to the coatings, the fibroblast adhesion increased and approached that of coatings with only one metal.[305] Since the nanotopography did not significantly differ between the different coatings, the present data indicates that the surface chemistry plays an important role. This role, however, seems to be rather complex depending on the amount of the individual metals and the possible interactions between them. Differences in electropotential on a surface and catalytic oxidation of silver, anticipated to occur on noble metal coatings, have previously shown antibacterial effects,[306,307] but their importance for inflammation and wound healing has not been assessed. Taking the inflammatory parameters at large, the inflammation around the materials in the present study was comparable to that of biocompatible titanium.[308]

The formation of fibrous capsules around the materials was evaluated after 21 days of implantation. Histomorphometric analysis revealed thinner capsules around non-coated PDMS, whereas the coatings gave rise to thicker capsules. Generally, an increasing amount of metals in the coatings correlated with a thicker fibrous capsule. Hence, no correlation could be made between the capsule thickness and the degree of inflammation around the materials. In contrast, the thicker capsule around copper compared with titanium was suggested to be related to extensive cell recruitment and initially increased IL-6, IL-1α and TNF-α levels.[308] The fibrous capsule has previously been shown to be thinner around materials with roughness on the microscale compared with smooth materials.[47,48] This has been coupled to the decreased micromotion of implants with rough surfaces, which in turn results in a lower extent of inflammation as well as a reduced amount of necrotic cells. In the present study,

few differences were found with respect to cell viability around the materials, but the coating that yielded the thickest capsule also showed (non-significantly) increased cell death at 21 days. Moreover, the small increase in nanoroughness of coated surfaces is not expected to affect implant stability and micromotions.

The presence of intermediate and high amounts of Pd in the coatings induced the thickest capsules, suggesting a triggering effect of Pd on fibroblast matrix deposition. Although an increased amount of TGF-β was produced by fibroblasts around noble metal coatings with high Pd content *in vitro*,[305] no modulatory effect on TGF-β levels by the different implants were detected *in vivo*. Capsule appearances and thicknesses around metals have previously been coupled to corrosion products and ion release.[309,310] However, the coatings in the present study contained very low total amount of metals (<2 μg/cm^2) and revealed no major release of the noble metals after 21 days of incubation *in vivo*. Previous studies have shown a dense, highly vascularised capsule with a large number of inflammatory cells and multinuclear giant cells around copper implants (thickness 160 μm), whereas titanium had a thinner (around 80 μm) capsule with fewer inflammatory cells and fewer and smaller blood vessels after 28 days of implantation.[50] In the present study the thickest capsules were in the same range as for copper, but all capsules were well organised and no adverse cellular reactions could be detected. It is therefore less likely that the increased capsule thickness around coated materials is a result of toxicity.

In the present study no attempts were made to evaluate the *in vivo* protein adsorption on the different surfaces. Protein adsorption onto implanted surfaces is unavoidable and may promote cellular adhesion to the surfaces, depending on protein type, concentration, conformation and orientation. Both topography and chemistry are important factors for protein adsorption. As shown earlier, both silver and gold have been found to adsorb more proteins than many other metals and polymers.[311] Differences in protein adsorption behaviour are therefore likely to have influenced the results.

5.3 Bone response to nanostructured noble metal coatings

In paper II, a noble metal coating was applied on machined titanium and evaluated with respect to osseointegration and biocompatibility in bone. Overall, a qualitatively and quantitatively similar bone response was observed for coated and non-coated titanium screws after 6 and 12 weeks in rabbit tibiae and femur. The amount of newly formed bone increased over time, whereas the bone–implant contact remained at the same level at the two evaluated time periods. However, a reduced bone–implant contact in femur was observed for coated implants in comparison

with controls after 12 weeks. On the other hand, the histological examination excluded adverse events such as persistent inflammation or bone resorption localised at the implant surfaces, two factors that may reduce osseointegration. Instead, an alternative explanation might be an increased remodelling of the bone within the proximity of the surface.

It has previously been stated that the properties of surface oxides play an important role for the osseointegration of titanium-based materials.[151,312] Noble metals, on the other hand, generally lack surface oxides and are also less well studied with respect to osseointegration. Earlier studies on machined gold implants have shown poor osseointegration.[151,313] In contrast, the results in the present study show that implants with a noble metal coated surface can indeed be well osseointegrated, which suggests that nanostructure played a beneficial role in the present study. Although relatively few *in vivo* experimental studies have been performed, recent observations demonstrate positive effects of titanium nanotopography on osseointegration when superimposed on a microtopography, as measured by histology, ultrastructure and removal torque.[127,160] Furthermore, several *in vitro* studies have shown higher differentiation and mineralisation of bone cells cultured on substrates with pronounced nanotopography.[140,141,148] Similar to the noble metal coatings used in the present thesis, most nanoscale surface modifications also alter the surface chemistry of the coating, making it difficult to separate the contributions of chemistry from that of topography. For example, surfaces modified with HA or calcium phosphate nanostructures, either on smooth or microtopographically complex surfaces, have shown increased bone–implant contact.[164,165] In a study comparing HA and titania nanofeatures on smooth titanium surfaces, an increased bone–implant contact was observed for the titania nanostructures after 4 weeks of implantation in rabbit tibia.[166] However, the titania nanostructured surfaces had slightly lower roughness and a higher nanofeature coverage compared with HA implants, leading the authors to suggest that bone integration is more dependent on the size and distribution of nanofeatures than on the chemistry. A recent study investigating differently sized nanobumps (60, 120 and 240 nm) on machined titanium showed an increased bone–implant contact for 60 nm bumps, indicating that size, but also density and curvature, affect bone integration.[169] Interestingly, the size range of the noble metal deposits on the screws in the present study varied between 10 and 150 nm, with the majority being less than 70 nm, thus being comparable in size with the 60 nm bumps. Moreover, the noble metal deposits were arranged in a disordered manner on the surface, which has previously been observed to increase osteoblast differentiation *in vitro*.[147]

An additional factor that might affect healing and osseointegration of an implant is the possible release or degradation of a coating. Major release from the noble metal coatings in the present study are, however, unlikely. First, very small amounts of

metals were present on the implants (<1 μg/cm^2). Second, an *in vitro* bench test evaluated the presumed worst-case scenario release of the coating, with 20–35% of the metals removed from the implant. This result was obtained after both insertion and removal of the implants in a rigid polyurethane foam under dry conditions. And third, a study of Ag-releasing implants inserted in rabbit femur showed no pathological findings or toxicological side effects.[314] *In vitro* studies of osteoblasts on Ag, Au and Pd have in general shown cell growth and differentiation as well as low cytotoxicity,[315-321] although negative effects on growth and differentiation have also been observed.[319]

In summary, noble metal coated titanium implants revealed a similar bone response to machined titanium implants and became osseointegrated, with the potential benefit of increased infection resistance. However, further studies are required to address long-term effects on osseointegration as well as biomechanical evaluation of implant stability prior to clinical introduction.

5.4 Host defence cell–bacteria interactions

The interactions between host defence cells and *S. epidermidis* at specific implant surfaces were investigated in two different settings: *in vitro* (paper III) and *in vivo* (paper IV). The surfaces presented to the cells were either smooth or nanostructured, with a single chemistry (gold or titanium) or with a mixed chemistry (silver, gold, palladium and titanium). In paper II, *S. aureus* adhesion to noble metal coated or non-coated machined titanium screws was assessed. A summary of the different experimental surfaces is shown in **Table 4** (section 3.1).

5.4.1 Host defence modulation by biomaterial presence

First, it is important to address whether there is an effect of the mere implant presence on the host defence cells. It is known from literature that a smaller inoculum of bacteria is needed to produce infection in the presence of a biomaterial and that otherwise non-virulent bacteria can gain access to the implant site and develop an infection.[183,184,277] It has been suggested that an immuno-incompetent zone prevails around the implant, with a subsequent inability of the host defence cells to clear infections.[4] This view is supported by the clinical experience that the most effective way to eradicate BAI is by removal of the medical device.[170,172,173]

In paper IV, during the early time points studied (4–72 hours), no signs of immune incompetence around the materials were observed. Taken together, in the presence of bacteria, the additional recruitment of inflammatory cells, the distribution of inflammatory cells in the interface zone and the higher gene expression activity of these cells suggest that a proper host defence was initiated at the implant site. In

addition, the PMN predominance at infected sites continued throughout the study, providing evidence of an ongoing acute inflammation with recruitment of new neutrophils. The comparison between biomaterial sites and sham sites (without material) showed many similarities. A higher number of inflammatory cells were recruited to the material sites, which may be explained by the presence of two stimuli: the bacteria and the implant. The proportion of PMN was similar between the biomaterial and sham sites in the infected animals. The exudate cell gene expression also showed similar levels, except for IL-6 that was more expressed at sham sites. However, the total number of viable *S. epidermidis* peaked at 24 hours, with a reduction of more than 5×10^3 CFU around the implant materials at 72 hours, whereas the sham sites showed only a modest decrease ($<10^3$ CFU) between 24 and 72 hours. Based on these observations it appears that the host defence is just as effective in the presence of these modified and non-modified titanium implants as in their absence.

Nevertheless, from the perspective of bacterial persistence, it cannot be concluded that the "race for the surface" was won by the host defence since a considerable number of viable *S. epidermidis* were still present at the implant site after 72 hours. The importance of the biomaterial is likely to become more evident over time. The material may promote persistence of the bacteria and host defence cells may become exhausted trying to eliminate the material,[41,185,322] leading to an inability to deal with residing bacteria. In the present study, neither the killing efficiency of exudate cells nor the functional behaviour of the implant-adherent cells have been assessed. Previous studies performed in mice have demonstrated the persistence of *S. epidermidis* in the tissue rather than on the biomaterial.[284,323,324] The bacteria were co-localised with host inflammatory cells, and even within macrophages, at distances up to >30 cell layers away from the implant.[284,323] In addition, an increase of *S. epidermidis* within the peri-implant tissue was demonstrated between day 14 and day 21.[324] The latter results which were obtained after longer implantation periods indicate that the implant itself does not harbour the infection and that an immuno-incompetent zone may develop over time and may extend hundreds of micrometers away from the implant.

5.4.2 Host defence modulation by biomaterial surface properties

Another important issue is if and in what direction the material surface properties affect the host defence. Large chemical variations have previously been found to cause a difference both in short- and long-term tissue interactions.[308] In the present thesis relatively small modifications, on the nano level, were added to the material surfaces and investigated either *in vitro* (paper III) or *in vivo* (paper IV).

In the *in vitro* study (paper III) the exclusive effect of nanotopography on monocytes was assessed. Smooth gold surfaces were immobilised with 35–40 nm gold nanoparticles, thus enabling the analysis of effects caused solely by the nanotopography, without changing the elemental composition. However, when changing surface properties (e.g. topography) on the nano level, other surface properties such as surface energy and wettability will inevitably change as well,[95] which may influence the results. This was demonstrated in paper III, in which the AuNP surfaces presented a higher hydrophilicity than the smooth gold. The results showed no major differences in monocyte adhesion and activity between the nanostructured and the smooth gold surfaces. On the contrary, both monocyte adhesion and activity were modulated when comparing unstimulated cells with zymosan and *S. epidermidis* stimulated cells, depending on the substrate being of gold or of polystyrene. Monocytes on gold lost their attachment upon stimulation and induced a more rapid ROS response, whereas monocytes on polystyrene increased their attachment upon stimulation and had a higher production of total ROS. Tentatively, these effects may be related to the expression of specific receptors depending on material, although this was not confirmed by gene expression analysis of four integrins (β1, β2, αv and αM). A previous study has reported the monocyte/macrophage phagocytosis efficiency to be higher in adherent cells compared with those in suspension.[325] Given that monocytes leave the gold surface more readily than polystyrene when exposed to stimuli, potentially by engagement of the same receptors, this could explain the lower peak and the lower total amount of ROS produced by cells on gold chemistry.

The IL-10 cytokine secretion was modified on the AuNP surface upon zymosan stimulation, pointing towards an anti-inflammatory/regulatory effect induced by the nanotopography when monocytes were exposed to a fungal stimulus. An elevated IL-10 gene expression level due to the microbial stimulus was also seen *in vivo* (paper IV) after 72 hours, but did not differ depending on the presence of nanostructures. In contrast to microtopography, which in several studies has demonstrated pro-inflammatory effects on monocytes,[56,60,61], nanotopographic features have previously shown a reduction in inflammatory mediators compared with smooth surfaces.[53,64] However, the present observations *in vitro* and in soft tissues *in vivo* do not support the latter findings.

To the author's knowledge, the effect of nanotopography has not been examined in an infection model previously. In paper IV, two very similar nanotopographies with distinct surface chemistries were compared with their smooth counterpart. The noble metal coated titanium had Ag, Au and Pd nanodeposits on the surface, whereas an on-top sputtered titanium layer effectively shielded the noble metal components keeping similar nanosized features. Both nanotextured surfaces (nNoble, nTi) had features ranging from a few nanometers to approximately 200 nm, covering

approximately 40% of the surface. The *in vivo* effect of these modifications was not pronounced during the initial 72 hours of implantation studied. However, results pointed towards the initiation of a more intense host defence around the nNoble implants with an associated decrease in the number of viable *S. epidermidis* cells. In both infected and control animals, the nNoble implants were associated with the highest recruitment of inflammatory cells at 24 h, a higher proportion of PMN at 24 hours and an initially higher TNF-α expression compared with the other materials. In addition, the lowest amount of total viable *S. epidermidis* at both 24 and 72 hours was found on and around the nNoble implants. These factors indicate an effect of the noble metal chemistry in combination with nanotexture on the host defence around titanium surfaces. It is therefore suggested that the nNoble surface may elicit a two-way mechanism against bacteria *in vivo*: a *direct* antibacterial effect reducing the adhesion/viability of *S. epidermidis* and an *indirect* antibacterial effect by greater host cell recruitment and activity.

The relatively few significant differences between the materials in paper IV may be a consequence of too small differences between the materials (on the nano level), the use of a too high inoculum for evaluation of non-bactericidal materials, or the use of too few animals/observations. In general, the nanotopographic features used in the present thesis did not induce major effects on host defence cells *in vitro* nor *in vivo*. Instead, the chemistry of the implants appeared to generate more differences in host cell behaviour.

5.4.3 Bacteria modulation by biomaterial properties

Bacterial adhesion and biofilm formation are considered important steps in the development of BAI. The interactions that take place between a bacterial cell and the material surface can depend on a direct interaction with the surface via physico-chemical forces such as electronic charge and hydrophobic interactions, or indirectly via the adhesion to adsorbed proteins on the surface. Both *S. aureus* and *S. epidermidis* express multiple adhesins, recognising several common proteins (e.g. fibrinogen, collagen, elastin) adsorbed onto the implant or present in the extracellular matrix. In the present thesis both the direct (paper II and III, no proteins) and indirect (paper IV, adsorbed proteins from blood and tissue) bacteria–surface interactions have been studied.

In paper III, fluorescent viability staining demonstrated less live *S. epidermidis* adherent onto AuNP compared with smooth Au, with a greater effect when nanostructure coverage increased. Furthermore, the bacterial layers closest to the surface exhibited significantly more bacterial cell death on the nanostructured surface. Since the gold nanoparticle release was considered minimal, this suggested a bactericidal effect upon contact with the immobilised nanoparticles. Interestingly, a

recent paper investigating nanostructured black silicon, analogue to the wings of the dragonfly, demonstrated a direct bactericidal effect on both gram-negative (*P. aeruginosa*) and gram-positive bacteria (*S. aureus*) upon contact, with a killing efficiency of 10^5 CFU per minute and square centimetre.[326] The nanofeatures were rather densely packed, spiky nanoprotrusions with a height of 240 nm (dragonfly) or 500 nm (black silicon). The authors suggested the bactericidal activity to depend on deformational stresses inside the bacteria enforced by the surface nanoarchitecture. Although the nanostructures used in paper III were not spiky and of considerably smaller height, the study by Ivanova *et al.*[326] suggests that a bactericidal effect, even on the thicker cell wall of gram-positives, can be acquired solely by the use of nanostructured surfaces. Other explanations for the bactericidal effect in paper III relates to the increased hydrophilicity of the nanostructured surfaces since hydrophilic surfaces have shown decreased bacterial attachment and less biofilm formation,[224,229] and to the creation of confined microenvironments underneath the bacterial cell. Indeed, cross sections of *S. epidermidis* on nanostructured surfaces revealed few discrete attachment points of the bacterial cell wall to the nanostructures. Albeit speculative, bacterial attachment could create narrow volumes beneath the cell body, which may exhibit special conditions, e.g. through the accumulation of waste products, change of pH, limited flow of nutrients, which in turn may influence bacterial viability.

Another important observation in paper III was the preferential spread of *S. epidermidis* in the horizontal plane on the nanostructured surfaces (more surface area covered by bacteria), whereas thicker layers of bacterial cells and more mature biofilm towers were observed on the smooth surfaces. Furthermore, the formation of intercellular adhesions between bacterial cells, typical for the accumulation step in biofilm formation, was observed earlier on the smooth surfaces. These observations indicate the importance of future molecular studies to evaluate the temporal development of biofilm formation related to the expression of genes belonging to the *icaADBC* operon, which codes for the enzymes involved in the production of PIA. Other factors such as accumulation-associated protein (aap), extracellular matrix binding protein (embp) and teichoic acid, are also involved in the intercellular aggregation events.[212,327,328] It would also be of interest to study if the *in vivo* gene expression of these biofilm-related factors differs in *S. epidermidis* depending on their distribution (on the implant surface, in the exudate and in the tissue). A recent study, evaluating *S. epidermidis* biofilm-related gene expression on hydrophilic and hydrophobic polymers over time *in vitro*, has indicated an increase of ica genes as well as aap, primarily between 12 and 24 hours.[329] This was correlated with the intercellular aggregation and proliferation of *S. epidermidis* on the same materials as observed with SEM.[229] However, whereas hydrophobic surfaces promoted much more bacterial growth and slime production, the gene expression did not differ between the surfaces.

In paper II, the *in vitro* adhesion of *S. aureus* to noble metal coated titanium screws was inhibited by 99% compared to non-coated implants. Again, a protein-free media was used, showing direct effects of the surface. No assessment of the bacterial viability was made since only viable cells were counted, making it difficult to elucidate the exact mechanism of action. The anti-infectious effect of noble metal coatings, observed also in clinical settings with the use of catheters,[7,248] has previously been attributed to anti-adhesiveness and galvanic mechanisms. Minute amounts of silver released from the coating have been detected in the present studies, making it unlikely that the mechanism of action relies on ion or particle release to the surroundings. The topography of the coating may also be an important factor, similar to the antimicrobial effect seen for gold nanoparticles immobilised on the surface in paper III. Noble metal coatings have a wider size range of the nanostuctures (approximately 10–200 nm) and sharper edges compared with the nanostructured gold surfaces (35–40 nm), and the surface coverage has been shown to vary depending on the location on the implant (screw valleys versus screw peaks).

In the *in vivo* infection study (paper IV) it was difficult to detect any direct effect of the different material surface features on *S. epidermidis*. One reason for this was the limited number of bacterial cells detected on the bare surface. Instead, the bacterial cells were seen in contact with the fibrinous matrix and in contact with inflammatory cells. Round protrusions of the host cell membranes, observed with SEM, and clusters of bacterial cells inside host defence cells, detected by FISH, indicated bacterial ingestion by host cells resident on the surface and in the interface tissue. Furthermore, despite high background fluorescence some evidence of a co-localisation of FISH-stained bacterial cells with DAPI-stained nuclei was found using CLSM (data not shown). Hence, at the present stage it is assumed that any bactericidal effects of the surfaces *in vivo* were related to ingestion of *S. epidermidis* by phagocytes rather than due to a direct contact-killing effect by the biomaterial surface. However, lower amounts of surface associated bacteria, although not significantly different, were found on the noble metal coated surfaces (nNoble). As previously discussed, it is possible that the nNoble surface exert a pro-inflammatory effect that protects the implant against microorganisms by attracting and activating more inflammatory cells to the site.

Hitherto, the clinical use of noble metal coated medical devices has been focused on their external use (urinary catheters, endotracheal tubes) and blood-contacting devices (central venous catheters). Noble metal coatings have been shown to have lower levels of fibrinogen deposition, lower levels of thrombocyte depletion and thrombin/antithrombin generation, but similar levels of C3a deposition compared with titanium after 1 hour exposure to blood *in vitro*.[330] However, the different biological environment in paper IV (connective tissue) versus blood for a minimal time of 4 hours did not avoid fibrinogen-deposition on the surface according to SEM

observations, suggesting that the situation on a totally internal device may be different.

Taken together, the results show that nanostructured gold surfaces reduce *S. epidermidis* viability *in vitro*, possibly due to mechanical stress enforced on the bacterial cell wall. Alternatively, the reduced bacterial cell viability may be a result of an increased surface hydrophilicity or a change in the microenvironment in the confined volume beneath the attached bacteria. Furthermore, noble metal coated titanium surfaces decreased *S. aureus* adhesion *in vitro*, although the mechanism of action remains unclear. A similar nanotopographic effect as for gold is suggested, even though previously forwarded mechanisms such as anti-adhesiveness and nanogalvanism cannot be ruled out. Nevertheless, a protein rich tissue environment may have masked the effect seen by direct bacteria–nanotopography interaction, and may instead be related to an increased infiltration and activation of inflammatory cells.

5.4.4 Monocyte/Macrophage activation

Two different soluble stimuli were utilised to study the immune cell activation on and adjacent to the implant surfaces: live *S. epidermidis* (paper III, IV) and zymosan (paper III), a cell wall product from yeast commonly used as a non-living microbial stimulus/phagocytic prey.

Phagocytosis of the different stimuli was confirmed both *in vitro* (paper III) and *in vivo* (paper IV). In paper III, as judged by SEM observations, different internalisation patterns were seen for opsonised zymosan and opsonised *S. epidermidis*. Zymosan was frequently associated with cell membrane pseudopods reaching out for their prey, whereas *S. epidermidis* more often were located on the phagocyte membrane, both *in vitro* and *in vivo*, without seemingly much effort by the immune cell. Interestingly, distinct phagocytic mechanisms have been identified in the case of complement-opsonised and IgG-opsonised particles, which is coupled to the receptors that are engaged.[331] Complement-aided phagocytosis has been identified as a relatively passive process in which the particles appear to sink into the cell. Since the stimuli used in the present thesis were opsonised in active serum, either prior to the incubation with monocytes *in vitro* or upon blood/plasma contact after the bacterial injection *in vivo*, this could explain the apparent "passive" behaviour of inflammatory cells upon *S. epidermidis* contact. It also indicates that opsonised zymosan was detected by additional receptors on the monocytes, e.g. the mannose receptor (recognising mannan), Dectin-1 and the complement receptor type 3 (CR3) (recognising β-glucan).[332-334] Moreover, complement-mediated phagocytosis has been suggested not to trigger the release of ROS,[335] which may explain the lower chemiluminescence response to *S. epidermidis* compared with zymosan. On the other

hand, the interaction between glucan and CR3 was shown to be responsible for the chemiluminescence production of blood phagocytes in response to non-opsonised zymosan.[336]

Overall, the production of ROS was very low in response to both gold and polystyrene surfaces, but was markedly higher in response to opsonised zymosan compared with opsonised *S. epidermidis*, confirming previous observations by other research groups.[274] Opsonisation was also noted as a requirement for detection of ROS in response to *S. epidermidis*, suggesting that not only complement receptors, but possibly also Fc-receptors, recognised the opsonised bacteria. TLR2, by recognising peptidoglycan and lipoteichoic acid, may also contribute to ROS production against gram-positive bacteria.[191,337] Despite the higher ROS induction for zymosan, monocytes were seen fully packed with internalised *S. epidermidis* when analysing FIB-prepared cross sections of the cells. An additional difference between zymosan and *S. epidermidis* is the ability to "fight back" and protect themselves from degrading enzymes. An AMP sensor system has been found in *S. epidermidis*, enabling them to escape the action of AMPs and thereby survive and persist within the phagocytes.[216] Although the killing efficiency was not assessed in the present studies, bacteria have smart ways to avoid being killed in contrast to zymosan, which may further explain the relatively low ROS production by monocytes. Moreover, gene expression analysis of superoxide dismutase 2 (SOD2) and cytochrome b-245 (Nox2), both relevant for the cell oxidative metabolism, did not correlate with the ROS production as measured with chemiluminescence. Instead, SOD2 was significantly up-regulated in response to *S. epidermidis* in comparison to zymosan. Collectively, these results indicate that ROS measurements alone are not a sufficient method to assess monocyte/macrophage activation.

A major difference between *in vitro* and *in vivo* experiments is the interaction with other immune cells to achieve further activation. For example, monocytes/macrophages are effective phagocytising cells, but they need additional signals such as TNF-α and IFN-γ to increase their bactericidal effectiveness.[338-340] TNF-α is produced by macrophages upon microbial stimulation and may act in an autocrine manner, whereas IFN-γ is produced by T helper cells and NK cells. Recently, an *in vitro* study with immobilised LPS (microbial signal) and/or IFN-γ on PEG surfaces to direct macrophages towards classical activation was performed.[341] The results revealed higher bacterial killing when IFN-γ or IFN-γ and LPS, but not LPS alone, were present on the surfaces. However, the induced response subsided after 24 hours and was virtually absent at 72 hours, as judged by IL-12 and nitric oxide production. It was also shown that the phagocytic capacity was reduced when the killing efficiency increased.

Despite the higher ROS production of monocytes/macrophages when stimulated with zymosan, the pro-inflammatory gene expression and TNF-α secretion of adherent monocytes were higher after stimulation with *S. epidermidis*. After 1 hour of *S. epidermidis* stimulation of monocyte cultures *in vitro*, the pro-inflammatory gene expression was intensively induced (10–250 fold increase) compared to non-challenged cells on smooth Au, AuNP and TCP, whereas zymosan caused a lower up-regulation (5–70 fold increase). The highest increase was seen for IL-1β and the lowest for IL-6. Also inflammatory cells from *in vivo* exudates showed increased gene expression levels of pro-inflammatory cytokines after 4 hours co-culture with *S. epidermidis*, although with a much more modest increase compared with *in vitro* results (2–30 fold increase). Under *in vivo* conditions, the highest up-regulation was observed for IL-6. Differences in gene expression between *in vitro* and *in vivo* could be explained by the different time points analysed, the different cell types (mononuclear cells are much more active in signalling events than PMN) and the considerably lower bacterial dose *in vivo* compared with the *in vitro* experiments. However, in order for the pro-inflammatory cytokines to exert their action the mRNA has to be translated into proteins. Secreted cytokines were measured *in vitro* and showed an increase only for TNF-α upon *S. epidermidis* stimulation. The low secretion of IL-6 and IL-1β in response to the different stimuli is most likely due to a too short time period for protein synthesis and secretion by the monocytes.[342,343]

In summary, the activation of the inflammatory cells upon stimulation with *S. epidermidis* and zymosan was evident both *in vivo* and *in vitro*, as indicated by increased inflammatory cell recruitment, phagocytosis, increased production of ROS, increased gene expression and increased cytokine release. As discussed previously, the surface chemistry played a larger role in inflammatory cell behaviour than nanotopography in the present studies. However, the response levels of the cells were highly affected by the type of stimulus presented. Zymosan induced high ROS production whereas *S. epidermidis* induced higher gene transcription of pro-inflammatory cytokines and SOD, as well as TNF-α secretion.

6 SUMMARY AND CONCLUSION

In summary,

- Differently modified noble metal coatings applied on silicone and on titanium were biocompatible with appropriate tissue responses in bone and soft tissue.
- Depending on the combination of Ag, Au and Pd, noble metal coatings modulated inflammation and fibrosis during integration in soft tissue.
- Noble metal coated titanium implants decreased adhesion of *Staphylococcus aureus in vitro* and exhibited osseointegration and a comparable bone response to that of non-coated clinically used machined titanium screws.
- The presence of nanostructures (35–40 nm spherical protrusions) on gold chemistry decreased *Staphylococcus epidermidis* viability, especially in the layers closest to the surface, and resulted in less mature biofilms compared with smooth surfaces. Although the mechanism behind these effects was not clarified, a direct contact-killing effect by mechano-induced stress may be one cause.
- Monocyte activity upon exposure to either zymosan particles or *Staphylococcus epidermidis* was not affected by the presence of nanostructures (35–40 nm spherical protrusions on gold). Instead, the response of the monocytes was largely determined by the soluble stimulus.
- An *in vivo* infection model was developed, allowing a quantification of biological events in association with biomaterial-associated infections. Significantly higher inflammatory cell recruitment, cell activity and cell death was demonstrated in the presence of *Staphylococcus epidermidis*. Viable bacteria were to a higher degree detected in the exudate than on the implant.

In conclusion, nanostructured noble metal coatings are biocompatible in soft tissue and bone, opening up possibilities for new application areas. The anti-infectious potential of nanostructured coatings may partly be related to physical interactions between bacteria and the surface nanostructures and partly related to an intensified inflammatory response due to the material surface chemistry.

7 FUTURE PERSPECTIVES

The findings in the present thesis demonstrate biocompatibility of nanostructured noble metal coatings in soft tissue as well as in bone, which render them a suitable option in many new application areas. Noble metal coatings may be of particular interest in applications associated with higher infection risks, e.g. transcutaneous amputation prostheses and dental implants breaking the mucosal lining. However, prior to evaluating the coating in load-bearing situations, a proper assessment of biomechanical stability and long-term bone response needs to be conducted. It would also be of interest to evaluate the effectiveness of the coatings in an infectious model in bone.

The mechanism of action for the anti-infectious effect of noble metal coatings has still not been fully elucidated. Furthermore, on the background of a direct killing upon contact of *S. epidermidis* on nanopatterned gold surfaces, the mechanism for this effect is a highly interesting area in the future. An *in vitro* and *in vivo* assessment of coatings with single or combined noble metals and systematically modified nanopatterns would be of interest for detailed analysis of bacterial viability, biofilm formation and bacterial gene expression in relation to the different events in biofilm formation. Furthermore, the potential impact of proteins on the bacterial adhesion to the coatings may contribute to an increased understanding of the events that take place in different biological fluids *in vivo*. Another future approach is to determine the bacterial gene expression *in vivo* depending on their distribution, i.e. on the implant surface, in the exudate or in the tissue. Indications of an increased inflammatory response around noble metal coated titanium implants is an interesting finding, which motivates additional research on the initial events around the coatings, e.g. assessment of host cell bactericidal efficiency and bacterial cell gene expression. In addition, investigations of the late inflammatory response as well as the survival and location of bacteria strains of different virulence would be highly relevant in order to address the final outcome of the infection, as the presence of the biomaterial is likely to alter this result.

ACKNOWLEDGEMENTS

This thesis is spanning across multiple disciplines and could not have been realised without the profound knowledge and support from several individuals.

First and foremost, I would like to thank my main supervisor **Peter Thomsen**, for believing in me and for providing me with the wonderful opportunity to perform research within the field of biomaterials. Your encouragement, support and wide knowledge has meant a lot to me.

I am very grateful for advice, input and discussions with my co-supervisors. **Felicia Suska**, thank you for introducing me to the research at the department, for your excellent surgical skills and for your enthusiasm. **Jukka Lausmaa**, I appreciate your accuracy and your valuable input and ideas about the material science aspect of the research. And **Margarita Trobos**, I am thankful to you for introducing me to the complex world of microbiology and for sharing your knowledge and friendship.

A special thanks to all co-authors, for your expertise, time and efforts within selected parts of this project.

I am very grateful to Bactiguard AB for providing me with the opportunity to perform research on a project so closely linked to industry and clinical practice. A special thanks to **Mattias Ohrlander**, **Linda Persson**, **Gunilla Rydja** and **Helen Bäckros** for providing coated materials, fruitful discussions and enjoyable collaboration throughout the years.

Many of the material analyses have been performed by **Sarunas Petronis** and **Benny Lyvén** (co-authors) and also by **Per Borchardt**, **Emma Fransson**, **Marie Ernstsson** and **Hossein Agheli** who are gratefully acknowledged.

Thank you **Anders Palmquist**, for discussions about science and various other topics, and for the beautiful cross sections of my small cells! Thank you **Mats Hulander** for your positive attitude and for sharing your gold surfaces, **Magnus Forsberg** for helpful hands in the lab and nice company in Davos, and **Forugh Vazirisani** for indispensable help during late lab hours.

All help and guidance for both big and small things from the laboratory personnel, **Anna Johansson**, **Lena Emanuelsson**, **Birgitta Norlindh** and **Maria Hoffman**, are highly appreciated.

I would also like to thank former and present colleagues at the Department of Biomaterials at the University of Gothenburg, within the BIOMATCELL centre and the IBCT alpha project. Thank you all for creating an inspiring work environment and thereby contributing to the completion of this thesis. A special thanks to **Cecilia Granéli**, **Sofia Almquist**, **Maria Lennerås**, **Magdalena Zaborowska**, **Patrik Stenlund**, **Omar Omar**, **Karin Ekström**, **Xiaoqin Wang**, **Necati Hermankaya**, **Giuseppe De Peppo** and **Victoria Fröjd** for friendship, laughs, energy and for always being helpful. Thanks also to **Maria Utterhall** and **Magnus Wassenius** for help with administrative matters and a special thanks to **Annika Juhlin** for careful proof reading of this thesis.

I am also grateful to the staff at the Electron Microscopy Unit for introducing me to the fine art of electron microscopy.

Last but not least, I would like to thank my family and friends for spreading joy and energy in my life. A special thanks to my parents, **Berit** and **Lars**, for always encouraging education, for love and support throughout my life and never failing baby-sitting assistance during these last few years. And to my brother **Johan**, for statistical advice, encouragement and putting things into perspective.

Finally, **Anton**, I am most grateful for all your love, support and for always being there for me during these past years. And **Noel**, my little prince and sunshine, for making me enjoy life so much more and appreciate the small things in life.

This research has been supported by the BIOMATCELL VINN Excellence Center of Biomaterials and Cell Therapy, the Swedish Research Council (K2012-52X-09495-25-3), the Västra Götaland Region, the Materials Area of Advance (SFO) at Chalmers and University of Gothenburg, the Hjalmar Svensson Foundation, the Adlerbertska Foundation and the IngaBritt and Arne Lundberg Foundation.

REFERENCES

1. Williams DF. *The Williams dictionary of biomaterials*. Liverpool, UK: Liverpool University Press; 1999.
2. Branemark PI, *et al.* Osseointegrated implants in the treatment of the edentulous jaw. Experience from a 10-year period. *Scand. J. Plast. Reconstr. Surg. Suppl.* 1977;16:1-132.
3. Campoccia D, *et al.* A review of the clinical implications of anti-infective biomaterials and infection-resistant surfaces. *Biomaterials*. Nov 2013;34(33):8018-29.
4. Gristina AG. Implant failure and the immuno-incompetent fibro-inflammatory zone. *Clin. Orthop.* Jan 1994(298):106-18.
5. Ceri H, *et al.* The Calgary Biofilm Device: new technology for rapid determination of antibiotic susceptibilities of bacterial biofilms. *J. Clin. Microbiol.* Jun 1999;37(6):1771-6.
6. Schwank S, *et al.* Impact of bacterial biofilm formation on in vitro and in vivo activities of antibiotics. *Antimicrob. Agents Chemother.* Apr 1998;42(4):895-8.
7. Schumm K, Lam Thomas BL. Types of urethral catheters for management of short-term voiding problems in hospitalised adults. *Cochrane Database Syst. Rev.* 2009(2).
8. Darouiche RO. Device-associated infections: a macroproblem that starts with microadherence. *Clin. Infect. Dis.* Nov 1 2001;33(9):1567-72.
9. Gordon RJ, *et al.* Ventricular assist device-related infections. *Lancet Infect. Dis.* 2006;6(7):426-37.
10. Hranjec T, *et al.* Surgical site infection prevention: How we do it. *Surgical Infections.* 2010;11(3):289-94.
11. Safdar N, *et al.* Clinical and economic consequences of ventilator-associated pneumonia: A systematic review. *Crit. Care Med.* 2005;33(10):2184-93.
12. Baddour LM, *et al.* Nonvalvular cardiovascular device-related infections. *Circulation.* Oct 21 2003;108(16):2015-31.
13. Attenello FJ, *et al.* Hospital costs associated with shunt infections in patients receiving antibiotic-impregnated shunt catheters versus standard shunt catheters. *Neurosurgery.* Feb 2010;66(2):284-9.
14. Morgan PB, *et al.* Incidence of keratitis of varying severity among contact lens wearers. *Br. J. Ophthalmol.* 2005;89(4):430-36.
15. Hughes DS, Hill RJ. Infectious endophthalmitis after cataract surgery. *Br. J. Ophthalmol.* Mar 1994;78(3):227-32.
16. Garellick G, *et al. Svenska höftprotesregistret. Årsrapport 2012.* Oct 2013 2013. ISBN: 978-91-980507-2-1.
17. Stefansdottir A. *The infected knee arthroplasty*. Lund: Department of Orthopaedics, Clinical Sciences Lund, Lund University, Sweden; 2010.
18. Young S, *et al.* Low infection rates after 34,361 intramedullary nail operations in 55 low- and middle-income countries: validation of the Surgical Implant Generation Network (SIGN) online surgical database. *Acta Orthop.* Dec 2011;82(6):737-43.
19. Diegelmann RF, Evans MC. Wound healing: an overview of acute, fibrotic and delayed healing. *Front. Biosci.* Jan 1 2004;9:283-9.
20. Laurens N, *et al.* Fibrin structure and wound healing. *J. Thromb. Haemost.* 2006;4(5):932-39.

21. Clark RAF. *The molecular and cellular biology of wound repair.* 2 ed. New York: Plenum Press; 1996.
22. Artuc M, *et al.* Mast cells and their mediators in cutaneous wound healing--active participants or innocent bystanders? *Exp. Dermatol.* Feb 1999;8(1):1-16.
23. Ryan GB, Majno G. Acute inflammation. *Am. J. Pathol.* 1977;86(1):183-276.
24. Fantone JC, Ward PA. Polymorphonuclear leukocyte-mediated cell and tissue injury: Oxygen metabolites and their relations to human disease. *Hum. Pathol.* 1985;16(10):973-78.
25. Fox S, *et al.* Neutrophil apoptosis: relevance to the innate immune response and inflammatory disease. *J. Innate Immun.* 2010;2(3):216-27.
26. Willenborg S, Eming SA. Macrophages - sensors and effectors coordinating skin damage and repair. *J. Dtsch. Dermatol. Ges.* Mar 2014;12(3):214-21.
27. Singer AJ, Clark RA. Cutaneous wound healing. *N. Engl. J. Med.* Sep 2 1999;341(10):738-46.
28. Park JE, Barbul A. Understanding the role of immune regulation in wound healing. *Am. J. Surg.* 2004;187(5 SUPPL. 1):11S-16S.
29. Johnston RB, Jr. Current concepts: immunology. Monocytes and macrophages. *N. Engl. J. Med.* Mar 24 1988;318(12):747-52.
30. Anderson JM. Chapter 4 Mechanisms of inflammation and infection with implanted devices. *Cardiovascular Pathology.* 1993;2(3 SUPPL.):33-41.
31. Sadana A. Protein adsorption and inactivation on surfaces. Influence of heterogeneities. *Chem. Rev.* 1992;92(8):1799-818.
32. Nakanishi K, *et al.* On the adsorption of proteins on solid surfaces, a common but very complicated phenomenon. *J. Biosci. Bioeng.* 2001;91(3):233-44.
33. Koegler P, *et al.* The influence of nanostructured materials on biointerfacial interactions. *Adv Drug Deliv Rev.* Dec 2012;64(15):1820-39.
34. Roach P, *et al.* Surface tailoring for controlled protein adsorption: effect of topography at the nanometer scale and chemistry. *J. Am. Chem. Soc.* Mar 29 2006;128(12):3939-45.
35. Holgers K-M, *et al.* Titanium in soft tissues. In: Brunette DM, Tengvall P, Textor M, Thomsen P, eds. *Titanium in medicine*. Berlin: Springer Verlag; 2001:513-60.
36. Veerman ECI, *et al.* SDS-PAGE analysis of the protein layers adsorbing in vivo and in vitro to bone substituting materials. *Biomaterials.* 1987;8(6):442-48.
37. Anderson JM, *et al.* Foreign body reaction to biomaterials. *Semin. Immunol.* 2008;20(2):86-100.
38. Rosengren A, *et al.* Immunohistochemical studies on the distribution of albumin, fibrinogen, fibronectin, IgG and collagen around PTFE and titanium implants. *Biomaterials.* Sep 1996;17(18):1779-86.
39. Rosengren A, *et al.* Method for immunolocalization of extracellular proteins in association with the implant-soft tissue interface. *Biomaterials.* 1994;15(1):17-24.
40. Eriksson AS, *et al.* Distribution of cells in soft tissue and fluid space around hollow and solid implants in the rat. *J. Mater. Sci.: Mater. Med.* 1994;5(5):269-78.
41. Henson PM. The immunologic release of constituents from neutrophil leukocytes. II. Mechanisms of release during phagocytosis, and adherence to nonphagocytosable surfaces. *J. Immunol.* Dec 1971;107(6):1547-57.
42. Henson PM. Mechanisms of exocytosis in phagocytic inflammatory cells. Parke-Davis Award Lecture. *Am. J. Pathol.* Dec 1980;101(3):494-511.

43. Gretzer C, *et al.* H2O2 production by cells on titanium and polystyrene surfaces using an in vivo model of exudate and surface related cell function. *J. Mater. Sci. Mater. Med.* Aug 2002;13(8):735-43.
44. Rosengren A, *et al.* Tissue reactions evoked by porous and plane surfaces made out of silicon and titanium. *IEEE Trans. Biomed. Eng.* Apr 2002;49(4):392-9.
45. Madden LR, *et al.* Proangiogenic scaffolds as functional templates for cardiac tissue engineering. *Proc. Natl. Acad. Sci. U. S. A.* Aug 24 2010;107(34):15211-6.
46. Parker JA, *et al.* Soft-tissue response to silicone and poly-L-lactic acid implants with a periodic or random surface micropattern. *J. Biomed. Mater. Res.* Jul 2002;61(1):91-8.
47. Rosengren A, *et al.* Tissue reactions to polyethylene implants with different surface topography. *J. Mater. Sci. Mater. Med.* Feb 1999;10(2):75-82.
48. Rosengren A, *et al.* Reactive capsule formation around soft-tissue implants is related to cell necrosis. *J. Biomed. Mater. Res.* Sep 15 1999;46(4):458-64.
49. Smith GC, *et al.* Soft tissue response to titanium dioxide nanotube modified implants. *Acta Biomater.* Aug 2011;7(8):3209-15.
50. Suska F, *et al.* Fibrous capsule formation around titanium and copper. *J. Biomed. Mater. Res. A.* Jun 15 2008;85(4):888-96.
51. Parker JA, *et al.* The effect of bone anchoring and micro-grooves on the soft tissue reaction to implants. *Biomaterials.* Sep 2002;23(18):3887-96.
52. Thomsen P, Gretzer C. Macrophage interactions with modified material surfaces. *Curr. Opin. Solid State Mater. Sci.* 2001;5(2-3):163-76.
53. Ainslie KM, *et al.* In vitro inflammatory response of nanostructured titania, silicon oxide, and polycaprolactone. *J. Biomed. Mater. Res. A.* Dec 2009;91(3):647-55.
54. Sethi RK, *et al.* Macrophage response to cross-linked and conventional UHMWPE. *Biomaterials.* Jul 2003;24(15):2561-73.
55. Bhardwaj RS, *et al.* Role of HSP70i in regulation of biomaterial-induced activation of human monocytes-derived macrophages in culture. *J. Mater. Sci.: Mater. Med.* Feb 2001;12(2):97-106.
56. Hamlet S, *et al.* The effect of hydrophilic titanium surface modification on macrophage inflammatory cytokine gene expression. *Clin. Oral Implants Res.* May 2012;23(5):584-90.
57. Suska F, *et al.* Monocyte viability on titanium and copper coated titanium. *Biomaterials.* Oct 2005;26(30):5942-50.
58. Gretzer C, *et al.* Adhesion, apoptosis and cytokine release of human mononuclear cells cultured on degradable poly(urethane urea), polystyrene and titanium in vitro. *Biomaterials.* Aug 2003;24(17):2843-52.
59. Quabius ES, *et al.* Dental implants stimulate expression of Interleukin-8 and its receptor in human blood - An in vitro approach. *J. Biomed. Mater. Res. B Appl. Biomater.* 2012;100 B(5):1283-88.
60. Ainslie KM, *et al.* In vitro immunogenicity of silicon-based micro- and nanostructured surfaces. *ACS Nano.* May 2008;2(5):1076-84.
61. Bota PC, *et al.* Biomaterial topography alters healing in vivo and monocyte/macrophage activation in vitro. *J. Biomed. Mater. Res. A.* Nov 2010;95(2):649-57.
62. Khang D, *et al.* Reduced responses of macrophages on nanometer surface features of altered alumina crystalline phases. *Acta Biomater.* Jun 2009;5(5):1425-32.
63. Wojciak-Stothard B, *et al.* Guidance and activation of murine macrophages by nanometric scale topography. *Exp. Cell Res.* Mar 15 1996;223(2):426-35.

64. Lee S, *et al.* Analysis on migration and activation of live macrophages on transparent flat and nanostructured titanium. *Acta Biomater.* May 2011;7(5):2337-44.
65. Rajyalakshmi A, *et al.* Reduced adhesion of macrophages on anodized titanium with select nanotube surface features. *Int. J. Nanomedicine.* 2011;6:1765-71.
66. Chamberlain LM, *et al.* Macrophage Inflammatory Response to TiO2 Nanotube Surfaces. *J. Biomater. Nanobiotechnol.* 2011(2):293-300.
67. Ferraz N, *et al.* Nanoporosity of alumina surfaces induces different patterns of activation in adhering monocytes/macrophages. *Int J Biomater.* 2010;2010:402715.
68. Karlsson M, *et al.* Nanoporous aluminum oxide affects neutrophil behaviour. *Microsc. Res. Tech.* Apr 1 2004;63(5):259-65.
69. Rice JM, *et al.* Quantitative assessment of the response of primary derived human osteoblasts and macrophages to a range of nanotopography surfaces in a single culture model in vitro. *Biomaterials.* Nov 2003;24(26):4799-818.
70. Mohiuddin M, *et al.* Control of growth and inflammatory response of macrophages and foam cells with nanotopography. *Nanoscale Res Lett.* 2012;7(1):394.
71. Meredith DO, *et al.* Human fibroblast reactions to standard and electropolished titanium and Ti-6Al-7Nb, and electropolished stainless steel. *J. Biomed. Mater. Res. A.* Dec 1 2005;75(3):541-55.
72. Kim SJ, *et al.* Evaluation of the biocompatibility of a coating material for an implantable bladder volume sensor. *Kaohsiung J. Med. Sci.* 2012;28(3):123-29.
73. Wrzeszcz A, *et al.* Dexamethasone released from cochlear implant coatings combined with a protein repellent hydrogel layer inhibits fibroblast proliferation. *J. Biomed. Mater. Res. A.* 2014;102(2):442-54.
74. Mirzadeh H, *et al.* Effect of silicon rubber crosslink density on fibroblast cell behavior in vitro. *J. Biomed. Mater. Res. A.* 2003;67(3):727-32.
75. Oakley C, Brunette DM. Topographic compensation: Guidance and directed locomotion of fibroblasts on grooved micromachined substrata in the absence of microtubules. *Cell Motil. Cytoskelet.* 1995;31(1):45-58.
76. Meyle J, *et al.* Surface micromorphology and cellular interactions. *J. Biomater. Appl.* 1993;7(4):362-74.
77. Oakley C, *et al.* Sensitivity of fibroblasts and their cytoskeletons to substratum topographies: Topographic guidance and topographic compensation by micromachined grooves of different dimensions. *Exp. Cell Res.* 1997;234(2):413-24.
78. Cousins BG, *et al.* The effect of silica nanoparticulate coatings on cellular response. *J. Mater. Sci.: Mater. Med.* 2004;15(4):355-59.
79. Curtis AS, *et al.* Cells react to nanoscale order and symmetry in their surroundings. *IEEE Trans. Nanobioscience.* Mar 2004;3(1):61-5.
80. Curtis ASG, *et al.* Substratum nanotopography and the adhesion of biological cells. Are symmetry or regularity of nanotopography important? *Biophys. Chem.* 2001;94(3):275-83.
81. Dalby MJ, *et al.* Polymer-demixed nanotopography: Control of fibroblast spreading and proliferation. *Tissue Eng.* 2002;8(6):1099-108.
82. Dalby MJ, *et al.* Rapid fibroblast adhesion to 27 nm high polymer demixed nano-topography. *Biomaterials.* Jan 2004;25(1):77-83.

83. Dalby MJ, *et al.* Increasing fibroblast response to materials using nanotopography: Morphological and genetic measurements of cell response to 13-nm-high polymer demixed islands. *Exp. Cell Res.* 2002;276(1):1-9.
84. Suska F, *et al.* In vivo/ex vivo cellular interactions with titanium and copper. *J. Mater. Sci.* Oct-Dec 2001;12(10-12):939-44.
85. Suska F, *et al.* IL-1alpha, IL-1beta and TNF-alpha secretion during in vivo/ex vivo cellular interactions with titanium and copper. *Biomaterials.* Feb 2003;24(3):461-8.
86. Suska F, *et al.* In vivo cytokine secretion and NF-kappaB activation around titanium and copper implants. *Biomaterials.* Feb 2005;26(5):519-27.
87. Johansson CB, *et al.* A quantitative comparison of the cell response to commercially pure titanium and Ti-6Al-4V implants in the abdominal wall of rats. *J. Mater. Sci.: Mater. Med.* 1992;3(2):126-36.
88. Eriksson AS, *et al.* Hollow implants in soft tissues allowing quantitative studies of cells and fluid at the implant interface. *Biomaterials.* Jan 1988;9(1):86-90.
89. Rosengren A, *et al.* Analysis of the inflammatory response to titanium and PTFE implants in soft tissue by macrophage phenotype quantification. *J. Mater. Sci.: Mater. Med.* 1998;9(7):415-20.
90. Kalltorp M, *et al.* In vivo cell recruitment, cytokine release and chemiluminescence response at gold, and thiol functionalized surfaces. *Biomaterials.* Nov 1999;20(22):2123-37.
91. Källtorp M. *Protein, cell and soft tissue interactions with thiol functionalized gold surfaces*. Göteborg, Sweden: Department of Biomaterials, Institute of Anatomy and Cell Biology, Göteborg University; 1999.
92. Ungersböck A, *et al.* Evaluation of the soft tissue interface at titanium implants with different surface treatments: experimental study on rabbits. *Biomed. Mater. Eng.* 1994;4(4):317-25.
93. Bryers JD, *et al.* Engineering biomaterials to integrate and heal: the biocompatibility paradigm shifts. *Biotechnol. Bioeng.* Aug 2012;109(8):1898-911.
94. Sussman EM, *et al.* Porous implants modulate healing and induce shifts in local macrophage polarization in the foreign body reaction. *Ann. Biomed. Eng.* Nov 19 2013.
95. Riehemann K, *et al.* Nanomedicine--challenge and perspectives. *Angewandte Chemie (International Edition in English).* 2009;48(5):872-97.
96. Marsell R, Einhorn TA. The biology of fracture healing. *Injury.* 2011;42(6):551-55.
97. Bolander ME. Regulation of fracture repair by growth factors. *Proc. Soc. Exp. Biol. Med.* Jun 1992;200(2):165-70.
98. Dimitriou R, *et al.* Current concepts of molecular aspects of bone healing. *Injury.* Dec 2005;36(12):1392-404.
99. Cho TJ, *et al.* Differential temporal expression of members of the transforming growth factor beta superfamily during murine fracture healing. *J. Bone Miner. Res.* Mar 2002;17(3):513-20.
100. Gerstenfeld LC, *et al.* Fracture healing as a post-natal developmental process: molecular, spatial, and temporal aspects of its regulation. *J. Cell. Biochem.* Apr 1 2003;88(5):873-84.
101. Tsukamoto T, *et al.* Platelet-derived growth factor B chain homodimer enhances chemotaxis and DNA synthesis in normal osteoblast-like cells (MC3T3-E1). *Biochem. Biophys. Res. Commun.* Mar 29 1991;175(3):745-51.
102. Oprea WE, *et al.* Effect of platelet releasate on bone cell migration and recruitment in vitro. *J. Craniofac. Surg.* May 2003;14(3):292-300.

103. Sfeir C, *et al.* Fracture repair. In: Lieberman JR, Frieadlaender GE, eds. Totowa, NJ: Humana Press; 2005:21-44.
104. Kon T, *et al.* Expression of osteoprotegerin, receptor activator of NF-kappaB ligand (osteoprotegerin ligand) and related proinflammatory cytokines during fracture healing. *J. Bone Miner. Res.* Jun 2001;16(6):1004-14.
105. Schindeler A, *et al.* Bone remodeling during fracture repair: The cellular picture. *Semin. Cell Dev. Biol.* Oct 2008;19(5):459-66.
106. Deschaseaux F, *et al.* Mechanisms of bone repair and regeneration. *Trends Mol. Med.* Sep 2009;15(9):417-29.
107. Einhorn TA. The cell and molecular biology of fracture healing. *Clin. Orthop.* Oct 1998;355(355 Suppl):S7-21.
108. Ai-Aql ZS, *et al.* Molecular mechanisms controlling bone formation during fracture healing and distraction osteogenesis. *J. Dent. Res.* Feb 2008;87(2):107-18.
109. Keramaris NC, *et al.* Fracture vascularity and bone healing: a systematic review of the role of VEGF. *Injury.* Sep 2008;39 Suppl 2(2):S45-57.
110. Takahashi N, *et al.* A new member of tumor necrosis factor ligand family, ODF/OPGL/TRANCE/RANKL, regulates osteoclast differentiation and function. *Biochem. Biophys. Res. Commun.* Mar 24 1999;256(3):449-55.
111. Katagiri T, Takahashi N. Regulatory mechanisms of osteoblast and osteoclast differentiation. *Oral Dis.* May 2002;8(3):147-59.
112. Larsson C, *et al.* The titanium-bone interface in vivo. In: Brunette DM, Tengvall P, Textor M, Thomsen P, eds. *Titanium in medicine*. Berlin: Springer Verlag; 2001:587-648.
113. Wennerberg A, Albrektsson T. Effects of titanium surface topography on bone integration: a systematic review. *Clin. Oral Implants Res.* Sep 2009;20(Suppl 4):172-84.
114. Masuda T, *et al.* Generalizations regarding the process and phenomenon of osseointegration. Part I. In vivo studies. *Int. J. Oral Maxillofac. Implants.* Jan-Feb 1998;13(1):17-29.
115. Davies JE. Understanding peri-implant endosseous healing. *J. Dent. Educ.* Aug 2003;67(8):932-49.
116. Palmquist A, *et al.* Titanium oral implants: surface characteristics, interface biology and clinical outcome. *J. R. Soc. Interface.* Oct 6 2010;7 Suppl 5:S515-27.
117. Anderson JM. Inflammation, wound healing, and the foreign-body response. In: Ratner BD, Hoffmann AS, Schoen FJ, Lemons JE, eds. *Biomaterials science: An introduction to materials in medicine*. San Diego, California: Elsevier Academic Press; 2004:296-304.
118. Tang Y, *et al.* TGF-beta1-induced migration of bone mesenchymal stem cells couples bone resorption with formation. *Nat. Med.* Jul 2009;15(7):757-65.
119. Gerstenfeld LC, *et al.* Impaired intramembranous bone formation during bone repair in the absence of tumor necrosis factor-alpha signaling. *Cells Tissues Organs.* 2001;169(3):285-94.
120. Omar O, *et al.* In vivo gene expression in response to anodically oxidized versus machined titanium implants. *J. Biomed. Mater. Res. A.* Mar 15 2010;92(4):1552-66.
121. Sennerby L, *et al.* Early tissue response to titanium implants inserted in rabbit cortical bone. Part II. Ultrastructural observations. *J. Mater. Sci.: Mater. Med.* 1993;4(5):494-502.
122. Cooper LF. Biologic determinants of bone formation for osseointegration: clues for future clinical improvements. *J. Prosthet. Dent.* Oct 1998;80(4):439-49.
123. Sennerby L, *et al.* Early tissue response to titanium implants inserted in rabbit cortical bone. Part I. Light microscopic observations. *J. Mater. Sci.: Mater. Med.* 1993;4(3):240-50.

124. Grandfield K, *et al.* Visualizing biointerfaces in three dimensions: electron tomography of the bone-hydroxyapatite interface. *J. R. Soc. Interface.* Oct 6 2010;7(51):1497-501.
125. Grandfield K, *et al.* Where bone meets implant: the characterization of nano-osseointegration. *Nanoscale.* May 21 2013;5(10):4302-8.
126. Thorfve A, *et al.* Hydroxyapatite coating affects the Wnt signaling pathway during peri-implant healing in vivo. *Acta Biomater.* Mar 2014;10(3):1451-62.
127. Palmquist A, *et al.* Biomechanical, histological and ultrastructural analyses of laser micro- and nano-structured titanium implant after 6 months in rabbit. *J. Biomed. Mater. Res. B Appl. Biomater.* May 2011;97(2):289-98.
128. Pilliar RM, *et al.* Observations on the effect of movement on bone ingrowth into porous-surfaced implants. *Clin. Orthop.* Jul 1986;208(208):108-13.
129. Kuzyk PR, Schemitsch EH. The basic science of peri-implant bone healing. *Indian J Orthop.* Mar 2011;45(2):108-15.
130. Branemark R, *et al.* Biomechanical characterization of osseointegration during healing: an experimental in vivo study in the rat. *Biomaterials.* Jul 1997;18(14):969-78.
131. Monsees TK, *et al.* Effects of different titanium alloys and nanosize surface patterning on adhesion, differentiation, and orientation of osteoblast-like cells. *Cells Tissues Organs.* 2005;180(2):81-95.
132. Lincks J, *et al.* Response of MG63 osteoblast-like cells to titanium and titanium alloy is dependent on surface roughness and composition. *Biomaterials.* Dec 1998;19(23):2219-32.
133. Ahmad M, *et al.* An in vitro model for mineralization of human osteoblast-like cells on implant materials. *Biomaterials.* Feb 1999;20(3):211-20.
134. Matsuzaka K, *et al.* The effect of poly-L-lactic acid with parallel surface micro groove on osteoblast-like cells in vitro. *Biomaterials.* Jul 1999;20(14):1293-301.
135. Liao H, *et al.* Response of rat osteoblast-like cells to microstructured model surfaces in vitro. *Biomaterials.* Feb 2003;24(4):649-54.
136. Ozawa S, Kasugai S. Evaluation of implant materials (hydroxyapatite, glass-ceramics, titanium) in rat bone marrow stromal cell culture. *Biomaterials.* Jan 1996;17(1):23-9.
137. Schwartz Z, *et al.* Effect of micrometer-scale roughness of the surface of Ti6Al4V pedicle screws in vitro and in vivo. *J. Bone Joint Surg. Am.* Nov 2008;90(11):2485-98.
138. Mendonca G, *et al.* Advancing dental implant surface technology--from micron- to nanotopography. *Biomaterials.* Oct 2008;29(28):3822-35.
139. Lord MS, *et al.* Influence of nanoscale surface topography on protein adsorption and cellular response. *Nano Today.* 2010;5(1):66-78.
140. Elias KL, *et al.* Enhanced functions of osteoblasts on nanometer diameter carbon fibers. *Biomaterials.* 2002;23(15):3279-87.
141. Popat KC, *et al.* Osteogenic differentiation of marrow stromal cells cultured on nanoporous alumina surfaces. *J. Biomed. Mater. Res. A.* 2007;80(4):955-64.
142. Popat KC, *et al.* Influence of engineered titania nanotubular surfaces on bone cells. *Biomaterials.* 2007;28(21):3188-97.
143. Boyan BD, *et al.* Osteoblasts generate an osteogenic microenvironment when grown on surfaces with rough microtopographies. *Eur. Cell. Mater.* Oct 24 2003;6:22-7.
144. Kunzler TP, *et al.* Systematic study of osteoblast response to nanotopography by means of nanoparticle-density gradients. *Biomaterials.* Nov 2007;28(33):5000-6.

145. Webster TJ, Ejiofor JU. Increased osteoblast adhesion on nanophase metals: Ti, Ti6Al4V, and CoCrMo. *Biomaterials.* Aug 2004;25(19):4731-9.
146. Advincula MC, *et al.* Osteoblast adhesion and matrix mineralization on sol-gel-derived titanium oxide. *Biomaterials.* 2006;27(10):2201-12.
147. Dalby MJ, *et al.* The control of human mesenchymal cell differentiation using nanoscale symmetry and disorder. *Nat. Mater.* Dec 2007;6(12):997-1003.
148. Kubo K, *et al.* Cellular behavior on TiO2 nanonodular structures in a micro-to-nanoscale hierarchy model. *Biomaterials.* Oct 2009;30(29):5319-29.
149. Johansson CB, *et al.* A quantitative comparison of machined commercially pure titanium and titanium-aluminum-vanadium implants in rabbit bone. *Int. J. Oral Maxillofac. Implants.* May-Jun 1998;13(3):315-21.
150. Johansson CB, *et al.* Commercially pure titanium and Ti6A14V implants with and without nitrogen-ion implantation: Surface characterization and quantitative studies in rabbit cortical bone. *J. Mater. Sci.: Mater. Med.* 1993;4(2):132-41.
151. Thomsen P, *et al.* Structure of the interface between rabbit cortical bone and implants of gold, zirconium and titanium. *J. Mater. Sci.: Mater. Med.* Nov 1997;8(11):653-65.
152. Jinno T, *et al.* Osseointegration of surface-blasted implants made of titanium alloy and cobalt-chromium alloy in a rabbit intramedullary model. *J. Biomed. Mater. Res.* 1998;42(1):20-29.
153. Cook SD, *et al.* Hydroxyapatite-coated titanium for orthopedic implant applications. *Clin. Orthop.* Jul 1988;232(232):225-43.
154. Vidigal GM, Jr., *et al.* Histomorphometric analyses of hydroxyapatite-coated and uncoated titanium dental implants in rabbit cortical bone. *Implant Dent.* 1999;8(3):295-302.
155. Le Guéhennec L, *et al.* Surface treatments of titanium dental implants for rapid osseointegration. *Dent. Mater.* Jul 2007;23(7):844-54.
156. Shalabi MM, *et al.* Implant surface roughness and bone healing: a systematic review. *J. Dent. Res.* Jun 2006;85(6):496-500.
157. Gotfredsen K, *et al.* Histomorphometric and removal torque analysis for TiO2-blasted titanium implants. An experimental study on dogs. *Clin. Oral Implants Res.* 1992;3(2):77-84.
158. Wennerberg A, *et al.* A histomorphometric and removal torque study of screw-shaped titanium implants with three different surface topographies. *Clin. Oral Implants Res.* 1995;6(1):24-30.
159. Wennerberg A, *et al.* Bone Tissue Response to Commercially Pure Titanium Implants Blasted with Fine and Coarse Particles of Aluminum Oxide. *Int. J. Oral Maxillofac. Implants.* 1996;11(1):38-45.
160. Branemark R, *et al.* Bone response to laser-induced micro- and nano-size titanium surface features. *Nanomed.* Apr 2011;7(2):220-7.
161. Lavenus S, *et al.* Cell differentiation and osseointegration influenced by nanoscale anodized titanium surfaces. *Nanomedicine (Lond).* Jul 2012;7(7):967-80.
162. Guo J, *et al.* The effect of hydrofluoric acid treatment of TiO2 grit blasted titanium implants on adherent osteoblast gene expression in vitro and in vivo. *Biomaterials.* Dec 2007;28(36):5418-25.
163. Berglundh T, *et al.* Bone healing at implants with a fluoride-modified surface: an experimental study in dogs. *Clin. Oral Implants Res.* Apr 2007;18(2):147-52.
164. Mendes VC, *et al.* Discrete calcium phosphate nanocrystalline deposition enhances osteoconduction on titanium-based implant surfaces. *J. Biomed. Mater. Res. A.* Aug 2009;90(2):577-85.

165. Meirelles L, *et al.* Nano hydroxyapatite structures influence early bone formation. *J. Biomed. Mater. Res. A.* Nov 2008;87(2):299-307.
166. Meirelles L, *et al.* Effect of hydroxyapatite and titania nanostructures on early in vivo bone response. *Clin. Implant Dent. Relat. Res.* Dec 2008;10(4):245-54.
167. Meirelles L, *et al.* Bone reaction to nano hydroxyapatite modified titanium implants placed in a gap-healing model. *J. Biomed. Mater. Res. A.* Dec 1 2008;87(3):624-31.
168. Schouten C, *et al.* In vivo bone response and mechanical evaluation of electrosprayed CaP nanoparticle coatings using the iliac crest of goats as an implantation model. *Acta Biomater.* Jun 2010;6(6):2227-36.
169. Ballo A, *et al.* Nanostructured model implants for in vivo studies: influence of well-defined nanotopography on de novo bone formation on titanium implants. *Int. J. Nanomedicine.* 2011;6:3415-28.
170. Darouiche RO. Treatment of infections associated with surgical implants. *N. Engl. J. Med.* Apr 1 2004;350(14):1422-9.
171. Grainger DW, *et al.* Critical factors in the translation of improved antimicrobial strategies for medical implants and devices. *Biomaterials.* 2013;34(37):9237-43.
172. Stocks G, Janssen HF. Infection in patients after implantation of an orthopedic device. *ASAIO J.* Nov-Dec 2000;46(6):S41-6.
173. Singhal AK, *et al.* Recent advances in management of intravascular catheter related infections. *Indian Journal of Medical and Paediatric Oncology.* 2005;26(1):31-40.
174. Kärrholm J. The swedish hip arthroplasty register (http://www.shpr.se). *Acta Orthop.* Feb 2010;81(1):3-4.
175. Wilson SK, Costerton JW. Biofilm and penile prosthesis infections in the era of coated implants: a review. *J. Sex. Med.* Jan 2012;9(1):44-53.
176. Busscher HJ, *et al.* Biomaterial-associated infection: locating the finish line in the race for the surface. *Sci. Transl. Med.* Sep 26 2012;4(153):1-10.
177. Campoccia D, *et al.* The significance of infection related to orthopedic devices and issues of antibiotic resistance. *Biomaterials.* Apr 2006;27(11):2331-9.
178. Costerton JW, *et al.* Bacterial biofilms: a common cause of persistent infections. *Science.* May 21 1999;284(5418):1318-22.
179. Augustyn B. Ventilator-associated pneumonia: risk factors and prevention. *Crit. Care Nurse.* 2007;27(4):32-39.
180. Baddour LM, *et al.* A summary of the update on cardiovascular implantable electronic device infections and their management: a scientific statement from the American Heart Association. *J. Am. Dent. Assoc.* Feb 2011;142(2):159-65.
181. Nahabedian MY, *et al.* Infectious complications following breast reconstruction with expanders and implants. *Plast. Reconstr. Surg.* Aug 2003;112(2):467-76.
182. Dutta D, *et al.* Factors influencing bacterial adhesion to contact lenses. *Mol. Vis.* 2012;18:14-21.
183. Elek SD, Conen PE. The virulence of Staphylococcus pyogenes for man; a study of the problems of wound infection. *Br. J. Exp. Pathol.* Dec 1957;38(6):573-86.
184. Zimmerli W, *et al.* Pathogenesis of foreign body infection: description and characteristics of an animal model. *J. Infect. Dis.* Oct 1982;146(4):487-97.
185. Zimmerli W, *et al.* Pathogenesis of foreign body infection. Evidence for a local granulocyte defect. *J. Clin. Invest.* 1984;73(4):1191-200.

186. Corbin A, *et al.* Antimicrobial penetration and efficacy in an in vitro oral biofilm model. *Antimicrob. Agents Chemother.* Jul 2011;55(7):3338-44.
187. Stewart PS. Mechanisms of antibiotic resistance in bacterial biofilms. *Int. J. Med. Microbiol.* Jul 2002;292(2):107-13.
188. König C, *et al.* Factors compromising antibiotic activity against biofilms of Staphylococcus epidermidis. *Eur. J. Clin. Microbiol. Infect. Dis.* 2001;20(1):20-26.
189. Arciola CR, *et al.* Antibiotic resistance in exopolysaccharide-forming Staphylococcus epidermidis clinical isolates from orthopaedic implant infections. *Biomaterials.* Nov 2005;26(33):6530-5.
190. Mogensen TH. Pathogen recognition and inflammatory signaling in innate immune defenses. *Clin. Microbiol. Rev.* 2009;22(2):240-73.
191. Schwandner R, *et al.* Peptidoglycan- and lipoteichoic acid-induced cell activation is mediated by toll-like receptor 2. *J. Biol. Chem.* Jun 18 1999;274(25):17406-9.
192. Takeuchi O, *et al.* Cutting edge: TLR2-deficient and MyD88-deficient mice are highly susceptible to Staphylococcus aureus infection. *J. Immunol.* Nov 15 2000;165(10):5392-6.
193. Echchannaoui H, *et al.* Toll-like receptor 2 deficient mice are highly susceptible to streptococcus pneumoniae meningitis because of reduced bacterial clearing and enhanced inflammation. *J. Infect. Dis.* September 15, 2002 2002;186(6):798-806.
194. Hemmi H, *et al.* A Toll-like receptor recognizes bacterial DNA. *Nature.* Dec 7 2000;408(6813):740-5.
195. Faustin B, *et al.* Reconstituted NALP1 inflammasome reveals two-step mechanism of caspase-1 activation. *Mol. Cell.* Mar 9 2007;25(5):713-24.
196. Girardin SE, *et al.* Nod2 is a general sensor of peptidoglycan through muramyl dipeptide (MDP) detection. *J. Biol. Chem.* Mar 14 2003;278(11):8869-72.
197. Kawai T, Akira S. The role of pattern-recognition receptors in innate immunity: update on Toll-like receptors. *Nat. Immunol.* May 2010;11(5):373-84.
198. Laarman A, *et al.* Complement inhibition by gram-positive pathogens: molecular mechanisms and therapeutic implications. *J. Mol. Med. (Berl.).* Feb 2010;88(2):115-20.
199. Walport MJ. Complement. First of two parts. *N. Engl. J. Med.* Apr 5 2001;344(14):1058-66.
200. Fernie-King BA, *et al.* Streptococcal inhibitor of complement (SIC) inhibits the membrane attack complex by preventing uptake of C567 onto cell membranes. *Immunology.* Jul 2001;103(3):390-8.
201. Mims C, *et al. Medical microbiology.* Second ed. Barcelona: Elsevier Science; 1998.
202. Harris LG, *et al.* An introduction to Staphylococcus aureus, and techniques for identifying and quantifying S. aureus adhesins in relation to adhesion to biomaterials: review. *Eur. Cell. Mater.* Dec 31 2002;4:39-60.
203. Zimmerli W, *et al.* Prosthetic-joint infections. *N. Engl. J. Med.* Oct 14 2004;351(16):1645-54.
204. Cheung GY, *et al.* Staphylococcus epidermidis strategies to avoid killing by human neutrophils. *PLoS Pathog.* 2010;6(10):e1001133.
205. Foster TJ. Immune evasion by staphylococci. *Nat. Rev. Microbiol.* Dec 2005;3(12):948-58.
206. Atshan SS, *et al.* Prevalence of adhesion and regulation of biofilm-related genes in different clones of Staphylococcus aureus. *J. Biomed. Biotechnol.* 2012;2012:976972.
207. O'Riordan K, Lee JC. Staphylococcus aureus capsular polysaccharides. *Clin. Microbiol. Rev.* Jan 2004;17(1):218-34.

208. Schwarz-Linek U, *et al.* The molecular basis of fibronectin-mediated bacterial adherence to host cells. *Mol. Microbiol.* May 2004;52(3):631-41.
209. Karavolos MH, *et al.* Role and regulation of the superoxide dismutases of Staphylococcus aureus. *Microbiology.* Oct 2003;149(Pt 10):2749-58.
210. Otto M. Phenol-soluble modulins. *Int. J. Med. Microbiol.* 2014.
211. Otto M. Staphylococcus epidermidis - The 'accidental' pathogen. *Nat. Rev. Microbiol.* 2009;7(8):555-67.
212. Otto M. Molecular basis of Staphylococcus epidermidis infections. *Semin Immunopathol.* Mar 2012;34(2):201-14.
213. Kocianova S, *et al.* Key role of poly-gamma-DL-glutamic acid in immune evasion and virulence of Staphylococcus epidermidis. *J. Clin. Invest.* Mar 2005;115(3):688-94.
214. Vuong C, *et al.* Polysaccharide intercellular adhesin (PIA) protects Staphylococcus epidermidis against major components of the human innate immune system. *Cell. Microbiol.* Mar 2004;6(3):269-75.
215. Kristian SA, *et al.* Biofilm formation induces C3a release and protects Staphylococcus epidermidis from IgG and complement deposition and from neutrophil-dependent killing. *J. Infect. Dis.* Apr 1 2008;197(7):1028-35.
216. Li M, *et al.* Gram-positive three-component antimicrobial peptide-sensing system. *Proc. Natl. Acad. Sci. U. S. A.* May 29 2007;104(22):9469-74.
217. Sutherland IW. The biofilm matrix--an immobilized but dynamic microbial environment. *Trends Microbiol.* May 2001;9(5):222-7.
218. Yao Y, *et al.* Genomewide analysis of gene expression in Staphylococcus epidermidis biofilms: insights into the pathophysiology of S. epidermidis biofilms and the role of phenol-soluble modulins in formation of biofilms. *J. Infect. Dis.* Jan 15 2005;191(2):289-98.
219. Nickel JC, *et al.* Tobramycin resistance of Pseudomonas aeruginosa cells growing as a biofilm on urinary catheter material. *Antimicrob. Agents Chemother.* Apr 1985;27(4):619-24.
220. Costerton JW, *et al.* Bacterial biofilms in nature and disease. *Annu. Rev. Microbiol.* 1987;41:435-64.
221. Otto M. Staphylococcal biofilms. *Curr. Top. Microbiol. Immunol.* 2008;322:207-28.
222. O'Gara JP. ica and beyond: biofilm mechanisms and regulation in Staphylococcus epidermidis and Staphylococcus aureus. *FEMS Microbiol. Lett.* May 2007;270(2):179-88.
223. Katsikogianni M, Missirlis YF. Concise review of mechanisms of bacterial adhesion to biomaterials and of techniques used in estimating bacteria-material interactions. *Eur. Cell. Mater.* Dec 7 2004;8:37-57.
224. An YH, Friedman RJ. Concise review of mechanisms of bacterial adhesion to biomaterial surfaces. *J. Biomed. Mater. Res.* Fall 1998;43(3):338-48.
225. Bos R, *et al.* Physico-chemistry of initial microbial adhesive interactions – its mechanisms and methods for study. *FEMS Microbiol. Rev.* 1999;23(2):179-230.
226. Tegoulia VA, Cooper SL. Staphylococcus aureus adhesion to self-assembled monolayers: effect of surface chemistry and fibrinogen presence. *Colloids Surf., B.* 2002;24(3-4):217-28.
227. Kiremitci-Gumusderelioglu M, Pesmen A. Microbial adhesion to ionogenic PHEMA, PU and PP implants. *Biomaterials.* Feb 1996;17(4):443-9.
228. Shi L, *et al.* Mucin coating on polymeric material surfaces to suppress bacterial adhesion. *Colloids Surf., B.* 2000;17(4):229-39.

229. Patel JD, *et al.* S. epidermidis biofilm formation: Effects of biomaterial surface chemistry and serum proteins. *J. Biomed. Mater. Res. A.* 2007;80(3):742-51.
230. Taylor RL, *et al.* The influence of substratum topography on bacterial adhesion to polymethyl methacrylate. *J. Mater. Sci.: Mater. Med.* 1998/01/01 1998;9(1):17-22.
231. Whitehead KA, Verran J. The effect of surface topography on the retention of microorganisms. *Food and Bioproducts Processing.* 2006;84(4 C):253-59.
232. Boyd RD, *et al.* Use of the atomic force microscope to determine the effect of substratum surface topography on bacterial adhesion. *Langmuir.* 2002/03/01 2002;18(6):2343-46.
233. Pereira da Silva CH, *et al.* Influence of titanium surface roughness on attachment of Streptococcus sanguis: an in vitro study. *Implant Dent.* Mar 2005;14(1):88-93.
234. Anselme K, *et al.* The interaction of cells and bacteria with surfaces structured at the nanometre scale. *Acta Biomater.* Oct 2010;6(10):3824-46.
235. Mitik-Dineva N, *et al.* Differences in colonisation of five marine bacteria on two types of glass surfaces. *Biofouling.* Oct 2009;25(7):621-31.
236. Mitik-Dineva N, *et al.* Escherichia coli, Pseudomonas aeruginosa, and Staphylococcus aureus attachment patterns on glass surfaces with nanoscale roughness. *Curr. Microbiol.* Mar 2009;58(3):268-73.
237. Puckett SD, *et al.* The relationship between the nanostructure of titanium surfaces and bacterial attachment. *Biomaterials.* Feb 2010;31(4):706-13.
238. Campoccia D, *et al.* Study of Staphylococcus aureus adhesion on a novel nanostructured surface by chemiluminometry. *Int. J. Artif. Organs.* Jun 2006;29(6):622-9.
239. Campoccia D, *et al.* A review of the biomaterials technologies for infection-resistant surfaces. *Biomaterials.* Nov 2013;34(34):8533-54.
240. Ruggieri MR, *et al.* Reduction of bacterial adherence to catheter surface with heparin. *J. Urol.* Aug 1987;138(2):423-6.
241. Nagaoka S, Kawakami H. Inhibition of bacterial adhesion and biofilm formation by a heparinized hydrophilic polymer. *ASAIO J.* Jul-Sep 1995;41(3):M365-8.
242. Kenan DJ, *et al.* Peptide-PEG amphiphiles as cytophobic coatings for mammalian and bacterial cells. *Chem. Biol.* Jul 2006;13(7):695-700.
243. Ostuni E, *et al.* Self-assembled monolayers that resist the adsorption of proteins and the adhesion of bacterial and mammalian cells. *Langmuir.* 2001;17(20):6336-43.
244. Park KD, *et al.* Bacterial adhesion on PEG modified polyurethane surfaces. *Biomaterials.* Apr-May 1998;19(7-9):851-9.
245. Cheng G, *et al.* Inhibition of bacterial adhesion and biofilm formation on zwitterionic surfaces. *Biomaterials.* Oct 2007;28(29):4192-9.
246. Karchmer TB, *et al.* A randomized crossover study of silver-coated urinary catheters in hospitalized patients. *Arch. Intern. Med.* Nov 27 2000;160(21):3294-8.
247. Saint S, *et al.* The efficacy of silver alloy-coated urinary catheters in preventing urinary tract infection: a meta-analysis. *Am. J. Med.* Sep 1998;105(3):236-41.
248. Goldschmidt H, *et al.* Prevention of catheter-related infections by silver coated central venous catheters in oncological patients. *Zentralblatt für Bakteriologie.* Dec 1995;283(2):215-23.
249. Popelka A, *et al.* Anti-bacterial treatment of polyethylene by cold plasma for medical purposes. *Molecules.* 2012;17(1):762-85.
250. Qu J, *et al.* Silver/hydroxyapatite composite coatings on porous titanium surfaces by sol-gel method. *J. Biomed. Mater. Res. B Appl. Biomater.* 2011;97 B(1):40-48.

251. Hilpert K, *et al.* Screening and characterization of surface-tethered cationic peptides for antimicrobial activity. *Chem. Biol.* 2009;16(1):58-69.
252. Raad I, *et al.* Central venous catheters coated with minocycline and rifampin for the prevention of catheter-related colonization and bloodstream infections. A randomized, double-blind trial. The Texas Medical Center Catheter Study Group. *Ann. Intern. Med.* Aug 15 1997;127(4):267-74.
253. Neut D, *et al.* Antibacterial efficacy of a new gentamicin-coating for cementless prostheses compared to gentamicin-loaded bone cement. *J. Orthop. Res.* Nov 2011;29(11):1654-61.
254. Liang J, *et al.* N-halamine/quat siloxane copolymers for use in biocidal coatings. *Biomaterials.* 2006;27(11):2495-501.
255. Jampala SN, *et al.* Plasma-enhanced synthesis of bactericidal quaternary ammonium thin layers on stainless steel and cellulose surfaces. *Langmuir.* Aug 19 2008;24(16):8583-91.
256. Foster HA, *et al.* Photocatalytic disinfection using titanium dioxide: Spectrum and mechanism of antimicrobial activity. *Appl. Microbiol. Biotechnol.* 2011;90(6):1847-68.
257. Pratap Reddy M, *et al.* Hydroxyapatite-supported Ag-TiO2 as Escherichia coli disinfection photocatalyst. *Water Res.* 2007;41(2):379-86.
258. Nablo BJ, *et al.* Inhibition of implant-associated infections via nitric oxide release. *Biomaterials.* 2005;26(34):6984-90.
259. Amitai G, *et al.* Polyurethane-based leukocyte-inspired biocidal materials. *Biomaterials.* 2009;30(33):6522-29.
260. Colon G, *et al.* Increased osteoblast and decreased Staphylococcus epidermidis functions on nanophase ZnO and TiO2. *J. Biomed. Mater. Res. A.* Sep 1 2006;78(3):595-604.
261. Evliyaoğlu Y, *et al.* The efficacy of a novel antibacterial hydroxyapatite nanoparticle-coated indwelling urinary catheter in preventing biofilm formation and catheter-associated urinary tract infection in rabbits. *Urol. Res.* 2011;39(6):443-49.
262. Zhao J, *et al.* Bactericidal and biocompatible properties of TiN/Ag multilayered films by ion beam assisted deposition. *J. Mater. Sci.: Mater. Med.* 2009;20(SUPPL. 1):S101-S05.
263. Hajipour MJ, *et al.* Antibacterial properties of nanoparticles. *Trends Biotechnol.* 2012;30(10):499-511.
264. Kaplan JB, *et al.* Recombinant human DNase I decreases biofilm and increases antimicrobial susceptibility in staphylococci. *J. Antibiot. (Tokyo).* Feb 2012;65(2):73-7.
265. Pavlukhina SV, *et al.* Noneluting enzymatic antibiofilm coatings. *ACS Appl. Mater. Interfaces.* 2012;4(9):4708-16.
266. Olofsson AC, *et al.* N-acetyl-L-cysteine affects growth, extracellular polysaccharide production, and bacterial biofilm formation on solid surfaces. *Appl. Environ. Microbiol.* Aug 2003;69(8):4814-22.
267. Belyansky I, *et al.* The addition of lysostaphin dramatically improves survival, protects porcine biomesh from infection, and improves graft tensile shear strength. *J. Surg. Res.* 2011;171(2):409-15.
268. Dean SN, *et al.* Natural and synthetic cathelicidin peptides with anti-microbial and anti-biofilm activity against Staphylococcus aureus. *BMC Microbiol.* 2011;11:114.
269. Lönn-Stensrud J, *et al.* Furanones, potential agents for preventing Staphylococcus epidermidis biofilm infections? *J. Antimicrob. Chemother.* 2009;63(2):309-16.
270. Darouiche RO, *et al.* Antimicrobial and antibiofilm efficacy of triclosan and DispersinB combination. *J. Antimicrob. Chemother.* Jul 2009;64(1):88-93.

271. Christensen LD, *et al.* Synergistic antibacterial efficacy of early combination treatment with tobramycin and quorum-sensing inhibitors against Pseudomonas aeruginosa in an intraperitoneal foreign-body infection mouse model. *J. Antimicrob. Chemother.* May 2012;67(5):1198-206.
272. Li B, *et al.* Multilayer polypeptide nanoscale coatings incorporating IL-12 for the prevention of biomedical device-associated infections. *Biomaterials.* 2009;30(13):2552-58.
273. Li B, *et al.* Evaluation of local MCP-1 and IL-12 nanocoatings for infection prevention in open fractures. *J. Orthop. Res.* 2010;28(1):48-54.
274. Wagner VE, Bryers JD. Poly(ethylene glycol)-polyacrylate copolymers modified to control adherent monocyte-macrophage physiology: interactions with attaching Staphylococcus epidermidis or Pseudomonas aeruginosa bacteria. *J. Biomed. Mater. Res. A.* Apr 1 2004;69(1):79-90.
275. Bryers JD. Medical biofilms. *Biotechnol. Bioeng.* May 1 2008;100(1):1-18.
276. Boelens JJ, *et al.* Interferon-gamma protects against biomaterial-associated Staphylococcus epidermidis infection in mice. *J. Infect. Dis.* Mar 2000;181(3):1167-71.
277. Gristina AG, *et al.* Infections from biomaterials and implants: a race for the surface. *Med. Prog. Technol.* 1988;14(3-4):205-24.
278. Costa P, *et al.* Directing cell migration using micropatterned and dynamically adhesive polymer brushes. *Acta Biomater.* Feb 6 2014.
279. Kantlehner M, *et al.* Surface coating with cyclic RGD peptides stimulates osteoblast adhesion and proliferation as well as bone formation. *Chembiochem.* Aug 18 2000;1(2):107-14.
280. Puckett SD, *et al.* Nanotextured titanium surfaces for enhancing skin growth on transcutaneous osseointegrated devices. *Acta Biomater.* Jun 2010;6(6):2352-62.
281. Maddikeri RR. Reduced medical infection related bacterial strains adhesion on bioactive RGD modified titanium surfaces: A first step toward cell selective surfaces. *J. Biomed. Mater. Res. A.* 2008;84(2):425-35.
282. Shi Z, *et al.* Bacterial adhesion and osteoblast function on titanium with surface-grafted chitosan and immobilized RGD peptide. *J. Biomed. Mater. Res. A.* 2008;86(4):865-72.
283. Wu Y, *et al.* Differential response of Staphylococci and osteoblasts to varying titanium surface roughness. *Biomaterials.* 2011;32(4):951-60.
284. Boelens JJ, *et al.* Biomaterial-associated persistence of Staphylococcus epidermidis in pericatheter macrophages. *J. Infect. Dis.* Apr 2000;181(4):1337-49.
285. Curtis J, Colas A. Medical applications of silicones. In: Ratner BD, Hoffmann AS, Schoen FJ, Lemons JE, eds. *Biomaterials science: An introduction to materials in medicine.* San Diego, California: Elsevier Academic Press; 2004.
286. Eisler R. Chrysotherapy: a synoptic review. *Inflamm. Res.* Dec 2003;52(12):487-501.
287. Hulander M, *et al.* Gradients in surface nanotopography used to study platelet adhesion and activation. *Colloids Surf B Biointerfaces.* Oct 1 2013;110:261-9.
288. Gabriel MM, *et al.* Effects of silver on adherence of bacteria to urinary catheters: in vitro studies. *Curr. Microbiol.* Jan 1995;30(1):17-22.
289. Jancinova V, *et al.* The combined luminol/isoluminol chemiluminescence method for differentiating between extracellular and intracellular oxidant production by neutrophils. *Redox Rep.* 2006;11(3):110-6.

290. Friedman PL, Ellisman MH. Enhanced visualization of peripheral nerve and sensory receptors in the scanning electron microscope using cryofracture and osmium-thiocarbohydrazide-osmium impregnation. *J. Neurocytol.* Feb 1981;10(1):111-31.
291. Palmquist A, *et al.* Morphological studies on machined implants of commercially pure titanium and titanium alloy (Ti6Al4V) in the rabbit. *J. Biomed. Mater. Res. B Appl. Biomater.* Oct 2009;91(1):309-19.
292. Mohammadi S, *et al.* Long-term bone response to titanium implants coated with thin radiofrequent magnetron-sputtered hydroxyapatite in rabbits. *Int. J. Oral Maxillofac. Implants.* Jul-Aug 2004;19(4):498-509.
293. Subbiahdoss G, *et al.* Mammalian cell growth versus biofilm formation on biomaterial surfaces in an in vitro post-operative contamination model. *Microbiology.* 2010;156(10):3073-78.
294. Lucke M, *et al.* Gentamicin coating of metallic implants reduces implant-related osteomyelitis in rats. *Bone.* May 2003;32(5):521-31.
295. Russo TA, *et al.* The effects of Escherichia coli capsule, O-antigen, host neutrophils, and complement in a rat model of Gram-negative pneumonia. *FEMS Microbiol. Lett.* Sep 26 2003;226(2):355-61.
296. Russo TA, *et al.* Rat pneumonia and soft-tissue infection models for the study of Acinetobacter baumannii biology. *Infect. Immun.* Aug 2008;76(8):3577-86.
297. Schaad HJ, *et al.* Comparative efficacies of imipenem, oxacillin and vancomycin for therapy of chronic foreign body infection due to methicillin-susceptible and -resistant Staphylococcus aureus. *J. Antimicrob. Chemother.* Jun 1994;33(6):1191-200.
298. Lindblad M, *et al.* Cell and soft tissue interactions with methyl- and hydroxyl-terminated alkane thiols on gold surfaces. *Biomaterials.* Aug 1997;18(15):1059-68.
299. Lewis JB, *et al.* Effect of subtoxic concentrations of metal ions on NFkappaB activation in THP-1 human monocytes. *J. Biomed. Mater. Res. A.* Feb 1 2003;64(2):217-24.
300. Shin SH, *et al.* The effects of nano-silver on the proliferation and cytokine expression by peripheral blood mononuclear cells. *Int. Immunopharmacol.* Dec 15 2007;7(13):1813-8.
301. Keller JC, *et al.* An in vivo method for the biological evaluation of metal implants. *J. Biomed. Mater. Res.* Sep 1984;18(7):829-44.
302. Wright JB, *et al.* Early healing events in a porcine model of contaminated wounds: effects of nanocrystalline silver on matrix metalloproteinases, cell apoptosis, and healing. *Wound Repair Regen.* May-Jun 2002;10(3):141-51.
303. Bhol KC, Schechter PJ. Topical nanocrystalline silver cream suppresses inflammatory cytokines and induces apoptosis of inflammatory cells in a murine model of allergic contact dermatitis. *Br. J. Dermatol.* Jun 2005;152(6):1235-42.
304. Bhol KC, Schechter PJ. Effects of nanocrystalline silver (NPI 32101) in a rat model of ulcerative colitis. *Dig. Dis. Sci.* Oct 2007;52(10):2732-42.
305. Suska F, *et al.* Noble metals as new antimicrobial and biocompatible coatings. *Clin. Oral Implants Res.* 2007;18(5):cxliii-cxliv.
306. Chiang W-C, *et al.* Bacterial inhibiting surfaces caused by the effects of silver release and/or electrical field. *Electrochim. Acta.* 2008;54(1):108-15.
307. Chang Q, *et al.* Bactericidal mechanism of Ag/Al2O3 against Escherichia coli. *Langmuir.* Oct 23 2007;23(22):11197-9.

308. Suska F. *On the initial inflammatory response to variations in biomaterial surface chemistry*. Göteborg, Sweden: Department of Biomaterials, Institute of Surgical Sciences, Sahlgrenska Academy at Göteborg University; 2004.
309. Williams DF. Tissue-biomaterial interactions. *J. Mater. Sci.* 1987/10/01 1987;22(10):3421-45.
310. Laing PG, *et al.* Tissue reaction in rabbit muscle exposed to metallic implants. *J. Biomed. Mater. Res.* Mar 1967;1(1):135-49.
311. Williams DF, *et al.* Protein absorption and desorption phenomena on clean metal surfaces. *J. Biomed. Mater. Res.* Mar 1985;19(3):313-20.
312. Lausmaa J. Mechanical, thermal, chemical and electrochemical surface treatment of titanium. In: Brunette D, Tengvall P, Thomsen P, Textor M, eds. *Titanium in Medicine*. Berlin: Springer Verlag; 2001.
313. Zainali K, *et al.* Effects of gold coating on experimental implant fixation. *J. Biomed. Mater. Res. A.* Jan 2009;88(1):274-80.
314. Gosheger G, *et al.* Silver-coated megaendoprostheses in a rabbit model--an analysis of the infection rate and toxicological side effects. *Biomaterials.* Nov 2004;25(24):5547-56.
315. Alt V, *et al.* An in vitro assessment of the antibacterial properties and cytotoxicity of nanoparticulate silver bone cement. *Biomaterials.* Aug 2004;25(18):4383-91.
316. Ewald A, *et al.* Antimicrobial titanium/silver PVD coatings on titanium. *Biomed. Eng. Online.* 2006;5:22.
317. Hardes J, *et al.* The influence of elementary silver versus titanium on osteoblasts behaviour in vitro using human osteosarcoma cell lines. *Sarcoma.* 2007;2007:26539.
318. Zheng X, *et al.* Antibacterial property and biocompatibility of plasma sprayed hydroxyapatite/silver composite coatings. *Journal of Thermal Spray Technology.* 2009:1-6.
319. Cortizo MC, *et al.* Metallic dental material biocompatibility in osteoblastlike cells: correlation with metal ion release. *Biol. Trace Elem. Res.* Aug 2004;100(2):151-68.
320. Lee YH, *et al.* Modified titanium surface with gelatin nano gold composite increases osteoblast cell biocompatibility. *Appl. Surf. Sci.* Aug 1 2010;256(20):5882-87.
321. Anselme K, Bigerelle M. Effect of a gold-palladium coating on the long-term adhesion of human osteoblasts on biocompatible metallic materials. *Surf. Coat. Technol.* Jun 20 2006;200(22-23):6325-30.
322. Kaplan SS, *et al.* Biomaterial-induced alterations of neutrophil superoxide production. *J. Biomed. Mater. Res.* 1992;26(8):1039-51.
323. Broekhuizen CA, *et al.* Peri-implant tissue is an important niche for Staphylococcus epidermidis in experimental biomaterial-associated infection in mice. *Infect. Immun.* Mar 2007;75(3):1129-36.
324. Broekhuizen CA, *et al.* Microscopic detection of viable Staphylococcus epidermidis in peri-implant tissue in experimental biomaterial-associated infection, identified by bromodeoxyuridine incorporation. *Infect. Immun.* Mar 2010;78(3):954-62.
325. Selvarajan K. *Adherent- and non-adherent macrophages in cell survival and death*. Ohio, USA: Integrated Biomedical Science Graduate Program, The Ohio State University; 2009.
326. Ivanova EP, *et al.* Bactericidal activity of black silicon. *Nat. Commun.* 2013;4:2838.
327. Mack D, *et al.* Staphylococcus epidermidis in biomaterial-associated infections. In: Moriarty TF, Zaat SAJ, Busscher HJ, eds. *Biomaterials associated infections*. New York: Springer; 2013:25-56.

328. Rohde H, *et al.* Induction of Staphylococcus epidermidis biofilm formation via proteolytic processing of the accumulation-associated protein by staphylococcal and host proteases. *Mol. Microbiol.* 2005;55(6):1883-95.
329. Patel JD, *et al.* Gene expression during S. epidermidis biofilm formation on biomaterials. *J. Biomed. Mater. Res. A.* 2012;100 A(11):2863-69.
330. Hulander M, *et al.* Blood Interactions with Noble Metals: Coagulation and Immune Complement Activation. *ACS Appl. Mater. Interfaces.* 2009;1(5):1053-62.
331. Allen LA, Aderem A. Molecular definition of distinct cytoskeletal structures involved in complement- and Fc receptor-mediated phagocytosis in macrophages. *J. Exp. Med.* Aug 1 1996;184(2):627-37.
332. Aderem A, Underhill DM. Mechanisms of phagocytosis in macrophages. *Annu. Rev. Immunol.* 1999;17:593-623.
333. Brown GD, *et al.* Dectin-1 is a major beta-glucan receptor on macrophages. *J. Exp. Med.* Aug 5 2002;196(3):407-12.
334. van Bruggen R, *et al.* Complement receptor 3, not Dectin-1, is the major receptor on human neutrophils for β-glucan-bearing particles. *Mol. Immunol.* 2009;47(2-3):575-81.
335. Wright SD, Silverstein SC. Receptors for C3b and C3bi promote phagocytosis but not the release of toxic oxygen from human phagocytes. *J. Exp. Med.* Dec 1 1983;158(6):2016-23.
336. Lindena J, *et al.* Mechanisms of non-opsonized zymosan-induced and luminol-enhanced chemiluminescence in whole blood and isolated phagocytes. *J. Clin. Chem. Clin. Biochem.* 1987;25(11):765-78.
337. Martinez-Martinez L, *et al.* Chemiluminescence of human polymorphonuclear leucocytes after stimulation with whole cells and cell-wall components of Staphylococcus epidermidis. *J. Med. Microbiol.* Sep 1993;39(3):196-203.
338. Nauciel C, Espinasse-Maes F. Role of gamma interferon and tumor necrosis factor alpha in resistance to Salmonella typhimurium infection. *Infect. Immun.* Feb 1992;60(2):450-4.
339. Murray HW. The interferons, macrophage activation, and host defense against nonviral pathogens. *J. Interferon Res.* Oct 1992;12(5):319-22.
340. Abbas AK, Lichtman AH. *Cellular and molecular biology.* fifth ed. Philadelphia: Saunders; 2003.
341. Park KR, Bryers JD. Effect of macrophage classical (M1) activation on implant-adherent macrophage interactions with Staphylococcus epidermidis: A murine in vitro model system. *J. Biomed. Mater. Res. A.* 2012;100 A(8):2045-53.
342. DeForge LE, Remick DG. Kinetics of TNF, IL-6, and IL-8 gene expression in LPS-stimulated human whole blood. *Biochem. Biophys. Res. Commun.* Jan 15 1991;174(1):18-24.
343. Hazuda DJ, *et al.* The kinetics of interleukin 1 secretion from activated monocytes. Differences between interleukin 1 alpha and interleukin 1 beta. *J. Biol. Chem.* Jun 15 1988;263(17):8473-9.